



THE UNIVERSITY  
*of* ADELAIDE

# **Investigating Amyloid Precursor Protein Derivatives As Novel Therapeutic Agents Following Traumatic Brain Injury**

Stephanie Lauren Plummer BHLthSc (Hons)

Discipline of Anatomy and Pathology  
Adelaide Medical School  
The University of Adelaide

December 2017

A thesis submitted to the University of Adelaide in partial fulfilment of the  
requirements for the degree of Doctor of Philosophy

# Contents

<b>Table of Figures</b> .....	<b>iv</b>
<b>Table of Tables</b> .....	<b>vi</b>
<b>Declaration</b> .....	<b>vii</b>
<b>Publications and Presentations</b> .....	<b>viii</b>
<b>Personal Acknowledgements</b> .....	<b>xii</b>
<b>Financial Support</b> .....	<b>xiv</b>
<b>Abbreviations</b> .....	<b>xv</b>
<b>Abstract</b> .....	<b>xvii</b>
<b>Chapter 1: The Neuroprotective Properties Of The Amyloid Precursor Protein Following Traumatic Brain Injury</b> .....	<b>1</b>
1.1 Synopsis.....	21
1.1.1 Hypothesis.....	21
1.1.2 Aims.....	21
<b>Chapter 2: Materials and Methods Part I: Experimental Procedures</b> .....	<b>22</b>
2.1 Ethics .....	23
2.2 Animals.....	23
2.3 Experimental Procedures .....	23
2.3.1 Anaesthesia .....	23
2.3.2 Impact Acceleration Weight Drop Model of Traumatic Brain Injury .....	24
2.3.3 APP Peptide Preparation .....	26
2.3.4 APP Peptide Administration .....	26
2.4 Neurological Assessment .....	27
2.4.1 Motor Outcome.....	27
2.4.2 Functional Outcome .....	29
2.5 Perfusions & Tissue Extraction .....	35
2.5.1 Formalin Fixed Tissue .....	35
2.5.2 Fresh Snap Frozen Tissue .....	35
2.6 Histological Analysis .....	36
2.6.1 Axonal Injury .....	37
2.6.2 Microglia.....	38
2.6.3 Astrocytes.....	39
2.7 Western Blot Analysis.....	40

2.8 Statistical Analysis .....	42
<b>Chapter 3: Materials &amp; Methods Part II: Troubleshooting.....</b>	<b>43</b>
3.1 Introduction.....	44
3.2 Animals.....	45
3.2.1 Sprague Dawley Rats .....	45
3.3 Pilot Study Examining Inter Strain Differences Between Sprague Dawley Rats Following TBI .....	47
3.4 Physical Outcome Prior to TBI.....	47
3.5 Physical Appearances Following TBI.....	48
3.6 Motor Outcome Following TBI .....	50
3.7 Histological Outcome Following TBI.....	51
3.8 Establishment of a Charles River Strain Breeding Colony .....	52
3.9 Long term Efficacy of APP96 110 Following TBI in The Adelaide University Bred Charles River Strain SD Rat .....	53
3.10 Summary .....	55
<b>Chapter 4: The Amyloid Precursor Protein Derivative, APP96-110, is Efficacious Following Intravenous Administration After Traumatic Brain Injury .....</b>	<b>56</b>
4.1 Abstract .....	59
4.2 Introduction.....	60
4.3 Methods .....	62
4.3.1 The APP96 110 Peptide.....	62
4.3.2 Evaluation of the Efficacy of IV APP96 110 Administered at 30 Minutes Following TBI .....	63
4.3.3 Evaluation of the Efficacy of IV APP96 110 Administered at 5 Hours Following TBI .....	66
4.3.4 Statistical Analysis .....	67
4.4 Results .....	67
4.4.1 Examining the Efficacy of IV APP96 110 Administered at 30 Minutes Following TBI .....	67
4.4.2 Evaluation of the Efficacy of IV APP96 110 Administered at 5 Hours Following TBI .....	74
4.5 Discussion.....	77
<b>Chapter 5: Enhanced Heparin Binding Affinity Of APP96-110 Results In Increased Neuroprotection Following Traumatic Brain Injury .....</b>	<b>83</b>
5.1 Introduction.....	84
5.2 Methods .....	85
5.2.1 APP96 110 Peptides .....	86

5.2.2 Chromatography Assay .....	86
5.2.3 In Vivo APP96 110 Preparation .....	87
5.2.4 Injury Induction .....	87
5.2.5 Assessment of Motor Outcome .....	87
5.2.6 Histological Assessment .....	88
5.2.7 Statistical Analysis .....	88
5.3 Results .....	89
5.3.1 Design of APP96 110 Mutant Peptides .....	89
5.3.2 Heparin Binding.....	90
5.3.3 Testing the Efficacy of the Mutant 3+APP96 110 Peptide Following TBI.....	91
5.3.4 Motor Outcome.....	91
5.3.5 Diffuse Axonal Injury .....	93
5.4 Discussion.....	96
<b>Chapter 6: The Long-Term Efficacy of APP96-110 Peptides Following TBI.....</b>	<b>101</b>
6.1 Introduction.....	102
6.2 Methods .....	103
6.2.1 APP96 110 Peptides .....	103
6.2.2 Animals.....	104
6.2.3 Injury Induction .....	104
6.2.4 Assessment of Motor Outcome .....	105
6.2.5 Assessment of Functional Outcome .....	105
6.2.6 Histological Assessment .....	106
6.2.7 Western Blot Analysis.....	106
6.2.8 Statistical Analysis .....	106
6.3 Results .....	107
6.3.1 Motor Outcome.....	107
6.3.2 Functional Outcome .....	109
6.3.3 Histological Analysis .....	115
6.3.4 Western Blot Analysis.....	119
6.4 Discussion.....	125
<b>Chapter 7: Summary &amp; Future Directions .....</b>	<b>131</b>
7.1 Future directions .....	135
<b>References .....</b>	<b>139</b>
<b>Appendix.....</b>	<b>144</b>
Multiplex .....	145

## Table of Figures

Figure 2.1: Image showing the injury apparatus for induction of the impact acceleration model of DAI.....	25
Figure 2.2: Representative photograph of the rotarod device used to assess motor outcome following TBI.....	28
Figure 2.3: Representative photograph of the Open Field, with the 10 x 10cm grid visible on the inside of the box.....	30
Figure 2.4: Representative photograph of the Elevated Plus Maze .....	31
Figure 2.5: Representative photograph of the Y Maze .....	32
Figure 2.6: Representative photograph of the Barnes Maze .....	33
Figure 2.7: Representative photograph showing the Forced Swim Test.....	34
Figure 2.8: Representative image demonstrating the regions of the cortex and corpus callosum that were used for IHC analysis.....	37
Figure 2.9: Representative images demonstrating the morphological differences between microglia activation states .....	38
Figure 2.10: Representative images demonstrating the morphological differences between astrocytes .....	39
Figure 3.1: A comparative image displaying the changes in motor outcome, and associated injury severity, over a period of 3 days over the course of the last 4 years in our laboratory.....	45
Figure 3.2: Injury severity of Charles River SD 24 hours post TBI, as assessed by the clinical record sheet criteria.....	49
Figure 3.3: 3 day motor outcome as assessed by the rotarod .....	50
Figure 3.4: Representative micrographs illustrating the extent of axonal injury in Harlan strain SDs post TBI .....	52
Figure 3.5: The coloured protocol created for establishment of the modified outbred Poiley system .....	53
Figure 3.6: 30 day motor outcome as assessed by the rotarod .....	54
Figure 3.7: 7 day motor outcome as assessed by the rotarod .....	55
Figure 4.1: Motor outcome illustrating the effect of treatment with 0.005mg/kg, 0.05mg/kg and 0.5mg/kg APP96 110 IV at 30 minutes post TBI .....	68
Figure 4.2: Representative micrographs showing the degree of DAI in the corpus callosum at 3 days following diffuse TBI.....	70
Figure 4.3: Representative micrographs showing the degree of neuroinflammation in the corpus callosum at 3 days following diffuse TBI.....	72
Figure 4.4: Representative micrographs showing the degree of neuroinflammation in the corpus callosum at 3 days following diffuse TBI.....	73
Figure 4.5: Motor outcome illustrating the effect of treatment with 0.05mg/kg and 0.5mg/kg APP96 110 IV at 5 hours post TBI .....	75
Figure 4.6: Representative micrographs showing the degree of axonal injury in the corpus callosum at 3 days following diffuse TBI .....	76
Figure 5.1: The structural configuration of APP96 110, inclusive of the $\beta$ hairpin loop constrained by a disulphide bond between cysteines 98 and 105.....	89
Figure 5.2: Heparin affinity chromatography showing the heparin binding affinity of WT APP96 110, 2+APP96 110 and 3+APP96 110 .....	90

Figure 5.3: Motor outcome illustrating the effect of treatment with doses of WT APP96 110 and 3+APP96 110 IV at 5 hours post TBI.....	92
Figure 5.4: Representative micrographs showing the degree of DAI in the corpus callosum at 3 days following diffuse TBI.....	95
Figure 6.1: Motor outcome illustrating the effect of treatment with IV 0.25mg/kg of WTAPP906 110 and 3APP96 110 at 5 hour post TBI over a 30 day period .....	108
Figure 6.2: Non significant functional outcome results from the Open Field, the Elevated Plus Maze and the Y Maze .....	111
Figure 6.3: Performance in the Barnes Maze .....	113
Figure 6.4: Time spent immobile throughout the Forced Swim Test.....	114
Figure 6.5: Representative micrographs demonstrating the percentage of activated microglia in the corpus callosum following TBI .....	116
Figure 6.6: Representative micrographs demonstrating the number of reactive astrocytes in the corpus callosum following TBI.....	118
Figure 6.7: Analysis of PSD 95 relative density within the cortex and hippocampus at 30 days following TBI.....	120
Figure 6.8: Analysis of synaptophysin relative density within the cortex and hippocampus at 30 days following TBI.....	121
Figure 6.9: Analysis of NF L relative density within the cortex and hippocampus at 30 days following TBI.....	122
Figure 6.10: Analysis of MBP relative density within the cortex and hippocampus at 30 days following TBI.....	123
Figure 6.11: Analysis of Tau 5 relative density within the cortex and hippocampus at 30 days following TBI.....	124

## Table of Tables

Table 2.1: The amino acid sequences of APP peptides used.....	26
Table 2.2: Schedule of the functional mazes and tests .....	29
Table 2.3: IHC antibodies analysed and their functions .....	37
Table 2.4: Western blot antibodies analysed and their functions .....	41
Table 3.1: Outcome of re characterisation of optimal weights of SDs pre injury to ensure consistency .....	49

# Declaration

I certify that this work contains no material which has been accepted for the award of any other degree or diploma in my name, in any university or other tertiary institution and, to the best of my knowledge and belief, contains no material previously published or written by another person, except where due reference has been made in the text. In addition, I certify that no part of this work will, in the future, be used in a submission in my name, for any other degree or diploma in any university or other tertiary institution without the prior approval of the University of Adelaide and where applicable, any partner institution responsible for the joint award of this degree.

I give consent to this copy of my thesis when deposited in the University Library, being made available for loan and photocopying, subject to the provisions of the Copyright Act 1968. I acknowledge that copyright of published works contained within this thesis resides with the copyright holder(s) of those works.

I also give permission for the digital version of my thesis to be made available on the web, via the University's digital research repository, the Library Search and also through web search engines, unless permission has been granted by the University to restrict access for a period of time. I acknowledge the support I have received for my research through the provision of an Australian Government Research Training Program Scholarship.

Stephanie Plummer

Date: 18<sup>th</sup> December, 2017



# Publications and Presentations

## Publications

### i. Reviews

**Plummer S**, Van Den Heuvel C, Thornton E, Corrigan F and Cappai R. (2016). The neuroprotective properties of the amyloid precursor protein following traumatic brain injury. *Online Journal of Aging and Disease*, Vol. 7 (2). 163 179

### ii. Original Research Papers

\* **Plummer SL**, Thornton E, Corrigan F, Woenig JA, Vink R, Cappai R and Van Den Heuvel C. (2018). The amyloid precursor protein derivative, APP96 110, is efficacious following intravenous administration after traumatic brain injury. *PLoS ONE*, Vol 13 (1).

## Abstracts

**Plummer SL**, Thornton E, Corrigan F, Vink R, Cappai R and Van Den Heuvel C. (2017). Evaluating the amyloid precursor protein derivative, APP96 110, as a novel therapeutic agent following traumatic brain injury. *Journal of Cerebral Blood Flow and Metabolism*. 37 (IS) BS12  
4. *Abstract*

**Plummer S**, Thornton E, Corrigan F, Vink R, Cappai R and Van Den Heuvel C. (2015). Investigation of the amyloid precursor protein derivative APP96 110 as a novel therapeutic agent following traumatic brain injury, *Journal of Neurochemistry*. 134. MTU05 26. *Abstract*

Inampudi C, Jana M, Ciccotosto G, **Plummer S**, Roberts B, Van Den Heuvel C and Cappai R. (2015). Identification of proteins interacting with amyloid precursor protein for neurotoxicity and neuroprotection. *Journal of Neurochemistry*. 134. MTU11 16. *Abstract*

**Plummer S**, Corrigan F, Thornton E, Vink R, Cappai R and Van Den Heuvel C. (2014). Evaluating APP96 110, a peptide derived from the Amyloid Precursor Protein, as a novel therapeutic agent against traumatic brain injury. *Journal of Neurotrauma: Abstract*

## **Presentations**

**Plummer SL**, Thornton E, Corrigan F, Cappai R and Van Den Heuvel C, **8<sup>th</sup> National Neurotrauma Symposium**, Oral Presentation, December 2017, Hobart, Australia

**Plummer SL**, Thornton E, Corrigan F, Vink R, Cappai R and Van Den Heuvel C, **28<sup>th</sup> Symposium on Cerebral Blood Flow, Metabolism and Function/13<sup>th</sup> Conference on Quantification of Brain Function with PET**, Oral Presentation, April 2017, Berlin, Germany

**Plummer SL**, Thornton E, Corrigan F, Cappai R and Van Den Heuvel C, **36<sup>th</sup> Meeting of the Australasian Neuroscience Society**, Poster Presentation, December 2016, Hobart, Australia

**Plummer SL**, Thornton E, Corrigan F, Cappai R and Van Den Heuvel C, **ANZSNP Neuropathology In Research Annual Scientific Meeting**, Oral Presentation, December 2016, Hobart, Australia

**Plummer SL**, Thornton E, Corrigan F, Cappai R and Van Den Heuvel C, **7<sup>th</sup> National Neurotrauma Symposium**, Poster Presentation, December 2016, Hobart, Australia

**Plummer SL**, Thornton E, Corrigan F, Cappai R and Van Den Heuvel C, **Florey Postgraduate Research Conference**, Poster Presentation, September 2016, Adelaide, Australia

**Plummer SL**, Thornton E, Corrigan F, Cappai R and Van Den Heuvel C, **Australian Society for Medical Research SA Annual Scientific Meeting**, Oral Presentation, June 2016 Adelaide, Australia

**Plummer SL**, Thornton E, Corrigan F, Cappai R and Van Den Heuvel C, **12<sup>th</sup> International Neurotrauma Symposium**, Poster Presentation *in absentia*, February 2016, Cape Town, South Africa

**Plummer SL**, Thornton E, Corrigan F, Cappai R and Van Den Heuvel C, **6<sup>th</sup> National Neurotrauma Symposium**, Oral Presentation, October 2015, Adelaide, Australia

**Plummer SL**, Thornton E, Corrigan F, Cappai R and Van Den Heuvel C, **Florey Postgraduate Research Conference**, Poster Presentation, September 2015, Adelaide, Australia

**Plummer SL**, Thornton E, Corrigan F, Vink R, Cappai R and Van Den Heuvel C, **25<sup>th</sup> ISN-APSN Biennial Meeting In Conjunction with ANS**, Poster Presentation, August 2015, Cairns, Australia

**Plummer SL**, Thornton E, Corrigan F, Vink R, Cappai R and Van Den Heuvel C, **Australian Society for Medical Research SA Annual Scientific Meeting**, Oral Presentation, June 2015, Adelaide, Australia

**Plummer SL**, Thornton E, Corrigan F, Vink R, Cappai R and Van Den Heuvel C, **5<sup>th</sup> National Neurotrauma Symposium**, Poster Presentation, October 2014, Adelaide, Australia

**Plummer SL**, Thornton E, Corrigan F, Vink R, Cappai R and Van Den Heuvel C, **Florey International Postgraduate Research Conference**, Poster Presentation, September 2014, Adelaide, Australia

**Plummer SL**, Thornton E, Corrigan F, Vink R, Cappai R and Van Den Heuvel C, **Australian Society for Medical Research SA Annual Scientific Meeting**, Oral Presentation, June 2014, Adelaide, Australia

**Plummer SL**, Thornton E, Corrigan F, Vink R, Cappai R and Van Den Heuvel C, **11<sup>th</sup> International Neurotrauma Symposium**, Oral Presentation, March 2014, Budapest, Hungary

**Plummer SL, Thornton E, Corrigan F, Vink R, Cappai R and Van Den Heuvel C, 34<sup>th</sup> Annual Meeting of the Australian Neuroscience Society, Poster Presentation, January 2014, Adelaide, Australia**

## **Invited Speaker**

**Neurosurgical Research Foundation Annual General Meeting, September 2017, Adelaide, Australia**

**36<sup>th</sup> Meeting of the Australasian Neuroscience Society, Invited co chair: Injury and Repair II Symposium, December 2016, Hobart Australia**

**Neurosurgical Research Foundation Annual General Meeting, August 2014, Adelaide, Australia**

## **Awards**

ISCBFM Early Career Researcher Travel Bursary for attendance at ISCBFM conference in April 2017, Berlin, Germany

University of Adelaide – School of Medicine Travel Award for attendance at NNT/ANZSNP/ANS conferences in December 2016, Hobart, Australia

Finalist in ‘Fresh Science’. 1 of 10 scientists selected in South Australia to participate in science communication and media training, June 2016

University of Adelaide – School Medical Sciences Travel Award for attendance at ISN/APSN/ANS conferences in August 2015, Cairns, Australia

Adelaide Research and Innovation (ARI) prize for the project with the most commercial potential, September 2014

# Personal Acknowledgements

The journey of this PhD has been a rollercoaster of emotions to say the least. But it would not have been possible without support from the following people.

First and foremost, I would like to thank my supervisors – A/Prof Corinna Van Den Heuvel, Dr Emma Thornton, Dr Frances Corrigan and Professor Roberto Cappai – all of whom have been instrumental for me during this journey.

Corinna, thank you for providing me with the opportunity to undertake this PhD (and honours) work under your supervision. I've loved being part of the APP group and continuing the research on the APP bandwagon. You have never faulted in your support, patience and encouragement of me, and have continuously gone out of your way to help me in any way you can. Your mentorship and friendship are incredibly important to me, and I look forward to working with you in a different manner next year.

Emma, you have been fantastic to have as a co supervisor throughout this PhD. Your knowledge of the APP story over the years has been instrumental, and your happiness and friendship has made this journey all the more bearable. Now that it looks like we might be semi neighbours, I hope we can continue our friendship in the years to come.

Frances, thank you for all your support and encouragement over the years. You have spent a considerable amount of time troubleshooting with me over the years, but the end result is finally something to be pleased with. Thank you for facilitating my dog fix and allowing me to take Harvey for walks, and for your continued friendship.

Roberto, you have been exceptionally fun at the many conference social events over the years, and your knowledge and support in this project have been instrumental. Despite the distance, you have always provided ideas, feedback and encouragement for the work, and you've been fantastic to have as a supervisor.

To my parents, Karin & Jim, thank you both for years of love, encouragement and support. You've both always enforced to me that I can achieve anything I want if I put my mind to it. My apologies for the (predominately adult) tears and tantrums, and my belief that despite your years of wisdom, I know better. Frankly, I don't. And I will always go to you both for advice and love.

To Jonny, my boyfriend and long time friend. You've experienced many of the highs, and more recently the lows, of this PhD with me, and despite the glazing over of your eyes when I explain my work to you, you've never faulted in your support and encouragement. Thank you for your patience, support and, importantly, your love.

To Emily, our somewhat unexpected and quite delayed friendship has become my most treasured. But as they say, better late than never! Thank you for your continuous love and support for me, and for wholeheartedly believing in me in when I clearly didn't in myself.

To past and present members of Team Neuro, particularly Renée, Anna, Josh, Lyndsey and Viyth, you have all been incredibly encouraging and supportive.

To Jaimee at the University of Adelaide animal house facility, thank you for your help in caring for my many animals over the years, and particularly for your help in troubleshooting and establishing the ARC breeding colony.

To Ginta & The Neurosurgical Research Foundation (NRF), thank you for your support of my research over the last few years, from promotion through facebook posts, to presentations at AGMs. It has been great to be a part of the NRF for so long and I hope to continue over the next few years.

And finally, I'd like to acknowledge and thank the hundreds of little rats that have been a part of this research, and have sacrificed their lives for the benefit of human scientific advancement. Without them, the progression of this work would not have been possible, and my absolute love for rats would not have developed. I hope heaven provides you with a

fountain of endless peanut butter and seeds. I have loved each and every one of you little munchkins.

## **Financial Support**

This research was funded by a project grant from the National Health & Medical Research Council (NHMRC), The Brain Foundation, and the Neurosurgical Research Foundation (NRF).

The facilitation of this work was made possible through funding by the Australian Government Research Training Program Scholarship (formally Australian Postgraduate Award).

# Abbreviations

A $\beta$  Amyloid beta  
AD – Alzheimer’s disease  
ADAM – A disintegrin and metalloprotease  
AI – Axonal injury  
ANOVA – Analysis of variance  
APLP – Amyloid precursor like protein  
APP – Amyloid precursor protein  
BBB – Blood brain barrier  
CNS – Central nervous system  
DAI – Diffuse axonal injury  
GFAP – Glial fibrillary acidic protein  
HSPGs – Heparin sulphate proteoglycans  
Iba1 – Ionized calcium binding adaptor molecule 1  
ICV – Intracerebroventricular  
IHC – Immunohistochemistry  
IL Interleukin  
IV – Intravenous  
LTP – Long term potentiation  
MANOVA – Multivariate analysis of variance  
MB – Myelin basic protein  
NFL – Neurofilament light  
NMDA – N methyl d aspartate  
PBS – Phosphate buffered saline  
PSD 95 – Post synaptic density protein 95  
RPM – Revolutions per minute  
RCF – Relative centrifugal force  
sAPP $\alpha$  Soluble amyloid precursor protein alpha  
sAPP $\beta$  Soluble amyloid precursor protein beta  
SDs – Sprague Dawley(s) (rats)  
SEM – Standard error of the mean



TBI – Traumatic brain injury

TBST – Tris buffered saline with tween

TNF $\alpha$  Tumour necrosis actor alpha

WB – Western Blot

# Abstract

Despite the significant health and economic burden that traumatic brain injury (TBI) places on society, the development of successful therapeutic agents to reduce its burden has not been successful. The Amyloid Precursor Protein (APP) is an ideal therapeutic candidate, as its acute upregulation following TBI has been shown to serve a number of neuroprotective roles following TBI. Recently, the APP derivative APP96 110, a 15 amino acid length peptide derivative, has continued to display these neuroprotective and neurotrophic functions. While the mechanisms for this remain unclear, it is hypothesized that these neuroprotective properties are linked to its ability to bind to heparin, and that these regions are responsible for the protection against neuronal injury and the improvement in neurological outcome following TBI. In order to further develop APP96 110 as a novel and clinically relevant therapeutic agent following TBI, it was essential to determine the optimal dose, route of and timepoint for administration, as well as examining ways in which the neuroprotective response of this peptide could be further enhanced.

In order to investigate these, a dose response study was carried out in male Sprague Dawley rats that was the first to assess the efficacy of intravenous (IV) APP96 110 acutely at 30 minutes post TBI, followed by the more clinically relevant 5 hour timepoint. IV administration of APP96 110 was shown to be neuroprotective for up to 5 hours post TBI, with animals demonstrating improvements in motor outcome and reductions in axonal injury (AI) and neuroinflammation when treated with the highest dose. Studies also assessed the ability to generate APP analogues with alterations to the amino acid sequence, to enhance the heparin binding affinity of the peptide, and examine whether this translated to increased

neuroprotection following TBI. Mutation of the APP96 110 peptide to enhance its heparin binding affinity resulted in a peptide with a stronger affinity for heparin (3+APP96 110), and *in vivo*, resulted in smaller doses conferring equal neuroprotective action to higher doses of wildtype (WT) APP96 110 post TBI. In addition, the long term efficacy of these APP96 110 derivatives was examined, with emphasis placed on assessing long term functional outcome, and beginning to elucidate the long term neuroinflammatory and neurodegenerative changes. Assessment of the long term efficacy demonstrated that, whilst WT and 3+APP96 110 produced similar protection for neuroinflammation, axonal structure, myelination, synaptogenesis and neurodegeneration, treatment with 3+APP96 110 significantly outperformed WT APP96 110 in its ability to improve functional outcome.

Together, results demonstrate that the neuroprotective benefits of APP96 110 may relate to its heparin binding ability, with this binding playing a crucial role in the mechanisms through which APP96 110 can exert their neuroprotective actions post TBI. Overall, APP96 110 shows promise as a novel and clinically relevant treatment option, that could overcome many of the challenges that have stalled development of efficacious treatments, by offering substantial neuroprotective and neurotrophic effects that reduce secondary injury and functional deficits associated with acute TBI.

# **Chapter 1: The Neuroprotective Properties Of The Amyloid Precursor Protein Following Traumatic Brain Injury**

# Statement of Authorship

Title of Paper	The Neuroprotective Properties of the Amyloid Precursor Protein Following Traumatic Brain Injury
Publication Status	<input checked="" type="checkbox"/> Published <input type="checkbox"/> Accepted for Publication <input type="checkbox"/> Submitted for Publication <input type="checkbox"/> Unpublished and Unsubmitted work written in manuscript style
Publication Details	Plummer S, Van Den Heuvel C, Thornton E, Corrigan F and Cappai R. (2016). The neuroprotective properties of the amyloid precursor protein following traumatic brain injury. <i>Online Journal of Aging and Disease</i> , Vol. 7 (2). 163-179

## Principal Author

Name of Principal Author (Candidate)	Stephanie Plummer		
Contribution to the Paper	Conceptualisation of the story, and contributed to the writing of the manuscript.		
Overall percentage (%)	75%		
Certification:	This paper reports on original research I conducted during the period of my Higher Degree by Research candidature and is not subject to any obligations or contractual agreements with a third party that would constrain its inclusion in this thesis. I am the primary author of this paper.		
Signature		Date	19/11/17

## Co-Author Contributions

By signing the Statement of Authorship, each author certifies that:

- i. the candidate's stated contribution to the publication is accurate (as detailed above);
- ii. permission is granted for the candidate to include the publication in the thesis; and
- iii. the sum of all co-author contributions is equal to 100% less the candidate's stated contribution.

Name of Co-Author	A/Prof Corinna Van Den Heuvel		
Contribution to the Paper	Conceptualisation of the story, and contributed to the writing of the manuscript.		
Signature		Date	30/11/17

Name of Co-Author	Dr Emma Thornton		
Contribution to the Paper	Conceptualisation of the story, and contributed to the writing of the manuscript.		
Signature		Date	26/11/17

Name of Co-Author	Dr Frances Corrigan		
Contribution to the Paper	Conceptualisation of the story, and contributed to the writing of the manuscript.		
Signature		Date	1/12/17.

Name of Co-Author	Professor Roberto Cappai		
Contribution to the Paper	Conceptualisation of the story, contributed to the writing of the manuscript, and lead the manuscript submission process.		
Signature		Date	3-Dec-2017

## Review Article

# The Neuroprotective Properties of the Amyloid Precursor Protein Following Traumatic Brain Injury

Stephanie Plummer<sup>1</sup>, Corinna Van den Heuvel<sup>1</sup>, Emma Thornton<sup>1</sup>, Frances Corrigan<sup>1</sup>, Roberto Cappai<sup>2,\*</sup>

<sup>1</sup>Adelaide Centre for Neuroscience Research, the University of Adelaide, South Australia, Australia

<sup>2</sup>Department of Pathology, the University of Melbourne, Victoria, Australia

[Received August 2, 2015; Revised September 1, 2015; Accepted September 7, 2015]

**ABSTRACT:** Despite the significant health and economic burden that traumatic brain injury (TBI) places on society, the development of successful therapeutic agents have to date not translated into efficacious therapies in human clinical trials. Injury to the brain is ongoing after TBI, through a complex cascade of primary and secondary injury events, providing a valuable window of opportunity to help limit and prevent some of the severe consequences with a timely treatment. Of note, it has been suggested that novel treatments for TBI should be multifactorial in nature, mimicking the body's own endogenous repair response. Whilst research has historically focused on the role of the amyloid precursor protein (APP) in the pathogenesis of Alzheimer's disease, recent advances in trauma research have demonstrated that APP offers considerable neuroprotective properties following TBI, suggesting that APP is an ideal therapeutic candidate. Its acute upregulation following TBI has been shown to serve a beneficial role following trauma and has led to significant advances in understanding the neuroprotective and neurotrophic functions of APP and its metabolites. Research has focused predominantly on the APP derivative sAPP $\alpha$ , which has consistently demonstrated neuroprotective and neurotrophic functions both *in vitro* and *in vivo* following various traumatic insults. Its neuroprotective activity has been narrowed down to a 15 amino acid sequence, and this region is linked to both heparan binding and growth-factor-like properties. It has been proposed that APP binds to heparan sulfate proteoglycans to exert its neuroprotective action. APP presents us with a novel therapeutic compound that could overcome many of the challenges that have stalled development of efficacious TBI treatments previously.

**Key words:** Amyloid precursor protein, traumatic brain injury, diffuse axonal injury, neuroprotection, heparan sulphate proteoglycans

## Introduction

Traumatic brain injury (TBI) is a major public health concern, and the World Health Organisation anticipates that TBI could become the leading cause of death and disability by 2020 [1]. Despite the clear significant burden that TBI places on society, to date there are no accepted pharmacological interventions to treat TBI. Current treatment methods including osmotic agents like mannitol and hypertonic saline, or surgical interventions like decompressive craniectomy that focus primarily on stabilising the patient and managing the complications

that may arise. However, these agents do not treat the underlying cause of the complications like cerebral oedema, nor are they applicable in many instances of TBI where oedema does not occur [2]. The amyloid precursor protein (APP) has a long association with TBI as its expression is dramatically upregulated in the brain following injury [3-6]. Although APP is best known and studied for its role as the source of the Amyloid- $\beta$  (A $\beta$ ) peptide in the pathogenesis of Alzheimer's disease, recent studies suggest that this upregulation of APP represents a neuroprotective response as a lack of APP impairs motor and cognitive outcomes, and enhances neuronal cell death

\*Correspondence should be addressed to: Roberto Cappai, Department of Pathology, the University of Melbourne, Victoria, Victoria, 3010 Australia. Email: [r.cappai@unimelb.edu.au](mailto:r.cappai@unimelb.edu.au)

Copyright: © 2016 Plummer S, et al. This is an open-access article distributed under the terms of the Creative Commons Attribution License, which permits unrestricted use, distribution, and reproduction in any medium, provided the original author and source are credited.

[7]. This makes APP a promising candidate upon which to develop a therapeutic treatment for TBI subjects. As such, this review will summarise the more salient aspects of the neuroprotective properties of APP, and highlight how these are beneficial in the setting of TBI.

### Traumatic Brain Injury

TBI is a debilitating and life-threatening injury to the brain, estimated to occur in approximately 54-60 million people worldwide each year [8]. In industrialised countries, TBI causes more deaths in people under the age of 45 than any other cause [9], with the majority of cases occurring in young adults, predominantly as a result of motor vehicle accidents, followed closely by falls and assaults [10]. The consequences of TBI can be severe. Survivors are often left with lasting neurological and cognitive impairments, placing an enormous emotional, health and economic burden on society. Depression, anxiety, changes in behaviour and personality and psychiatric disorders are among the many lasting effects following TBI.

Following TBI, extensive neuronal damage is ongoing through a complex cascade of deleterious physiological events that occur in the ensuing minutes to days to weeks. Many of these deleterious events could be reversed if targeted with an appropriate therapy, preventing serious complications and reducing the burden on society.

### Pathophysiology of TBI

TBI is a complex injury that encompasses changes to both molecular and gross anatomical brain structure. Injury can occur through either impaction of the head against an object, or commonly, through acceleration/deceleration forces [11, 12]. Whilst linear acceleration movements will cause damage such as contusions and haemorrhage to superficial grey matter, rotational acceleration movements are not well tolerated by the brain, and will result in injury of greater severity [12-14]. Injury, measured on a continuum of mild, moderate and severe, will cause extensive neuronal death through a cascade of deleterious physiological events that follow the initial impact. As a result, cell death is caused by both primary and secondary injury mechanisms.

#### Primary Injury

Occurring at the moment of insult, primary injury is the result of mechanical forces causing deformation of blood vessels, axons, glia and neurons [11, 14, 15], through axonal stretching, lacerations, tears,

contusions and haemorrhage. Injuries are classified as either focal or diffuse, with focal injuries a result of collision forces that cause localised injuries including skull fracture and contusion. In contrast, diffuse injuries are typically the result of rapid acceleration/deceleration forces, resulting in diffuse axonal injury (DAI) [11-14]. However, both focal and diffuse injuries are often seen simultaneously [12, 16]. Unfortunately, primary injury is irreversible, and efforts should therefore focus on injury prevention, via airbags in cars and helmets for cyclists [9, 17]. In contrast, secondary injury is potentially reversible.

#### Secondary Injury

Secondary injury involves a delayed and deleterious cascade of biochemical and physiological events that occur as a result of the primary injury [11, 14, 17]. Occurring in the minutes to days to weeks following the initial insult, it encompasses a range of harmful, often synergistic, effects that compound the existing injury, including glutamate excitotoxicity, oxidative stress, irreversible cell injury and death, inflammation, blood-brain-barrier (BBB) disruption, mitochondrial dysfunction and changes in ionic homeostasis [2, 9, 11, 14].

One of the most significant consequences of secondary injury following TBI is cell death, which can occur via controlled programmed cell death (PCD) through apoptosis, or unregulated death through necrosis. It has been proposed that cell death mechanisms may actually represent a continuum between apoptotic and necrotic pathways [18]. It is well established that free radicals, increases in intracellular calcium and excitatory amino acids are all implicated in the development of apoptosis. However, it is now also believed that a shift in the balance between pro-apoptotic factors like Bcl-2, Bcl-x and extracellular signal-regulated kinases, and anti-apoptotic factors, such as Bax, c-Jun N-terminal kinase, tumor-suppressor gene, p53 and calpain and caspase proteases, also play a role in influencing cell death following trauma [18].

Many of these serious secondary injury events have the potential to be reversed [9], but without treatment will often compound leading to further consequences such as ischaemia, brain dysfunction, cerebral oedema and often death [17]. Fortunately, the delayed onset and potentially reversible nature of these secondary events provides a novel window of opportunity for a therapy to reduce neuronal damage and help limit/prevent the associated morbidity and mortality [9]. It has been suggested that therapeutic interventions should be multifactorial in nature,



targeting multiple elements of the secondary injury cascade [9, 19, 20]. One proposed approach is to emulate the body's endogenous repair response.

### **Diffuse Axonal Injury**

One of the most common and significant features of TBI is DAI, which currently lacks an efficacious treatment. DAI is defined as the occurrence of diffuse damage to axons in the cerebral hemispheres, in the corpus callosum, in the brain stem and sometimes in the cerebellum resulting from a head injury [21]. DAI occurs as result of rapid acceleration/deceleration forces, causing deformation of brain tissue through shearing forces and stretching. Regions of varying densities stretch over each other, giving rise to widespread damage throughout the cerebral hemispheres, corpus callosum, and brain stem [16, 21]. Estimates suggest that DAI occurs in more than 80% of all motor vehicle induced TBI cases, and is consistently associated with worse outcome post-injury [2, 15, 16, 22]. Indeed, it has been reported that 58% of patients who had sustained a TBI and died within subsequent months demonstrated DAI [22]. Due to its nature, DAI is typically only detectable microscopically in post-mortem tissue, unless severe injury results in macroscopic white matter tears [16, 21]. As a result, diagnosing DAI in patients with conventional imaging techniques is difficult, and thus, the incidence of DAI may be under-diagnosed in TBI cases [16].

DAI was initially thought to be exclusively a primary injury event, a result of primary axotomy upon impact. However, recent studies have led to the understanding that DAI is in fact a progressive insult that leads to and prolongs neurological damage [15, 23, 24]. Axons are typically not completely torn upon the primary impact, but rather stretched, causing a localised intra-axonal change to the cytoskeleton. It is not until the secondary injury cascade commences that existing cytoskeletal damage causes disruption to the anterograde axoplasmic transport leading to axonal swelling with subsequent axonal disconnection [23, 25]. Furthermore, this cytoskeletal damage can disrupt sodium channel action, resulting in an influx of sodium and subsequent damage to voltage-gated calcium channels, causing a deleterious calcium influx. This in turn instigates the production of phospholipases and proteases, like calpains, damaging mitochondria and resulting in complete axonal separation and subsequent cell death [16, 25]. Undoubtedly, the consequences of DAI are often serious, as it is the most common cause of vegetative state and coma following TBI [16, 21, 26]. Many

remain comatose, while survivors often have a poor quality of life due to considerable disability and impairment.

It is important to note that APP is frequently used as a highly sensitive marker of axonal injury [3, 4]. APP is typically transported via fast axonal transport in an anterograde direction, although a fraction of APP can travel retrogradely [27, 28]. Damage and stretching of axons through injury results in localised intra-axonal changes to the axolemma, disrupting fast axonal transport and facilitating accumulation of APP, which can be observed as early as 30 minutes following trauma [11]. Consequently, APP accumulations or swellings can be observed at the site of damage, and are easily detectable via immunohistochemistry [3, 4]. Whilst in this context APP can be used as a marker for injury, this is not its primary role in TBI.

### **The Amyloid Precursor Protein**

APP is best known and studied for its role as the source of the Amyloid- $\beta$  (A $\beta$ ) peptide. The deposition of A $\beta$  plaques is believed to play an important role in the pathogenesis of Alzheimer's disease (AD), and accordingly, a vast amount of literature exists about the pathological roles of APP and its proteolytic products. However, the normal biological functions and actions of APP are yet to be clearly defined and understood.

APP is a constitutively expressed, highly conserved type-1 transmembrane glycoprotein. APP isoforms can be found in a number of places throughout the body including the spleen, thymus, kidney, lungs, liver, brain, heart, and platelets (reviewed in [29]), suggesting diverse physiological roles. Whilst APP is expressed in all cells that undergo cell-to-cell interactions, its expression is highest in neuronal cells and glia, particularly within the central nervous system (CNS). Here, APP serves a synaptic function [30], and is increasingly expressed in brain regions that undergo greater levels of synaptic modification, with expression of APP mRNA far greater in the foetal and developing brain than in the adult brain [31]. In neurons, APP is localised not only to somatodendritic and axonal compartments [27], but also to the presynaptic active zone [32].

### **APP Isoforms & Structure**

As a single membrane-spanning protein of typically between 695 to 770 amino acids in length, APP comprises of a long extracellular N-terminal domain or ectodomain, a transmembrane region and a short

intracellular C-terminal domain [33] (see Figure 1). The gene for APP is located on chromosome 21, and consists of 19 exons. Exons 7, 8 and 15 can be alternatively spliced to produce APP isoforms of which APP695, APP751 and APP770, defined by the number of amino acids they contain, are the most commonly studied [34]. Exon 7 codes for a Kunitz-type protease inhibitor (KPI) domain, found in only the APP751 and APP770 isoforms. In contrast, APP695 lacks the KPI domain [30, 34]. In addition, APP770 contains an OX-2 related domain [34]. Alternate splicing involving exon 15 typically occurs in leukocytes, and in the central nervous system in activated microglia and astrocytes, forming the leukocyte derived L-APP. Here, exon 15 is missing and exons 14 and 16 subsequently fuse together [30]. Whilst APP695 is found almost exclusively in neurons, APP751 and APP770 are found more extensively throughout other organs. However, they are expressed within glial cells, although at a considerably lower concentration than APP695 [35,

36].

Structurally, the APP extracellular domain comprises of up to six different sub-domains, depending on its isoform. These include the growth-factor like domain (D1), the copper binding domain (D2), an acidic domain (D3), a KPI and OX-2 domain (for isoforms APP751 and APP770 only) and a carbohydrate domain (D6) [37]. The combination of the D1 and D2 domains can also be referred to as the E1 domain. The D6 carbohydrate domain can be further divided into an E2 domain (D6a) and a juxtamembrane domain (D6b). APP has been shown to bind a variety of ligands, including metals, such as copper, iron and zinc, to cell surface and secreted molecules, as well as to heparan [38, 39]. Of particular interest is the heparan binding domain of the growth-factor like domain, which as discussed later, may mediate the neuroprotective activity of APP in TBI.

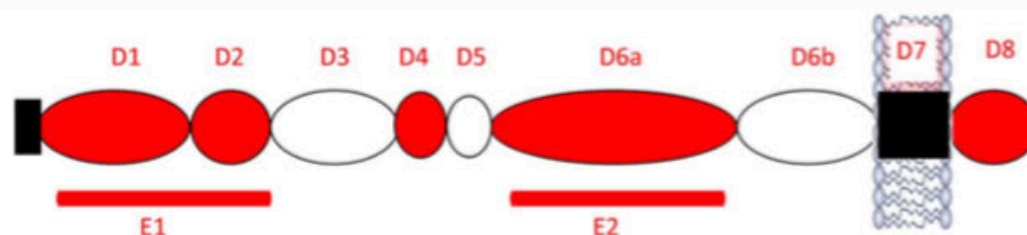


**Figure 1. Representation of the structure of APP, highlighting its extracellular, transmembrane and intracellular domains.**

### APP Synthesis & Transport

APP is synthesised and translated in the endoplasmic reticulum, prior to travelling to the Golgi complex [32, 40]. Here, APP matures through the constitutive secretory pathway, and undergoes a variety of post-translational modifications including tyrosine sulphation, O- and N-linked glycosylation and phosphorylation [32, 41, 42]. APP is concentrated in the Golgi complex, and from here, travels through the central vacuolar system *en route* to the plasma membrane [27, 41]. Once attached, it must be cleaved via  $\alpha$ -,  $\beta$ - and  $\gamma$ -secretase enzymes to produce APP fragments before these fragments can be released.

Alternatively, APP may be internalized at the plasma membrane via clathrin- and dynamin-dependent pathways, and is either recycled back to the plasma membrane to follow the secretory pathway, or targeted towards the endosomal/lysosomal pathway [27, 43]. Only a fraction of synthesised APP will reach the cell surface for secretion, with only a small percentage of this APP actually being released [43, 44].

Transport of APP within neurons in the central nervous system varies slightly to that of other systems. APP is axonally sorted to vesicular compartments, and using kinesin and microtubules for transport, travels via fast axonal transport to the

presynapse [27, 28, 32]. Here, it is incorporated into the presynaptic membrane, specifically into the presynaptic active zone, and to a lesser extent to free synaptic vesicles, suggesting a role in the physiology of neurotransmitter release [32].

**APP Proteolytic Processing**

Once mature, APP is able to undergo proteolytic cleavage on, or in close proximity, to the cell surface

to produce smaller APP-derived metabolites [40]. Through cleavage, the integral transmembrane and C-terminal domains remain adhered to the cell membrane, with the extracellular domain released through a process referred to as ectodomain shedding [45, 46]. This cleavage process follows one of two major pathways, termed either the amyloidogenic or non-amyloidogenic pathway (see Figure 2).

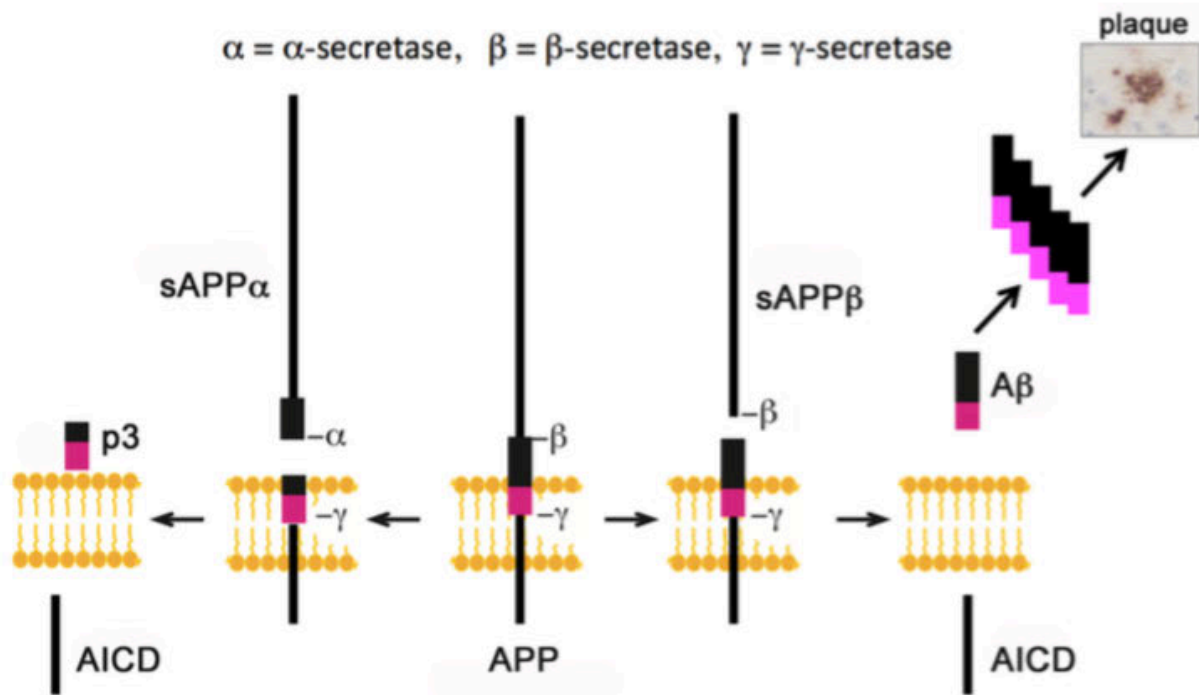


Figure 2. Representation summarising the major pathways of APP proteolytic processing via the α-, β- and γ-secretase enzymes.

**Amyloidogenic processing**

Cleavage via the amyloidogenic pathway is a complex process involving cleavage of APP by the enzyme β-secretase BACE1 (Beta-site APP Cleaving Enzyme 1) to release the APP-β (sAPPβ) ectodomain and the 99 amino acid C-terminal membrane bound fragment C99. Further cleavage of C99 by the γ-secretase enzyme complex, that includes presenilin, results in the production of the neurotoxic amyloid-β (Aβ) peptide and the APP intracellular domain (AICD) (reviewed in [45]).

**Non-amyloidogenic processing**

APP is preferentially cleaved via the non-amyloidogenic pathway, which occurs within the secretory pathway in the trans Golgi network and the cell surface [40]. Cleavage via α-secretase enzyme cleaves APP between amino acids 612 and 613 [44] producing the neuroprotective soluble APP-α (sAPPα) fragment and an 83 amino acid C-terminal fragment C83. Further cleavage via γ-secretase cleaves C83, producing the remaining AICD [45]. Importantly, cleavage via α-secretase cleaves APP in the middle of the region coding for Aβ, precluding Aβ formation [44, 47-49]. The majority of APP cleavage

is via  $\alpha$ -secretase, and not  $\beta$ - and  $\gamma$ -secretases as previously thought [43, 47, 48].

The enzymes responsible for endogenous  $\alpha$ -secretase cleavage belong to the family of a disintegrin and metalloprotease (ADAM) enzymes. Specifically, the ADAM subtypes ADAM9, ADAM10 and ADAM17 have been shown to be the predominant  $\alpha$ -secretase enzymes involved in APP cleavage [45, 49-51]. However, it appears that ADAM10 is the major  $\alpha$ -secretase cleavage enzyme [45, 49], as even moderate neuronal overexpression was shown to strongly stimulate  $\alpha$ -secretase cleavage of APP, delaying plaque formation, and alleviating cognitive defects in a transgenic AD mouse model [52, 53].

### The Functions of APP

Whilst the physiological function(s) of APP are yet to be fully understood, a variety of actions have been described and range from roles in metal homeostasis [54-57], binding and metabolism of proteoglycans [58-62], neuritogenesis [63], haemostasis and thrombosis [64, 65], glucose homeostasis [66], synaptogenesis and neuroprotection [67-70] and regulation of intracellular signalling [71, 72]. Many of these functions may account for the neuroprotective actions following brain trauma.

Knockout of APP leads to a range of deficits including reductions in body weight, grip strength, locomotor activity and brain weight, as well as age-related deficits in spatial learning [73]. Furthermore, histological analysis of the brain also revealed areas of gliosis, decreased neocortical and hippocampal levels of synaptophysin, and reduced dendritic lengths of hippocampal neurons with age [73, 74]. This supports a role for APP in a variety of cellular functions such as cell adhesion, neurite outgrowth and synaptogenesis.

APP belongs to a family of proteins that contains the APP homologues APP-like proteins, APLP1 and APLP2. The functions of these proteins greatly resemble APP, and differ mainly in their inability to produce A $\beta$  plaques, the hallmark pathological feature of AD. It is believed that APLP1 and APLP2 may be able to take over the role of APP in APP knockout models [75, 76].

Particular focus has been placed on APP's role in cell adhesion as a contact receptor, binding to other cells or to components of the extracellular matrix. This function is particularly important, as adhesion is known to regulate proliferation [77]. APP and its family members have been shown to form homo- and hetero-dimerisation complexes, associated with cell-

cell adhesion promotion and subsequent *trans*-cellular adhesion *in vivo* [78].

In addition to its cell adhesion properties, APP has been proposed to play a role in neurotrophic and synaptotrophic functions such as neurogenesis, neurite outgrowth and synaptogenesis [79]. APP has been shown to promote functional synapse formation [63, 80], whilst reductions in APP expression have been associated with impaired neurite outgrowth and synaptic activity *in vivo* [81-83]. Indeed, APP's metabolite sAPP $\alpha$ , has been shown to lead to neurite outgrowth like processes in cultured fibroblasts, cortical hippocampal neurons and in human neuroblastoma cells [84-90].

APP can also play a significant role in memory and cognitive function, most likely through being involved in processes like synaptogenesis, cell adhesion and neurite outgrowth. Knockout of APP in mice demonstrated age-related cognitive deficits including impairment in conditioned avoidance and Morris Water Maze tasks, highlighting a role for APP in processes that underlie learning and memory [74, 91, 92]. Furthermore, improvements in performing cognitive tasks were seen in an animal that had been exposed to an enriched environment, and was associated with a four-fold increase in APP protein levels, as well as an overall increase in the percentage of APP containing synapses in the hippocampus [93].

### Neuroprotective Actions of APP Derivatives

Whilst the proteolytic cleavage of APP produces a number of derivatives with varying pathological and physiological roles, it is the neuroprotective properties of these derivatives that are of particular importance in the context of brain trauma.

#### sAPP $\beta$

sAPP $\beta$ , the often forgotten peptide following  $\beta$ - and  $\gamma$ -secretase cleavage, has been considerably less studied than other metabolites like A $\beta$  or sAPP $\alpha$ . sAPP $\beta$  shares the same extracellular sequence as sAPP $\alpha$ , with the exception of the final 16 amino acid sequence at the C-terminal. This sharing of the major domains results in sAPP $\beta$  and sAPP $\alpha$  having similar actions, including promotion of neurite and axonal outgrowth [94]. However, a number of differences have been observed. sAPP $\beta$  has been shown to offer almost 100 times less neuroprotective activity than sAPP $\alpha$ , particularly regarding protection from glucose deprivation and excitotoxicity [94, 95]. Furthermore, whilst sAPP $\beta$  has additionally been shown to help promote axonal elongation when added

to cultured neurons, its effect is ten times lower than sAPP $\alpha$  [27, 96]. Additionally, key differences in sAPP $\beta$  appear to lie in its lack of activity in long-term potentiation (LTP) [96], as exogenous sAPP $\beta$  was less potent at restoring LTP levels to normal in rats [97]. Little is known about the role of sAPP $\beta$  in TBI, with one study showing sAPP $\beta$  levels were unchanged in the CSF of amateur boxers following a bout [98]. Given its reduced potency and efficacy in a variety of physiological settings, it is unlikely to confer the same level of neuroprotection in TBI as sAPP $\alpha$ . But this is a gap in the field that warrants further investigation to clarify sAPP $\beta$ 's role in TBI.

### sAPP $\alpha$

The APP metabolite with the greatest neuroprotective activity is sAPP $\alpha$ . *In vitro* studies have highlighted a number of functions of sAPP $\alpha$  (Table 1). sAPP $\alpha$  is able to enhance the long-term survival of cultured cortical neurons [99] and is believed to play a key role in the protection of cultured neuroblastoma cells

against glutamate toxicity [100], as it can protect cultured neuronal cells from excitotoxic, metabolic and oxidative insults [29, 99, 101]. While these *in vitro* studies demonstrate the favourable properties of sAPP $\alpha$ , they often fail to take into account the heterogeneous nature of various ischaemic and traumatic insults, including those occurring in TBI, in both animals and humans. Accordingly, *in vivo* studies are typically more translatable to human conditions, assessing the dynamic nature of the diverse systems that interact during an injury.

*In vivo* studies have highlighted similar actions to those of *in vitro* studies (Table 2). sAPP $\alpha$  can enhance neurite outgrowth and promote cortical synaptogenesis [29, 99, 101]. Interestingly, sAPP $\alpha$  can also act synergistically with epidermal growth factor as a growth factor for neuronal progenitor cells in the subventricular zone of the lateral ventricle in adult mice [102]. This suggests a role for sAPP $\alpha$  in adult neurogenesis, as these cells retain the capacity to produce new neurons throughout adulthood.

**Table 1.** The neuroprotective and neurotrophic functions of sAPP *in vitro*

Model/Method	<i>In vitro</i> Neuroprotective & Neurotrophic Functions of sAPP	References
Cultured rat cortical neurons	Enhances long-term neuronal survival and neuronal extension	[84]
Cultured rat hippocampal and septal neurons & human cortical neurons	Protects against hypoglycaemic damage	[67]
	Reduces calcium ions; prevents calcium-mediated hypoglycaemia	
	Protects against glutamate excitotoxicity	
Application of A $\beta$ to cultured rat hippocampal neurons	Reduces A $\beta$ -induced injury	[149]
	Attenuates induction of reactive oxygen species	
	Attenuates elevated intracellular calcium levels	
	Protects against iron-induced oxidative injury	
Cultured embryonic rat hippocampal neurons	Suppresses NMDA-induced currents	[99]
Cultured mouse epidermal growth factor responsive neurospheres	Regulates progenitor proliferation in the subventricular zone of lateral ventricle	[102]
Cultured mouse and rat hippocampal neurons	Regulates function of full-length APP in neurite outgrowth	[141]

### APP Has a Neuroprotective Role In TBI

APP has a long and significant association with TBI. As previously discussed, APP is acutely upregulated in injured neurons and astrocytes following TBI. Increases in APP protein levels within neuronal cell bodies and reactive astrocytes have been observed following experimental TBI including in rats [6, 103], pigs [104] and sheep [5], with similar findings in

humans [3]. Increases in APP mRNA expression were seen as early as 30 minutes in the cerebral hemispheres, cerebellum and brainstem following diffuse TBI in sheep [5]. APP mRNA expression is regulated by many genes and proteins that are acutely increased following TBI including heat shock proteins and immediate early genes such as c-fos and c-jun [105].

**Table 2.** The neuroprotective and neurotrophic functions of sAPP *in vivo*

Model/Method	<i>In vivo</i> Neuroprotective & Neurotrophic Functions of sAPP $\alpha$	References
<b>TBI models</b>		
Impact-acceleration model of diffuse TBI in rats	Improves motor outcome and attenuates axonal injury and neuronal cell loss	[124]
Controlled cortical impact (focal) TBI in mice followed by intracerebroventricular infusion	Improves motor and cognitive outcome	[152]
Controlled cortical impact (focal) TBI in APP <sup>-/-</sup> mice followed by intracerebroventricular infusion	Significantly improves cortical and hippocampal injury Improves functional outcome, and reduces cortical and hippocampal cell damage Rescues deficits in APP <sup>-/-</sup> mice to be no longer significantly different to APP <sup>+/+</sup> mice	[131]
Weight-drop mechanical percussion model in mice	Etazolate, an $\alpha$ -secretase activator, reduces inflammation and cerebral oedema, improves memory and motor outcome and protects tissue	[132]
<b>Other injury models (non-TBI)</b>		
Four-vessel occlusion model of transient ischaemia in rat hippocampal neurons	Protects against transient cerebral ischaemic brain injury	[68]
Lateral ventricle infusion in rats	Increases synaptic density and memory retention; promotes synaptogenesis	[150]
Intracerebroventricular infusion	Enhances short- and long-term memory performance Blocks learning deficits induced by scopolamine	[151]
Lateral ventricle infusion in mice	Increases number of epidermal growth factor responsive progenitors through increasing proliferation	[102]
Bilateral intrahippocampal electrode and cannula recordings & intrahippocampal infusion	Facilitates a role in LTP induction processes in rat dentate gyrus with effect isolated to sAPP $\alpha$ domain of APP Inhibition of $\alpha$ -secretase reduces LTP whilst exogenous sAPP $\alpha$ rescues it Endogenous sAPP $\alpha$ is a key contributor to synaptic plasticity and spatial memory	[97]
Transgenic mouse model with bovine ADAM10 over-expression	$\alpha$ -secretase over-expression shows neurotrophic effect of cortical cholinergic, glutamatergic and GABAergic presynaptic bouton populations	[101]

Initially, the purpose of the acutely increased APP expression after TBI was unclear. Due to the formation of the neurotoxic A $\beta$  from APP cleavage, it had often been suggested that increased APP expression following TBI was detrimental, and would increase the risk of deposition of these A $\beta$  plaques with the subsequent development of AD [106-108], particularly in susceptible individuals with the APOE  $\epsilon$ 4 allele [109, 110]. While this may represent a long term and unintended consequence of the upregulation of APP in response to acute brain injury, this theory has not been conclusively proven, with studies producing contradictory results. Whilst epidemiological reports have suggested there is a positive association between TBI and AD [108, 109, 111], other studies have found that TBI may not be a risk factor for the later development of AD [112, 113]. Similarly while some histopathological studies of

individuals who died after suffering a single severe TBI demonstrate widespread A $\beta$  deposition irrespective of age [114-116], others have concluded that A $\beta$  deposition in victims below the age of 60 is a rare occurrence [117, 118]. Furthermore, the presence of A $\beta$  plaques after TBI appears to decrease over time, with this attributed to an increase in the levels of the A $\beta$  degrading enzyme, neprilysin [119]. This correlates with experimental studies employing transgenic mice with mutations which enable the development of AD-like pathology, which have not found that TBI accelerates A $\beta$  deposition [120-122], unless a repetitive model of injury was used [123].

In contrast, Van den Heuvel and colleagues were the first to suggest that the upregulation of APP following TBI was actually beneficial and not detrimental, as increases in APP corresponded with increased preservation of neurons [5]. This not only

identified that APP mRNA was a potential sensitive early indicator of neuronal injury, but importantly, that upregulation of APP serves as an adaptive and protective response to injury [5]. This hypothesis was supported, in part by our study by Corrigan and colleagues, reaffirming that endogenous APP serves a beneficial role following TBI [7]. Here, a lack of APP, through studying TBI in APP knockout mice (APP<sup>-/-</sup>), rendered the APP<sup>-/-</sup> mice more vulnerable to injury following a mild diffuse TBI. APP<sup>-/-</sup> mice demonstrated greater motor and cognitive deficits, increased vulnerability of neurons to injury and a defective reparative response to injury, compared to wildtype mice [7]. This was thought to be attributable to a lack of the metabolite sAPP $\alpha$ .

sAPP $\alpha$  is the metabolite that is believed to mediate the neuroprotective activity of APP, due to its previously described neuroprotective and neurotrophic actions in distinct injury models [67, 68]. Thornton and colleagues were the first to examine the neuroprotective role of exogenous sAPP $\alpha$  *in vivo* TBI [124]. sAPP $\alpha$  was administered via intracerebroventricular (ICV) infusion at 30 minutes following diffuse impact-acceleration TBI in rats, a clinically relevant model of TBI that produces DAI to mimic that seen in humans [125]. Rats treated with sAPP $\alpha$  after injury showed significant improvements in motor outcome over the seven day testing period when assessed on the rotarod when compared to vehicle control rats, and had reached baseline levels by day four post-injury [124]. Importantly, sAPP $\alpha$  was able to profoundly reduce the amount of axonal injury, and therefore injury severity, in the corpus callosum on day one following injury, reaching significance at days three and seven post-injury. This suggested that sAPP $\alpha$  may be efficacious at reducing the as-yet untreatable DAI. Furthermore, sAPP $\alpha$  administration was able to protect hippocampal neurons, significantly reducing the number of caspase-3 apoptotic cells in the hippocampus to a level that was only slightly more than non-injured [124]. Similar findings were observed following transient global ischaemia in rats, where post-traumatic ICV administration of sAPP $\alpha$  protected hippocampal neurons against ischaemic injury, as determined by the increased in neuronal survival and associated preservation of neuronal function [68].

Several mechanisms have been postulated as to how sAPP $\alpha$  exerts its neuroprotective effects. sAPP $\alpha$  can activate high conductance potassium channels, leading to hyperpolarisation of the cell and the suppression of calcium entry through voltage-

dependent channels and NMDA receptors [95, 99, 126]. This will have a protective effect as excess calcium influx, which can commonly occur following excitotoxicity, can activate a number of destructive enzymes such as proteases and DNases, which initiate cytoskeletal collapse. This may be a factor in the reduction of axonal injury mediated by sAPP $\alpha$  following TBI, as calcium induced activation of calpain pathways are capable of degrading the cytoskeletal network within the axon. Calpain-mediated degradation of the cytoskeleton has been shown to occur at sites of axonal damage and disconnection in numerous immunohistochemical studies employing antibodies directed towards its specific proteolytic breakdown products [127, 128]. Other mechanisms via which sAPP $\alpha$  may be neuroprotective include the ability to activate the transcription factor nuclear factor kappa B (NF $\kappa$ B) [129], which is important in promoting neuronal survival. This occurs by suppressing the expression of pro-apoptotic genes whilst upregulating anti-apoptotic genes [130].

Confirmation that sAPP $\alpha$  is the primary mediator of the neuroprotective activity of APP following TBI was that its administration restored deficits seen in APP<sup>-/-</sup> mice following trauma [131]. APP<sup>-/-</sup> mice demonstrated significantly poorer motor and cognitive outcomes following TBI when compared to wildtype mice, as assessed on the ledged beam and Barnes Maze, respectively. Following treatment with sAPP $\alpha$ , APP<sup>-/-</sup> mice performed no differently to wildtype mice on these assessments [131]. sAPP $\alpha$  treated APP<sup>-/-</sup> mice also demonstrated significant reductions in both cortical and hippocampal cell damage at both 24 hours and 7 days following trauma compared to untreated APP<sup>-/-</sup> mice, again resembling levels of wildtype mice in all instances [131]. These results, taken together with our earlier study in rats [124], highlight the neuroprotective effect of sAPP $\alpha$  following trauma.

Endogenous sAPP $\alpha$  levels can also be altered through pharmacological modulation of APP metabolism by using the  $\alpha$ -secretase activator, Etazolate [132]. Etazolate treatment increased production of sAPP $\alpha$ , and was able to attenuate IL-1-mediated inflammation following TBI, including microglial activation, with a resultant improvement in cerebral oedema formation. This led to lasting memory improvements and motor performance due to the protection of cerebral tissue though the increase in sAPP $\alpha$  levels [132]. However, since  $\alpha$ -secretase cleaves a number of other substrates besides APP, these effects by Etazolate cannot be unequivocally

attributed to APP.

The modulation of other APP secretases has been recently applied as a therapeutic approach for TBI. Loane and colleagues used the inhibition of  $\beta$ - and  $\gamma$ -secretases to attenuate motor and cognitive deficits and reduce cell loss in mice following TBI [133]. This could be partially attributed to increases in sAPP $\alpha$  levels, as prevention of amyloidogenic processing could lead to increases in processing via the non-amyloidogenic pathway. Nonetheless, the aforementioned studies all indicate the potential of APP and sAPP $\alpha$  as a potential therapeutic agent.

### The Neuroprotective Active Site of APP in TBI

The specific regions within sAPP $\alpha$  that are responsible for conferring its neuroprotective activity have been identified. Assessment of both motor and cognitive outcome demonstrated that the D1 and D6a but not D2 domains (Figure 1) were equally as effective as full-length sAPP $\alpha$  [134]. Furthermore, administration of the D1 and D6a domains to rats post-TBI was able to significantly reduce axonal injury in the corpus callosum similar to that seen with sAPP $\alpha$  treatment, when compared to vehicle control and D2 treated rats [134].

Given the efficacy of the D1 and D6a domains, but not D2, it was hypothesised that a common functional site may exist governing this neuroprotective activity. It was postulated that a likely common functional feature is heparan binding, which is evident within both domains [94, 135]. The D1 domain has high structural similarity to growth-factor like domains, and displays strong affinity to heparan, particularly to heparan sulfate proteoglycans (HSPGs) [136-138]. Indeed, heparanases are able to prevent sAPP $\alpha$  from protecting cultured cells against glutamate toxicity and glucose-deprivation-induced injury [95].

To explore this hypothesis, treatment with a peptide encompassing the heparan binding domain in D1, namely APP residues 96-110 was investigated. ICV injection following trauma demonstrated continued efficacy in both APP $^{-/-}$  mice and in rats following diffuse TBI [139]. In APP $^{-/-}$  mice, APP96-110 was able to restore motor and cognitive deficits, associated with greater preservation of cortical and hippocampal tissue, so that they were no longer significantly different to APP wildtypes [139]. In diffuse TBI, APP96-110 was shown to improve motor and cognitive abilities of injured rats, and significantly reduced axonal injury in the corpus callosum at seven days post-injury [139]. Importantly,

APP96-110 showed no difference in efficacy to the intact D1 protein indicating it was as fully active as D1 and sAPP $\alpha$ .

The efficacy of APP96-110 was related to APP's heparan binding ability, since an APP96-110 analogue with reduced heparan binding, made by mutating the proposed heparan binding residues, had no neuroprotective effect [139]. This established that the neuroprotective activity of APP96-110 correlated to its ability to bind heparan.

### Proposed Mechanisms of Action

APP96-110 is able to bind to cell-surface or extracellular matrix bound HSPGs to elicit a neurotogenic response [135, 137, 140]. The APP96-110 region contains a  $\beta$  hairpin loop formed by a disulphide bond between cysteines 98 and 105 [138, 140]. The presence of this bond has been shown to be critical for promoting neurite outgrowth [141] and the activation of MAP kinase [142]. Indeed, binding of this region to HSPGs can promote neurite outgrowth from central and peripheral neurons [140, 143, 144]. Furthermore, an antibody that binds to this region inhibits functional synapse formation [80], completely abolishes depolarisation induced neurite outgrowth [145].

HSPGs can act as either receptors or co-receptors [146], and the binding of sAPP $\alpha$ , through APP96-110, is proposed to lead to key physiological changes such as the regulation of cell adhesion, synaptogenesis, cell signalling and neurite outgrowth [135, 138, 140]. These changes are all important steps in promoting neuroplasticity and subsequent neurogenesis following TBI. Since HSPGs such as glypican and perlecan can inhibit the ability of APP to stimulate neurite outgrowth [144], there may be an interplay between APP and different HSPGs for APP96-110 to mediate its neuroprotective effects. As such, HSPGs may not be the target receptors for sAPP $\alpha$  or APP96-110 alone, rather HSPGs could bind to APP96-110 and aid in the binding of APP96-110 to its true neuroprotective receptor. Accordingly, identification of the definitive APP neuroprotective ligand remains an important goal to resolve the mechanism of action of sAPP in TBI.

### Development of Potential Therapeutics for TBI

Until this point, research has focused solely on achieving neuroprotective effects of exogenous APP molecules following ICV administration after TBI. However, the clinical application of a TBI therapy



would ideally be via intravenous (IV), rather than ICV administration. This would facilitate an earlier administration by paramedics rather than requiring transport to a trauma unit. A challenge for many IV drugs that target the brain is the ability to penetrate the BBB. Following trauma, ensuing damage to the BBB facilitates a localised increase in permeability of blood contents into the brain parenchyma as early as 15 minutes after injury, lasting for up to four to six hours for large molecules. Permeability for smaller molecules, however, can last up to three to four days [147, 148]. Whilst this permeability does contribute to the injury process, it also provides a window of opportunity through which therapeutics may gain easier entry to the brain they otherwise may not [148].

An additional therapeutic challenge that often slows bench to bedside progress for TBI is that much experimental research focuses on an immediate time point after injury, generally up to an hour post-TBI. As the time frame between injury and the medical diagnosis of trauma in human situations may often far exceed one hour, an ideal therapy for TBI should demonstrate efficacy up to several hours post injury. As such, research focusing on more clinically relevant time frames would help overcome this therapeutic challenge.

### Conclusion

This review has focused on the neuroprotective actions conferred by APP following TBI. Acute upregulation of APP has been shown to serve a protective, rather than detrimental role following trauma. This is now believed to be due to the presence of sAPP $\alpha$ , a metabolite that may bind to HSPGs or another receptor via its heparan binding sites, in particular, amino acid residues 96-110. A peptide encompassing APP96-110 has been shown to offer potent neuroprotective activity following TBI, including improved motor and cognitive outcome and reduced tissue loss. Most importantly, treatment with APP96-110 reduced axonal injury and overall injury severity. Accordingly, further development of APP96-110 as a therapeutic for TBI, and particularly DAI which currently lacks an efficacious treatment, is warranted as its efficacy at improving functional outcome and reducing injury severity is significant. Therefore, sAPP $\alpha$ /APP96-110 present as a novel and viable treatment offering substantial neuroprotective and neurotrophic effects for ameliorating acute brain injury.

### Acknowledgements

The authors have received funding from the National Health and Medical Research Council of Australia and the Australian Research Council.

### References

- [1] Hyder AA, Wunderlich CA, Puvanachandra P, Gururaj G, Kobusingye OC (2007). The impact of traumatic brain injuries: a global perspective. *NeuroRehabilitation*, 22: 341-353
- [2] Maas AI, Stocchetti N, Bullock R (2008). Moderate and severe traumatic brain injury in adults. *Lancet Neurol*, 7: 728-741
- [3] Gentleman SM, Nash MJ, Sweeting CJ, Graham DI, Roberts GW (1993). Beta-amyloid precursor protein (beta APP) as a marker for axonal injury after head injury. *Neurosci Lett*, 160: 139-144
- [4] Blumbergs PC, Scott G, Manavis J, Wainwright H, Simpson DA, McLean AJ (1994). Staining of amyloid precursor protein to study axonal damage in mild head injury. *Lancet*, 344: 1055-1056
- [5] Van den Heuvel C, Blumbergs PC, Finnie JW, Manavis J, Jones NR, Reilly PL, et al. (1999). Upregulation of amyloid precursor protein messenger RNA in response to traumatic brain injury: an ovine head impact model. *Exp Neurol*, 159: 441-450
- [6] Pierce JE, Trojanowski JQ, Graham DI, Smith DH, McIntosh TK (1996). Immunohistochemical characterization of alterations in the distribution of amyloid precursor proteins and beta-amyloid peptide after experimental brain injury in the rat. *J Neurosci*, 16: 1083-1090
- [7] Corrigan F, Vink R, Blumbergs PC, Masters CL, Cappai R, van den Heuvel C (2012). Characterisation of the effect of knockout of the amyloid precursor protein on outcome following mild traumatic brain injury. *Brain Res*, 1451: 87-99
- [8] Feigin VL, Theadom A, Barker-Collo S, Starkey NJ, McPherson K, Kahan M, et al. (2013). Incidence of traumatic brain injury in New Zealand: a population-based study. *Lancet Neurol*, 12: 53-64
- [9] Vink R, Van Den Heuvel C (2004). Recent advances in the development of multifactorial therapies for the treatment of traumatic brain injury. *Expert Opin Investig Drugs*, 13: 1263-1274
- [10] Myburgh JA, Cooper DJ, Finfer SR, Venkatesh B, Jones D, Higgins A, et al. (2008). Epidemiology and 12-month outcomes from traumatic brain injury in Australia and New Zealand. *J Trauma*, 64: 854-862
- [11] Finnie JW, Blumbergs PC (2002). Traumatic brain injury. *Vet Pathol*, 39: 679-689
- [12] Gaetz M (2004). The neurophysiology of brain injury. *Clin Neurophysiol*, 115: 4-18
- [13] Blennow K, Hardy J, Zetterberg H (2012). The neuropathology and neurobiology of traumatic brain injury. *Neuron*, 76: 886-899

- [14] Greve MW, Zink BJ (2009). Pathophysiology of traumatic brain injury. *Mt Sinai J Med*, 76: 97-104
- [15] Heath DL, Vink R (1999). Improved motor outcome in response to magnesium therapy received up to 24 hours after traumatic diffuse axonal brain injury in rats. *J Neurosurg*, 90: 504-509
- [16] Smith DH, Meaney DF, Shull WH (2003). Diffuse axonal injury in head trauma. *J Head Trauma Rehabil*, 18: 307-316
- [17] Finfer SR, Cohen J (2001). Severe traumatic brain injury. *Resuscitation*, 48: 77-90
- [18] Raghupathi R (2004). Cell death mechanisms following traumatic brain injury. *Brain Pathol*, 14: 215-222
- [19] Faden AI, Stoica B (2007). Neuroprotection: challenges and opportunities. *Arch Neurol*, 64: 794-800
- [20] Vink R, Nimmo AJ (2002). Novel therapies in development for the treatment of traumatic brain injury. *Expert Opin Investig Drugs*, 11: 1375-1386
- [21] Adams JH, Doyle D, Ford I, Gennarelli TA, Graham DI, McLellan DR (1989). Diffuse axonal injury in head injury: definition, diagnosis and grading. *Histopathology*, 15: 49-59
- [22] Adams JH, Jennett B, Murray LS, Teasdale GM, Gennarelli TA, Graham DI (2011). Neuropathological findings in disabled survivors of a head injury. *J Neurotrauma*, 28: 701-709
- [23] Povlishock JT (1993). Pathobiology of traumatically induced axonal injury in animals and man. *Ann Emerg Med*, 22: 980-986
- [24] Maxwell WL, Watt C, Graham DI, Gennarelli TA (1993). Ultrastructural evidence of axonal shearing as a result of lateral acceleration of the head in non-human primates. *Acta Neuropathol*, 86: 136-144
- [25] Buki A, Povlishock JT (2006). All roads lead to disconnection?--Traumatic axonal injury revisited. *Acta Neurochir (Wien)*, 148: 181-193
- [26] Gennarelli TA, Thibault LE, Adams JH, Graham DI, Thompson CJ, Marcincin RP (1982). Diffuse axonal injury and traumatic coma in the primate. *Ann Neurol*, 12: 564-574
- [27] Brunholz S, Sisodia S, Lorenzo A, Deyts C, Kins S, Morfini G (2012). Axonal transport of APP and the spatial regulation of APP cleavage and function in neuronal cells. *Exp Brain Res*, 217: 353-364
- [28] Koo EH, Sisodia SS, Archer DR, Martin LJ, Weidemann A, Beyreuther K, et al. (1990). Precursor of amyloid protein in Alzheimer disease undergoes fast anterograde axonal transport. *Proc Natl Acad Sci U S A*, 87: 1561-1565
- [29] Mattson MP (1997). Cellular actions of beta-amyloid precursor protein and its soluble and fibrillogenic derivatives. *Physiol Rev*, 77: 1081-1132
- [30] Beyreuther K, Pollwein P, Multhaup G, Monning U, König G, Dyrks T, et al. (1993). Regulation and expression of the Alzheimer's beta/A4 amyloid protein precursor in health, disease, and Down's syndrome. *Ann N Y Acad Sci*, 695: 91-102
- [31] Moya KL, Benowitz LI, Schneider GE, Allinquant B (1994). The amyloid precursor protein is developmentally regulated and correlated with synaptogenesis. *Dev Biol*, 161: 597-603
- [32] Lassek M, Weingarten J, Einsfelder U, Brendel P, Müller U, Volkandt W (2013). Amyloid precursor proteins are constituents of the presynaptic active zone. *J Neurochem*, 127: 48-56
- [33] Kang J, Lemaire HG, Unterbeck A, Salbaum JM, Masters CL, Grzeschik KH, et al. (1987). The precursor of Alzheimer's disease amyloid A4 protein resembles a cell-surface receptor. *Nature*, 325: 733-736
- [34] Sandbrink R, Masters CL, Beyreuther K (1994). APP gene family: unique age-associated changes in splicing of Alzheimer's beta A4-amyloid protein precursor. *Neurobiol Dis*, 1: 13-24
- [35] Forloni G, Demicheli F, Giorgi S, Bendotti C, Angeretti N (1992). Expression of amyloid precursor protein mRNAs in endothelial, neuronal and glial cells: modulation by interleukin-1. *Brain Res Mol Brain Res*, 16: 128-134
- [36] König G, Monning U, Czech C, Prior R, Banati R, Schreiter-Gasser U, et al. (1992). Identification and differential expression of a novel alternative splice isoform of the beta A4 amyloid precursor protein (APP) mRNA in leukocytes and brain microglial cells. *J Biol Chem*, 267: 10804-10809
- [37] Reinhard C, Hebert SS, De Strooper B (2005). The amyloid-beta precursor protein: integrating structure with biological function. *EMBO J*, 24: 3996-4006
- [38] Bayer TA, Cappai R, Masters CL, Beyreuther K, Multhaup G (1999). It all sticks together--the APP-related family of proteins and Alzheimer's disease. *Mol Psychiatry*, 4: 524-528
- [39] Perreau VM, Orchard S, Adlard PA, Bellingham SA, Cappai R, Ciccotosto GD, et al. (2010). A domain level interaction network of amyloid precursor protein and Abeta of Alzheimer's disease. *Proteomics*, 10: 2377-2395
- [40] Tomita S, Kirino Y, Suzuki T (1998). Cleavage of Alzheimer's amyloid precursor protein (APP) by secretases occurs after O-glycosylation of APP in the protein secretory pathway. Identification of intracellular compartments in which APP cleavage occurs without using toxic agents that interfere with protein metabolism. *J Biol Chem*, 273: 6277-6284
- [41] Caporaso GL, Takei K, Gandy SE, Matteoli M, Mundigl O, Greengard P, et al. (1994). Morphologic and biochemical analysis of the intracellular trafficking of the Alzheimer beta/A4 amyloid precursor protein. *J Neurosci*, 14: 3122-3138
- [42] Sisodia SS, Koo EH, Beyreuther K, Unterbeck A, Price DL (1990). Evidence that beta-amyloid protein in Alzheimer's disease is not derived by normal processing. *Science*, 248: 492-495
- [43] Koo EH, Squazzo SL, Selkoe DJ, Koo CH (1996). Trafficking of cell-surface amyloid beta-protein precursor. I. Secretion, endocytosis and recycling as detected by labeled monoclonal antibody. *J Cell Sci*, 109 (Pt 5): 991-998
- [44] De Strooper B, Annaert W (2000). Proteolytic

- processing and cell biological functions of the amyloid precursor protein. *J Cell Sci*, 113 ( Pt 11): 1857-1870
- [45] Prox J, Rittger A, Saftig P (2012). Physiological functions of the amyloid precursor protein secretases ADAM10, BACE1, and presenilin. *Exp Brain Res*, 217: 331-341
- [46] Lichtenthaler SF (2006). Ectodomain shedding of the amyloid precursor protein: cellular control mechanisms and novel modifiers. *Neurodegener Dis*, 3: 262-269
- [47] Hiltunen M, van Groen T, Jolkkonen J (2009). Functional roles of amyloid-beta protein precursor and amyloid-beta peptides: evidence from experimental studies. *J Alzheimers Dis*, 18: 401-412
- [48] Suh YH, Checler F (2002). Amyloid precursor protein, presenilins, and alpha-synuclein: molecular pathogenesis and pharmacological applications in Alzheimer's disease. *Pharmacol Rev*, 54: 469-525
- [49] Kuhn PH, Wang H, Dislich B, Colombo A, Zeitschel U, Ellwart JW, et al. (2010). ADAM10 is the physiologically relevant, constitutive alpha-secretase of the amyloid precursor protein in primary neurons. *EMBO J*, 29: 3020-3032
- [50] Buxbaum JD, Liu KN, Luo Y, Slack JL, Stocking KL, Peschon JJ, et al. (1998). Evidence that tumor necrosis factor alpha converting enzyme is involved in regulated alpha-secretase cleavage of the Alzheimer amyloid protein precursor. *J Biol Chem*, 273: 27765-27767
- [51] Asai M, Hattori C, Szabo B, Sasagawa N, Maruyama K, Tanuma S, et al. (2003). Putative function of ADAM9, ADAM10, and ADAM17 as APP alpha-secretase. *Biochem Biophys Res Commun*, 301: 231-235
- [52] Postina R, Schroeder A, Dewachter I, Bohl J, Schmitt U, Kojro E, et al. (2004). A disintegrin-metalloproteinase prevents amyloid plaque formation and hippocampal defects in an Alzheimer disease mouse model. *J Clin Invest*, 113: 1456-1464
- [53] Lichtenthaler SF (2011). alpha-secretase in Alzheimer's disease: molecular identity, regulation and therapeutic potential. *J Neurochem*, 116: 10-21
- [54] White AR, Reyes R, Mercer JF, Camakaris J, Zheng H, Bush AI, et al. (1999). Copper levels are increased in the cerebral cortex and liver of APP and APLP2 knockout mice. *Brain Res*, 842: 439-444
- [55] Maynard CJ, Cappai R, Volitakis I, Cherny RA, White AR, Beyreuther K, et al. (2002). Overexpression of Alzheimer's disease amyloid-beta opposes the age-dependent elevations of brain copper and iron. *J Biol Chem*, 277: 44670-44676
- [56] Duce JA, Tsatsanis A, Cater MA, James SA, Robb E, Wikke K, et al. (2010). Iron-export ferroxidase activity of beta-amyloid precursor protein is inhibited by zinc in Alzheimer's disease. *Cell*, 142: 857-867
- [57] Needham BE, Ciccotosto GD, Cappai R (2014). Combined deletions of amyloid precursor protein and amyloid precursor-like protein 2 reveal different effects on mouse brain metal homeostasis. *Metallomics*, 6: 598-603
- [58] Multhaup G, Mechler H, Masters CL (1995). Characterization of the high affinity heparin binding site of the Alzheimer's disease beta A4 amyloid precursor protein (APP) and its enhancement by zinc(II). *J Mol Recognit*, 8: 247-257
- [59] Cappai R, Cheng F, Ciccotosto GD, Needham BE, Masters CL, Multhaup G, et al. (2005). The amyloid precursor protein (APP) of Alzheimer disease and its paralog, APLP2, modulate the Cu/Zn-Nitric Oxide-catalyzed degradation of glypican-1 heparan sulfate in vivo. *J Biol Chem*, 280: 13913-13920
- [60] Klaver D, Hung AC, Gasperini R, Foa L, Aguilar MI, Small DH (2010). Effect of heparin on APP metabolism and Abeta production in cortical neurons. *Neurodegener Dis*, 7: 187-189
- [61] Cheng F, Cappai R, Lidfeldt J, Belting M, Fransson LA, Mani K (2014). Amyloid precursor protein (APP)/APP-like protein 2 (APLP2) expression is required to initiate endosome-nucleus-autophagosome trafficking of glypican-1-derived heparan sulfate. *J Biol Chem*, 289: 20871-20878
- [62] Hoefgen S, Coburger I, Roeser D, Schaub Y, Dahms SO, Than ME (2014). Heparin induced dimerization of APP is primarily mediated by E1 and regulated by its acidic domain. *J Struct Biol*, 187: 30-37
- [63] da Rocha JF, da Cruz ESOA, Vieira SI (2015). Analysis of the Amyloid Precursor Protein (APP) role in neurogenesis reveals a biphasic SH-SY5Y neuronal cell differentiation model. *J Neurochem*, 134: 288-301
- [64] Xu F, Previti ML, Nieman MT, Davis J, Schmaier AH, Van Nostrand WE (2009). AbetaPP/APLP2 family of Kunitz serine proteinase inhibitors regulate cerebral thrombosis. *J Neurosci*, 29: 5666-5670
- [65] Henry A, Li QX, Galatis D, Hesse L, Multhaup G, Beyreuther K, et al. (1998). Inhibition of platelet activation by the Alzheimer's disease amyloid precursor protein. *Br J Haematol*, 103: 402-415
- [66] Needham BE, Wlodek ME, Ciccotosto GD, Fam BC, Masters CL, Proietto J, et al. (2008). Identification of the Alzheimer's disease amyloid precursor protein (APP) and its homologue APLP2 as essential modulators of glucose and insulin homeostasis and growth. *J Pathol*, 215: 155-163
- [67] Mattson MP, Cheng B, Culwell AR, Esch FS, Lieberburg I, Rydel RE (1993). Evidence for excitoprotective and intraneuronal calcium-regulating roles for secreted forms of the beta-amyloid precursor protein. *Neuron*, 10: 243-254
- [68] Smith-Swintosky VL, Pettigrew LC, Craddock SD, Culwell AR, Rydel RE, Mattson MP (1994). Secreted forms of beta-amyloid precursor protein protect against ischemic brain injury. *J Neurochem*, 63: 781-784
- [69] Gralle M, Botelho MG, Wouters FS (2009). Neuroprotective secreted amyloid precursor protein acts by disrupting amyloid precursor protein dimers. *J Biol Chem*, 284: 15016-15025
- [70] Milosch N, Tanriover G, Kundu A, Rami A, Francois JC, Baumkötter F, et al. (2014). Holo-APP and G-protein-mediated signaling are required for sAPPalpha-induced activation of the Akt survival pathway. *Cell Death Dis*, 5: e1391

- [71] Pardossi-Piquard R, Petit A, Kawarai T, Sunyach C, Alves da Costa C, Vincent B, et al. (2005). Presenilin-dependent transcriptional control of the Abeta-degrading enzyme neprilysin by intracellular domains of betaAPP and APLP. *Neuron*, 46: 541-554
- [72] Kerridge C, Belyaev ND, Nalivaeva NN, Turner AJ (2014). The Abeta-clearance protein transthyretin, like neprilysin, is epigenetically regulated by the amyloid precursor protein intracellular domain. *J Neurochem*, 130: 419-431
- [73] Zheng H, Jiang M, Trumbauer ME, Sirinathsinghji DJ, Hopkins R, Smith DW, et al. (1995). beta-Amyloid precursor protein-deficient mice show reactive gliosis and decreased locomotor activity. *Cell*, 81: 525-531
- [74] Dawson GR, Seabrook GR, Zheng H, Smith DW, Graham S, O'Dowd G, et al. (1999). Age-related cognitive deficits, impaired long-term potentiation and reduction in synaptic marker density in mice lacking the beta-amyloid precursor protein. *Neuroscience*, 90: 1-13
- [75] Heber S, Herms J, Gajic V, Hainfellner J, Aguzzi A, Rulicke T, et al. (2000). Mice with combined gene knock-outs reveal essential and partially redundant functions of amyloid precursor protein family members. *J Neurosci*, 20: 7951-7963
- [76] Weyer SW, Zagrebelsky M, Herrmann U, Hick M, Ganss L, Gobbert J, et al. (2014). Comparative analysis of single and combined APP/APLP knockouts reveals reduced spine density in APP-KO mice that is prevented by APP $\alpha$  expression. *Acta Neuropathol Commun*, 2: 36
- [77] Gralle M, Ferreira ST (2007). Structure and functions of the human amyloid precursor protein: the whole is more than the sum of its parts. *Prog Neurobiol*, 82: 11-32
- [78] Soba P, Eggert S, Wagner K, Zentgraf H, Siehl K, Kreger S, et al. (2005). Homo- and heterodimerization of APP family members promotes intercellular adhesion. *EMBO J*, 24: 3624-3634
- [79] Octave JN, Pierrot N, Ferao Santos S, Nalivaeva NN, Turner AJ (2013). From synaptic spines to nuclear signaling: nuclear and synaptic actions of the amyloid precursor protein. *J Neurochem*, 126: 183-190
- [80] Morimoto T, Ohsawa I, Takamura C, Ishiguro M, Kohsaka S (1998). Involvement of amyloid precursor protein in functional synapse formation in cultured hippocampal neurons. *J Neurosci Res*, 51: 185-195
- [81] Allinquant B, Hantraye P, Mailleux P, Moya K, Bouillot C, Prochiantz A (1995). Downregulation of amyloid precursor protein inhibits neurite outgrowth in vitro. *J Cell Biol*, 128: 919-927
- [82] Herard AS, Besret L, Dubois A, Dauguet J, Delzescaux T, Hantraye P, et al. (2006). siRNA targeted against amyloid precursor protein impairs synaptic activity in vivo. *Neurobiol Aging*, 27: 1740-1750
- [83] Perez RG, Zheng H, Van der Ploeg LH, Koo EH (1997). The beta-amyloid precursor protein of Alzheimer's disease enhances neuron viability and modulates neuronal polarity. *J Neurosci*, 17: 9407-9414
- [84] Araki W, Kitaguchi N, Tokushima Y, Ishii K, Aratake H, Shimohama S, et al. (1991). Trophic effect of beta-amyloid precursor protein on cerebral cortical neurons in culture. *Biochem Biophys Res Commun*, 181: 265-271
- [85] Bhasin R, Van Nostrand WE, Saitoh T, Donets MA, Barnes EA, Quitschke WW, et al. (1991). Expression of active secreted forms of human amyloid beta-protein precursor by recombinant baculovirus-infected insect cells. *Proc Natl Acad Sci U S A*, 88: 10307-10311
- [86] Jin LW, Ninomiya H, Roch JM, Schubert D, Masliah E, Otero DA, et al. (1994). Peptides containing the RERMS sequence of amyloid beta/A4 protein precursor bind cell surface and promote neurite extension. *J Neurosci*, 14: 5461-5470
- [87] Ohsawa I, Takamura C, Kohsaka S (1997). The amino-terminal region of amyloid precursor protein is responsible for neurite outgrowth in rat neocortical explant culture. *Biochem Biophys Res Commun*, 236: 59-65
- [88] Qiu WQ, Ferreira A, Miller C, Koo EH, Selkoe DJ (1995). Cell-surface beta-amyloid precursor protein stimulates neurite outgrowth of hippocampal neurons in an isoform-dependent manner. *J Neurosci*, 15: 2157-2167
- [89] Saitoh T, Sundsmo M, Roch JM, Kimura N, Cole G, Schubert D, et al. (1989). Secreted form of amyloid beta protein precursor is involved in the growth regulation of fibroblasts. *Cell*, 58: 615-622
- [90] Wang Y, Ha Y (2004). The X-ray structure of an antiparallel dimer of the human amyloid precursor protein E2 domain. *Mol Cell*, 15: 343-353
- [91] Tremml P, Lipp HP, Muller U, Ricceri L, Wolfer DP (1998). Neurobehavioral development, adult openfield exploration and swimming navigation learning in mice with a modified beta-amyloid precursor protein gene. *Behav Brain Res*, 95: 65-76
- [92] Tremml P, Lipp HP, Muller U, Wolfer DP (2002). Enriched early experiences of mice underexpressing the beta-amyloid precursor protein restore spatial learning capabilities but not normal openfield behavior of adult animals. *Genes Brain Behav*, 1: 230-241
- [93] Huber G, Bailly Y, Martin JR, Mariani J, Brugg B (1997). Synaptic beta-amyloid precursor proteins increase with learning capacity in rats. *Neuroscience*, 80: 313-320
- [94] Chasseigneaux S, Allinquant B (2012). Functions of Abeta, sAPP $\alpha$  and sAPP $\beta$ : similarities and differences. *J Neurochem*, 120 Suppl 1: 99-108
- [95] Furukawa K, Sopher BL, Rydel RE, Begley JG, Pham DG, Martin GM, et al. (1996). Increased activity-regulating and neuroprotective efficacy of alpha-secretase-derived secreted amyloid precursor protein conferred by a C-terminal heparin-binding domain. *J Neurochem*, 67: 1882-1896
- [96] Chasseigneaux S, Dinc L, Rose C, Chabret C, Coulpier F, Topilko P, et al. (2011). Secreted amyloid precursor protein beta and secreted amyloid precursor protein alpha induce axon outgrowth in vitro through Egr1 signaling pathway. *PLoS one*, 6: e16301
- [97] Taylor CJ, Ireland DR, Ballagh I, Bourne K, Marechal NM, Turner PR, et al. (2008). Endogenous secreted

- amyloid precursor protein-alpha regulates hippocampal NMDA receptor function, long-term potentiation and spatial memory. *Neurobiol Dis*, 31: 250-260
- [98] Neselius S, Zetterberg H, Blennow K, Marcusson J, Brisby H (2013). Increased CSF levels of phosphorylated neurofilament heavy protein following bout in amateur boxers. *PLoS one*, 8: e81249
- [99] Furukawa K, Mattson MP (1998). Secreted amyloid precursor protein alpha selectively suppresses N-methyl-D-aspartate currents in hippocampal neurons: involvement of cyclic GMP. *Neuroscience*, 83: 429-438
- [100] Schubert D, Behl C (1993). The expression of amyloid beta protein precursor protects nerve cells from beta-amyloid and glutamate toxicity and alters their interaction with the extracellular matrix. *Brain Res*, 629: 275-282
- [101] Bell KF, Zheng L, Fahrenholz F, Cuello AC (2008). ADAM-10 over-expression increases cortical synaptogenesis. *Neurobiol Aging*, 29: 554-565
- [102] Caille I, Allinquant B, Dupont E, Bouillot C, Langer A, Muller U, et al. (2004). Soluble form of amyloid precursor protein regulates proliferation of progenitors in the adult subventricular zone. *Development*, 131: 2173-2181
- [103] Bramlett HM, Kraydieh S, Green EJ, Dietrich WD (1997). Temporal and regional patterns of axonal damage following traumatic brain injury: a beta-amyloid precursor protein immunocytochemical study in rats. *J Neuropathol Exp Neurol*, 56: 1132-1141
- [104] Chen XH, Siman R, Iwata A, Meaney DF, Trojanowski JQ, Smith DH (2004). Long-term accumulation of amyloid-beta, beta-secretase, presenilin-1, and caspase-3 in damaged axons following brain trauma. *Am J Pathol*, 165: 357-371
- [105] Dewji NN, Do C (1996). Heat shock factor-1 mediates the transcriptional activation of Alzheimer's beta-amyloid precursor protein gene in response to stress. *Brain Res Mol Brain Res*, 35: 325-328
- [106] Fleminger S, Oliver DL, Lovestone S, Rabe-Hesketh S, Giora A (2003). Head injury as a risk factor for Alzheimer's disease: the evidence 10 years on; a partial replication. *J Neurol Neurosurg Psychiatry*, 74: 857-862
- [107] Mortimer JA, van Duijn CM, Chandra V, Fratiglioni L, Graves AB, Heyman A, et al. (1991). Head trauma as a risk factor for Alzheimer's disease: a collaborative re-analysis of case-control studies. EURODEM Risk Factors Research Group. *Int J Epidemiol*, 20 Suppl 2: S28-35
- [108] Salib E, Hillier V (1997). Head injury and the risk of Alzheimer's disease: a case control study. *Int J Geriatr Psychiatry*, 12: 363-368
- [109] Guo Z, Cupples LA, Kurz A, Auerbach SH, Volicer L, Chui H, et al. (2000). Head injury and the risk of AD in the MIRAGE study. *Neurology*, 54: 1316-1323
- [110] Mayeux R, Ottman R, Maestre G, Ngai C, Tang MX, Ginsberg H, et al. (1995). Synergistic effects of traumatic head injury and apolipoprotein-epsilon 4 in patients with Alzheimer's disease. *Neurology*, 45: 555-557
- [111] Rasmusson DX, Brandt J, Martin DB, Folstein MF (1995). Head injury as a risk factor in Alzheimer's disease. *Brain Inj*, 9: 213-219
- [112] Fratiglioni L, Ahlbom A, Viitanen M, Winblad B (1993). Risk factors for late-onset Alzheimer's disease: a population-based, case-control study. *Ann Neurol*, 33: 258-266
- [113] Launer LJ, Andersen K, Dewey ME, Letenneur L, Ott A, Amaducci LA, et al. (1999). Rates and risk factors for dementia and Alzheimer's disease: results from EURODEM pooled analyses. EURODEM Incidence Research Group and Work Groups. *European Studies of Dementia. Neurology*, 52: 78-84
- [114] Gentleman SM, Greenberg BD, Savage MJ, Noori M, Newman SJ, Roberts GW, et al. (1997). A beta 42 is the predominant form of amyloid beta-protein in the brains of short-term survivors of head injury. *Neuroreport*, 8: 1519-1522
- [115] Ikonomic MD, Uryu K, Abrahamson EE, Ciallella JR, Trojanowski JQ, Lee VM, et al. (2004). Alzheimer's pathology in human temporal cortex surgically excised after severe brain injury. *Exp Neurol*, 190: 192-203
- [116] Roberts GW, Gentleman SM, Lynch A, Graham DI (1991). beta A4 amyloid protein deposition in brain after head trauma. *Lancet*, 338: 1422-1423
- [117] Adle-Biassette H, Duyckaerts C, Wasowicz M, He Y, Fornes P, Foncin JF, et al. (1996). Beta AP deposition and head trauma. *Neurobiol Aging*, 17: 415-419
- [118] Braak H, Braak E (1997). Frequency of stages of Alzheimer-related lesions in different age categories. *Neurobiol Aging*, 18: 351-357
- [119] Chen XH, Johnson VE, Uryu K, Trojanowski JQ, Smith DH (2009). A lack of amyloid beta plaques despite persistent accumulation of amyloid beta in axons of long-term survivors of traumatic brain injury. *Brain Pathol*, 19: 214-223
- [120] Murai H, Pierce JE, Raghupathi R, Smith DH, Saatman KE, Trojanowski JQ, et al. (1998). Twofold overexpression of human beta-amyloid precursor proteins in transgenic mice does not affect the neuromotor, cognitive, or neurodegenerative sequelae following experimental brain injury. *J Comp Neurol*, 392: 428-438
- [121] Nakagawa Y, Reed L, Nakamura M, McIntosh TK, Smith DH, Saatman KE, et al. (2000). Brain trauma in aged transgenic mice induces regression of established abeta deposits. *Exp Neurol*, 163: 244-252
- [122] Smith DH, Nakamura M, McIntosh TK, Wang J, Rodriguez A, Chen XH, et al. (1998). Brain trauma induces massive hippocampal neuron death linked to a surge in beta-amyloid levels in mice overexpressing mutant amyloid precursor protein. *Am J Pathol*, 153: 1005-1010
- [123] Uryu K, Laurer H, McIntosh T, Pratico D, Martinez D, Leight S, et al. (2002). Repetitive mild brain trauma accelerates Abeta deposition, lipid peroxidation, and cognitive impairment in a transgenic mouse model of Alzheimer amyloidosis. *J Neurosci*, 22: 446-454
- [124] Thornton E, Vink R, Blumbergs PC, Van Den Heuvel C (2006). Soluble amyloid precursor protein alpha reduces

- neuronal injury and improves functional outcome following diffuse traumatic brain injury in rats. *Brain Res*, 1094: 38-46
- [125] Marmarou A, Foda MA, van den Brink W, Campbell J, Kita H, Demetriadou K (1994). A new model of diffuse brain injury in rats. Part I: Pathophysiology and biomechanics. *J Neurosurg*, 80: 291-300
- [126] Mattson MP (1999). Impairment of membrane transport and signal transduction systems by amyloidogenic proteins. *Methods Enzymol*, 309: 733-746
- [127] Buki A, Koizumi H, Povlishock JT (1999). Moderate posttraumatic hypothermia decreases early calpain-mediated proteolysis and concomitant cytoskeletal compromise in traumatic axonal injury. *Exp Neurol*, 159: 319-328
- [128] Saatman KE, Abai B, Grosvenor A, Vorwerk CK, Smith DH, Meaney DF (2003). Traumatic axonal injury results in biphasic calpain activation and retrograde transport impairment in mice. *J Cereb Blood Flow Metab*, 23: 34-42
- [129] Cheng G, Yu Z, Zhou D, Mattson MP (2002). Phosphatidylinositol-3-kinase-Akt kinase and p42/p44 mitogen-activated protein kinases mediate neurotrophic and excitoprotective actions of a secreted form of amyloid precursor protein. *Exp Neurol*, 175: 407-414
- [130] Yang L, Tao LY, Chen XP (2007). Roles of NF-kappaB in central nervous system damage and repair. *Neurosci Bull*, 23: 307-313
- [131] Corrigan F, Vink R, Blumbergs PC, Masters CL, Cappai R, van den Heuvel C (2012). sAPPalpha rescues deficits in amyloid precursor protein knockout mice following focal traumatic brain injury. *J Neurochem*, 122: 208-220
- [132] Siopi E, Llufriu-Daben G, Cho AH, Vidal-Lletjos S, Plotkine M, Marchand-Leroux C, et al. (2013). Etazolate, an alpha-secretase activator, reduces neuroinflammation and offers persistent neuroprotection following traumatic brain injury in mice. *Neuropharmacology*, 67: 183-192
- [133] Loane DJ, Pocivavsek A, Moussa CE, Thompson R, Matsuoka Y, Faden AI, et al. (2009). Amyloid precursor protein secretases as therapeutic targets for traumatic brain injury. *Nat Med*, 15: 377-379
- [134] Corrigan F, Pham CL, Vink R, Blumbergs PC, Masters CL, van den Heuvel C, et al. (2011). The neuroprotective domains of the amyloid precursor protein, in traumatic brain injury, are located in the two growth factor domains. *Brain Res*, 1378: 137-143
- [135] Clarris HJ, Cappai R, Heffernan D, Beyreuther K, Masters CL, Small DH (1997). Identification of heparin-binding domains in the amyloid precursor protein of Alzheimer's disease by deletion mutagenesis and peptide mapping. *J Neurochem*, 68: 1164-1172
- [136] Narindrasorasak S, Lowery D, Gonzalez-DeWhitt P, Poorman RA, Greenberg B, Kisilevsky R (1991). High affinity interactions between the Alzheimer's beta-amyloid precursor proteins and the basement membrane form of heparan sulfate proteoglycan. *J Biol Chem*, 266: 12878-12883
- [137] Small DH, Nurcombe V, Moir R, Michaelson S, Monard D, Beyreuther K, et al. (1992). Association and release of the amyloid protein precursor of Alzheimer's disease from chick brain extracellular matrix. *J Neurosci*, 12: 4143-4150
- [138] Rossjohn J, Cappai R, Feil SC, Henry A, McKinstry WJ, Galatis D, et al. (1999). Crystal structure of the N-terminal, growth factor-like domain of Alzheimer amyloid precursor protein. *Nat Struct Biol*, 6: 327-331
- [139] Corrigan F, Thornton E, Roisman LC, Leonard AV, Vink R, Blumbergs PC, et al. (2014). The neuroprotective activity of the amyloid precursor protein against traumatic brain injury is mediated via the heparin binding site in residues 96-110. *J Neurochem*, 128: 196-204
- [140] Small DH, Nurcombe V, Reed G, Clarris H, Moir R, Beyreuther K, et al. (1994). A heparin-binding domain in the amyloid protein precursor of Alzheimer's disease is involved in the regulation of neurite outgrowth. *J Neurosci*, 14: 2117-2127
- [141] Young-Pearse TL, Chen AC, Chang R, Marquez C, Selkoe DJ (2008). Secreted APP regulates the function of full-length APP in neurite outgrowth through interaction with integrin beta1. *Neural Dev*, 3: 15
- [142] Greenberg SM, Qiu WQ, Selkoe DJ, Ben-Itzhak A, Kosik KS (1995). Amino-terminal region of the beta-amyloid precursor protein activates mitogen-activated protein kinase. *Neurosci Lett*, 198: 52-56
- [143] Williamson TG, Nurcombe V, Beyreuther K, Masters CL, Small DH (1995). Affinity purification of proteoglycans that bind to the amyloid protein precursor of Alzheimer's disease. *J Neurochem*, 65: 2201-2208
- [144] Williamson TG, Mok SS, Henry A, Cappai R, Lander AD, Nurcombe V, et al. (1996). Secreted glypican binds to the amyloid precursor protein of Alzheimer's disease (APP) and inhibits APP-induced neurite outgrowth. *J Biol Chem*, 271: 31215-31221
- [145] Gakhar-Koppole N, Hundeshagen P, Mandl C, Weyer SW, Allinquant B, Muller U, et al. (2008). Activity requires soluble amyloid precursor protein alpha to promote neurite outgrowth in neural stem cell-derived neurons via activation of the MAPK pathway. *Eur J Neurosci*, 28: 871-882
- [146] Sarrazin S, Lamanna WC, Esko JD (2011). Heparan sulfate proteoglycans. *Cold Spring Harb Perspect Biol*, 3: pii: a004952
- [147] Baskaya MK, Rao AM, Dogan A, Donaldson D, Dempsey RJ (1997). The biphasic opening of the blood-brain barrier in the cortex and hippocampus after traumatic brain injury in rats. *Neurosci Lett*, 226: 33-36
- [148] Habgood MD, Bye N, Dziegielewska KM, Ek CJ, Lane MA, Potter A, et al. (2007). Changes in blood-brain barrier permeability to large and small molecules following traumatic brain injury in mice. *Eur J Neurosci*, 25: 231-238
- [149] Goodman Y, Mattson MP (1994). Secreted forms of beta-amyloid precursor protein protect hippocampal neurons against amyloid beta-peptide-induced oxidative injury. *Exp Neurol*, 128: 1-12
- [150] Roch JM, Masliah E, Roch-Levecq AC, Sundsmo MP,

- Otero DA, Veinbergs I, et al. (1994). Increase of synaptic density and memory retention by a peptide representing the trophic domain of the amyloid beta/A4 protein precursor. *Proc Natl Acad Sci U S A*, 91: 7450-7454
- [151] Meziane H, Dodart JC, Mathis C, Little S, Clemens J, Paul SM, et al. (1998). Memory-enhancing effects of secreted forms of the beta-amyloid precursor protein in normal and amnesic mice. *Proc Natl Acad Sci U S A*, 95: 12683-12688
- [152] Corrigan F, Vink R, Blumbergs PC, Masters CL, Cappai R, van den Heuvel C (2012). Evaluation of the effects of treatment with sAPPalpha on functional and histological outcome following controlled cortical impact injury in mice. *Neurosci Lett*, 515: 50-5

## 1.1 Synopsis

TBI is a life threatening injury, and yet despite its serious nature, there are currently no effective therapeutic agents to treat the condition. The following research examines the neuroprotective role of the APP96 110 peptide following TBI, with the goal of progressing the pre clinical development of this peptide as a novel therapeutic agent. This was achieved through the assessment of intravenous delivery as a viable route, determining the optimal timepoint of administration, the development of novel analogues with enhanced therapeutic action, and the assessment of the efficacy of long term administration on outcome, neuroinflammation and neurodegeneration.

### 1.1.1 Hypothesis

The neuroprotective properties of APP96 110 following TBI are linked to its heparin binding sites, and these specific regions are therefore responsible for APP protecting against neuronal injury and improving neurological outcome following TBI.

### 1.1.2 Aims

- To determine the efficacy of intravenous (IV) APP96 110, along with the most clinically relevant time of administration, following moderate severe diffuse TBI.
- To mutate key amino acid residues within the APP96 110 sequence to create APP analogues with an enhanced heparin binding affinity, and subsequently examine whether this enhancement would confer greater neuroprotective activity *in vivo* following TBI.
- To assess the long term efficacy of both wildtype and mutated APP96 110 following TBI, and examine their effects on long term neuroinflammation and neurodegeneration.



## **Chapter 2: Materials and Methods Part I: Experimental Procedures**

## **2.1 Ethics**

All experimental protocols were performed within the guidelines established by the National Health and Medical Research Council of Australia and was approved by the Animal Ethics Committee of the University of Adelaide, Australia (Ethics numbers: M 2012 213 and M 2014 131).

## **2.2 Animals**

For this research, male Sprague Dawley rats the equivalent of 10 12 weeks of age were used for all experiments. For Chapters 4 and 5, all animals used in experiments were bred from the Harlan strain, whilst those used in experiments in Chapter 6 were bred from the Charles River strain (for detailed justification, see Material & Methods Part II). Studies have shown Charles River strain SDs to demonstrate a number of differences to other SD strains, in particular the Harlan strain. These differences include differences in growth rate and body composition, including a higher body fat mass, higher gross liver weight, lower testicular weight and lower cholesterol levels (Brower et al., 2015). All animals were group housed in a controlled temperature environment under a 12 hour light dark cycle and fed and watered *ad libitum*.

## **2.3 Experimental Procedures**

### **2.3.1 Anaesthesia**

The induction of anaesthesia was conducted using isoflurane. Animals were placed in a transparent plastic induction chamber with isoflurane delivered at 5% in 1.4L/min N<sub>2</sub> and 0.6L/min O<sub>2</sub> for 5 minutes. Animals were intubated with a 16G x 2" sized IV catheter and maintained on a normoxic mix with 3% isoflurane (1.4L/min N<sub>2</sub> and 0.6L/min O<sub>2</sub>) via mechanical ventilation throughout the procedure.

### **2.3.2 Impact Acceleration Weight-Drop Model of Traumatic Brain Injury**

TBI was induced using the impact acceleration model of diffuse axonal injury (DAI) (Marmarou et al., 1994). This injury model produces a range of injury severities from moderate through to moderate severe, and its heterogeneity provides a clinically relevant model to test neuroprotective therapeutics. To induce the injury, animals were anaesthetised as previously described, and upon the absence of pain reflexes, a midline incision was made centrally on the skull between the eyes and ears, before a metallic disk (10mm in diameter and 3mm in depth) was adhered onto the skull with polyacrylamide centrally between lambda and bregma sutures. Animals were placed on a foam bed of 10cm height, and injured by releasing a 450g weight from 2 metres onto the metallic disk (Marmarou et al., 1994) (Figure 2.1). This produces widespread damage to axons, particularly in white matter tracts of the brain. Directly following injury, animals received 10 minutes of hypoxia (2L/min N<sub>2</sub> and 0.2L/min of O<sub>2</sub>) to replicate the hypoxia typically induced by diffuse TBI under controlled circumstances (Hellewell et al., 2010). Our previous unpublished studies demonstrated that 10 minutes of hypoxia was sufficient to exacerbate TBI but prevent a predominantly hypoxic injury. Sham animals were surgically prepared but not injured and did not receive hypoxia.

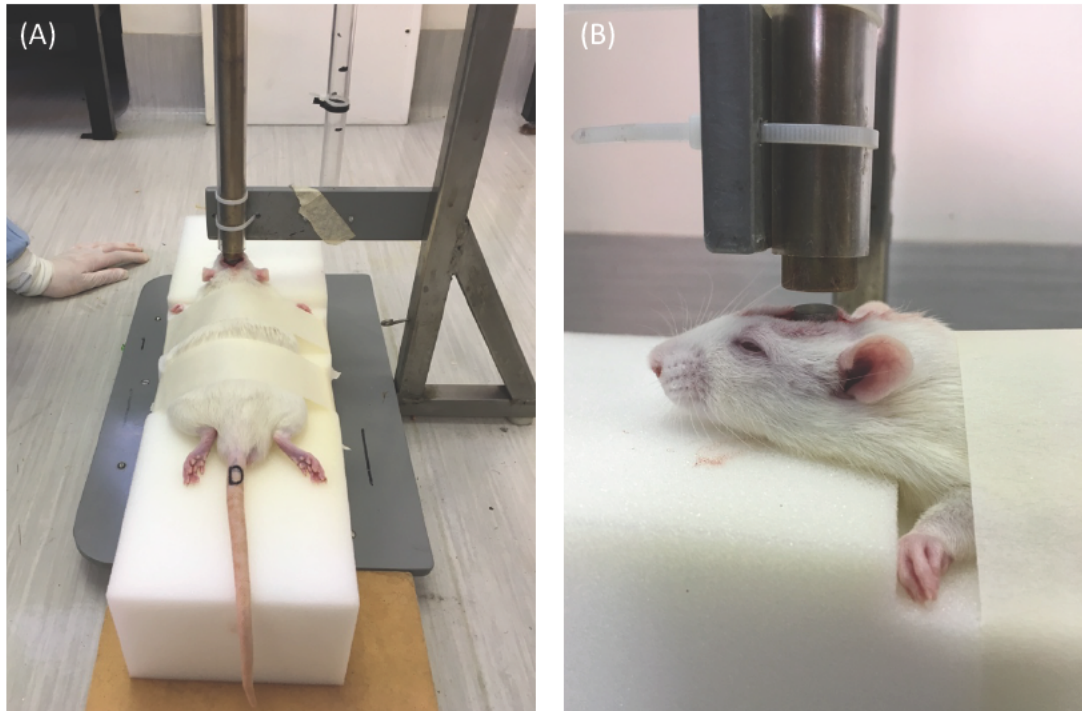


**Figure 2.1:** Image showing the injury apparatus for induction of the impact acceleration model of DAI. Image (A) shows the Perspex tube containing the 450g weight, which is lined up to fall directly onto the metallic disk adhered to the rat's skull (B).

Following TBI, all rats were monitored extensively using a clinical record sheet. Intensive continuous monitoring of the animals was provided for the first 2 hours post procedure and animals were then checked at least hourly for the next 4 hours. If signs of clinical deterioration were evident, the frequency of monitoring was adjusted accordingly so that appropriate intervention could occur. Following this initial period, animals were monitored twice daily with clinical record sheets maintained to assess the following criteria: daily weight loss, appearance and texture of their coats, posture, changes in social behaviour, as well as the presence or absence of stress marks, circling behaviour, operation site swelling, and paresis. Weight loss of greater than 5 10% of their pre surgical body weight was treated with subcutaneous saline to prevent dehydration.

### 2.3.3 APP Peptide Preparation

For all experiments, APP peptides were custom synthesized by *Auspep* (Tullamarine, Victoria, Australia) and were all N terminally acetylated and C terminally amidated (see Table 2.1). Peptides were received as lyophilized powder and dissolved in distilled water to produce 1mM stock solutions, before diluted accordingly to the required concentrations for each study.

**Table 2.1: The amino acid sequences of APP peptides used**

APP Derivative Name	Amino Acid Sequence
WT APP96 110	NWCKRGRKQCKTHPH
2+ APP96 110	NWCRRGRKQCKTRPH
3+ APP96 110	RWCRRGRKQCKTRPH

### 2.3.4 APP Peptide Administration

Following TBI, animals in all experiments received their treatments intravenously (IV) via the tail vein. For experiments outlined in chapter 4, the initial cohort of animals received their treatments at 30 minutes post TBI, whereas the second cohort received treatment at 5 hours post TBI. For all further experiments outlined in Chapters 5 and 6, animals were administered treatment at 5 hours post TBI due to the efficacy of this treatment timepoint demonstrated in chapter 4. Animals were returned to their home cage to recover once normal behaviour was established.

## **2.4 Neurological Assessment**

To effectively assess the efficacy of various APP derivatives on outcome following TBI, a range of neurological assessments, including motor and cognitive assessments, were undertaken. For all cognitive assessments, Any Maze Software was used to track, observe and record all testing. This allowed observation from afar, as the experimenter was not present in the room during testing. In order to remove scent trails, all mazes were wiped with 70% ethanol prior to use, and between each animal and each trial on the maze.

### **2.4.1 Motor Outcome**

#### **Rotarod**

The rotarod is a sensitive test of motor ability that assesses a rat's locomotion, balance and grip strength (Hamm et al., 1994). The rotarod comprises of 18 rotating metallic rods on which the animal is required to balance and walk (Figure 2.2). The speed of the rotarod is increased from 6 to 36 revolutions per minute (RPM) in intervals of by 3 RPM every 10 seconds. Animals are trained daily on the rotarod for 4 5 days prior to injury until they can complete 120 seconds to ensure an even baseline for all treatment groups. The length of time, in seconds, that animals are successfully able to walk on the rotarod post injury is recorded. Testing concludes when the rat can walk successfully for 120 seconds, falls off the device or completes consecutive loops, indicating a loss of balance.

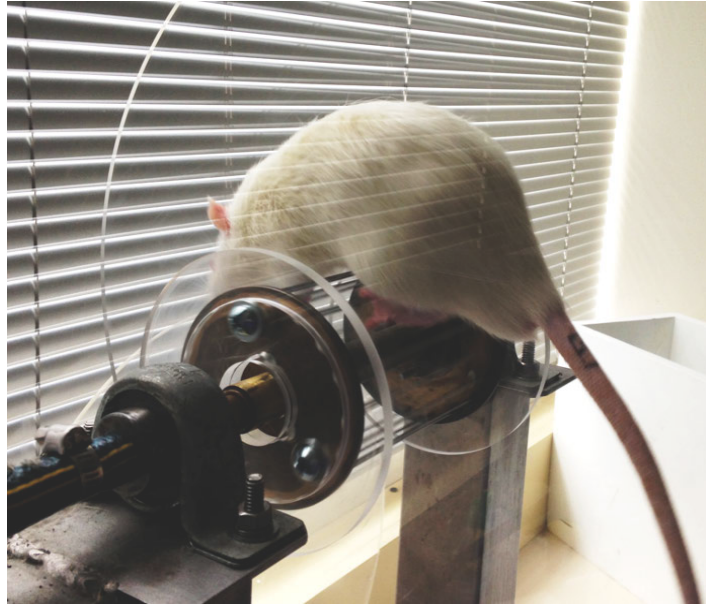


**Figure 2.2: Representative photograph of the rotarod device used to assess motor outcome following TBI.**

## 2.4.2 Functional Outcome

Functional deficits post TBI were assessed using a number of mazes and tests including the Open Field, Elevated Plus Maze, Y Maze, Barnes Maze and the Forced Swim Test. All tests were performed in order of least stressful to most stressful to ensure animals were given sufficient time to recover from the already stressful injury, and to minimize pre existing stress from the impact on functional testing.

**Table 2.2: Schedule of the functional mazes and tests**

<b>Maze/Test</b>	<b>Schedule post-TBI</b>	<b>Function</b>
Open Field	Day 7 & Day 21	Locomotion & anxiety
Elevated Plus Maze	Day 6 & Day 22	Anxiety
Y Maze	Day 5 & Day 23	Hippocampal dependent spatial & recognition memory
Barnes Maze	Days 24, 25, 26 & 28	
Forced Swim Test	Day 29	Depressive like behaviour



## Open Field

In the studies contained within this thesis the open field was used as a measure of locomotion and anxiety. The test consists of a square box (95 x 95 x 44.5cm) divided internally into a grid shape (10 x 10cm) (Figure 2.3). The grid is further divided into inner and outer zones. Rats were placed in the centre of the grid and given 5 minutes to explore at will. Rats demonstrating locomotor deficits are expected to travel a reduced distance in the grid, and are likely to spend less time in the inner zone and more time in the outer zones.

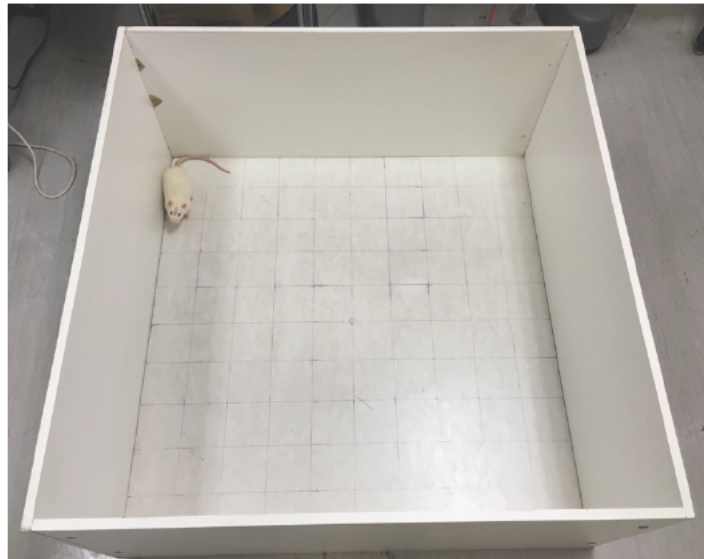


**Figure 2.3: Representative photograph of the Open Field, with the 10 x 10cm grid visible on the inside of the box.**

## Elevated Plus Maze

The Elevated Plus Maze is a measure of anxiety (Pellow et al., 1985). The maze consists of a + shaped device consisting of four arms: two opposite enclosed arms and two opposite open arms (Figure 2.4). Rats were placed in the lowest open arm and given 5 minutes to explore the maze. The time spent in the open arms versus the closed arms was recorded. Rats demonstrating an increased level of anxiety should choose to spend more time in the enclosed arms.

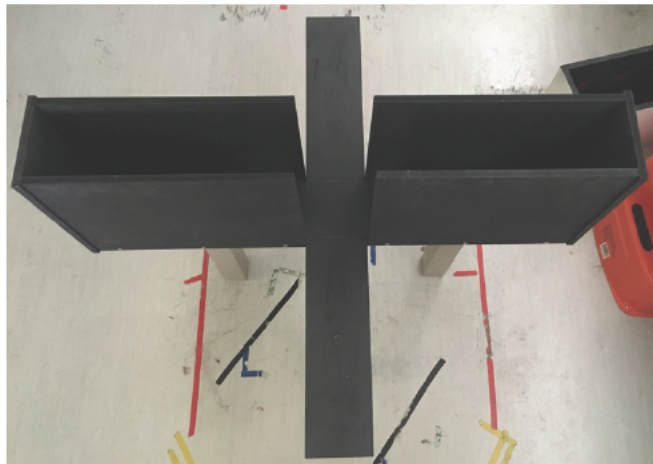


**Figure 2.4: Representative photograph of the Elevated Plus Maze, with the open arms visible vertically, and the closed arms visible horizontally.**

## Y-Maze

The Y Maze is a measure of hippocampal dependent spatial and recognition memory (Conrad et al., 1996). The maze consists of a Y shaped device which consists of 3 arms: the start, other and novel arms (Figure 2.5). For the first trial, the novel arm was closed off, with rats placed in the start arm and given 3 minutes to explore the start and other arms. An hour later, the rats were placed back in the start arm, now with the novel and other arms open, and given 3 minutes to explore. The amount of time spent exploring each arm was recorded. Rats will typically spend more time in the novel arm than the start and other arms in the second trial, however this will not be the case for rats displaying deficits in spatial and recognition memory.

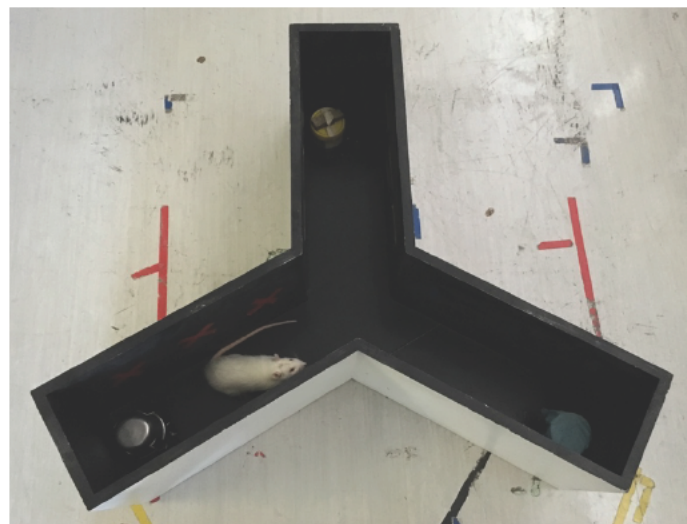


**Figure 2.5: Representative photograph of the Y-Maze during the second phase of the trial with all three arms accessible. At the end of each arm is a container covered in a metal dish, a piece of foam and a plastic glove as viewed clockwise from left. These provide the animals with spatial information and an incentive to keep exploring**

## Barnes Maze

The Barnes Maze aims to assess learning and memory (Barnes, 1979). The maze consists of a 1.2 metre diameter circular base with 18 escape holes around the circumference (Figure 2.6). An escape box is located underneath one of the escape holes. Rats were placed in the centre of the maze, a flood light was turned on to act as an aversive stimulus, and the time taken to find the escape box was recorded. Once rats found the location of the escape box, the flood light was turned off, and the time taken to find the escape box is recorded. Rats underwent two trials, 15 minutes apart, each day for 3 days. On day 5 of testing, following a rest day on day 4, the location of the escape box was moved 90° to test cognitive flexibility. Rats underwent two trials, 1 hour apart, and the time taken to find both the old and new escape boxes were recorded.



**Figure 2.6: Representative photograph of the Barnes Maze showing the circular maze with 18 escape holes around the circumference, and an escape box located underneath one (visible to far right of image).**

## Forced Swim Test

The Forced Swim Test aims to measure depressive like behaviour (Yankelevitch Yahav et al., 2015). A cylindrical vase (25 x 60cm) was filled to a depth of 30cm with water between 23-25° Celsius, before rats were placed in the cylinder for 5 minutes and required to swim (Figure 2.7). The time spent swimming versus immobility/floating was recorded. Rats displaying a higher level of depressive like behaviour will likely spend more time immobile. Rats are removed from the water, towel dried, and placed on a 37° Celsius heat pad to recover.

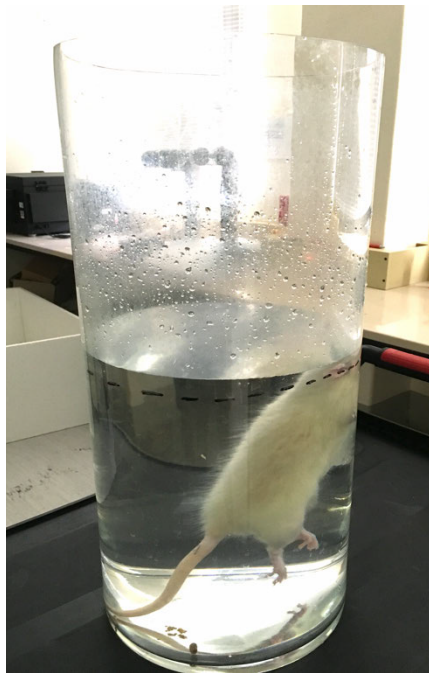


**Figure 2.7: Representative photograph showing the Forced Swim Test cylindrical vase.**

## **2.5 Perfusions & Tissue Extraction**

All animals were sacrificed humanely following ethical guidelines. For experiments in Chapters 4 and 5, all brain tissue was formalin fixed. For experiments in Chapter 6, brain tissue was both formalin fixed and fresh snap frozen in liquid nitrogen.

### **2.5.1 Formalin Fixed Tissue**

At pre determined time points post TBI, animals were anaesthetised with 5% isoflurane (2L/min of O<sub>2</sub>) of isoflurane for 5 minutes. Upon the absence of pain reflexes, animals were transcardially perfused with 10% formalin. Fixed bodies were allowed to rest for a minimum of 1 hour, before fixed brains were extracted and placed in containers of formalin to continue emersion fixation for a minimum of 7 days. Fixed brains were sectioned into 2mm coronal sections and embedded in paraffin wax.

### **2.5.2 Fresh Snap Frozen Tissue**

At pre determined time points post TBI, animals were anaesthetised with 5% isoflurane (2L/min of O<sub>2</sub>) of isoflurane for 3 minutes. Upon the absence of pain reflexes, the heart was exposed, and arterial blood was taken from the aorta. Animals were then transcardially perfused with sodium chloride solution (Baxter). Brains were extracted immediately and dissected to remove the left and right frontal cortex, the corpus callosum and the left and right hippocampus, before being snap frozen in liquid nitrogen. Blood samples were

centrifuged at 1000 relative centrifugal force (RCF) at 4° Celsius for 10 minutes before plasma was removed and stored alongside brains at 80° Celsius.

## **2.6 Histological Analysis**

Histological analysis of brain tissue in Chapters, 4, 5 and 6 was undertaken using immunohistochemistry (IHC). IHC is a semi quantitative method of analysis that allows visualisation of intact tissue and cellular architecture, distribution and appearance in paraffin fixed tissue (Duraiyan et al., 2012). IHC was performed on 5µm coronal slices and performed following standard procedure. Following overnight incubation with the appropriate primary antibody (Table 2.3), slides were incubated with the appropriate secondary antibody (1:250, Vector), before incubation with streptavidin peroxidase conjugate (SPC – 1:1000). This was followed by antigen detection with 3,3' Diaminobenzidine tetrahydrochloride (DAB) for 7 minutes, and sections counterstained with haematoxylin. Sections were digitally scanned using the Nanozoomer slide scanner (*Hamamatsu*, Hamamatusu City, Shizuoka, Japan), and the associated software (NDPview) used to view and analyze the images. All histological counts were done blinded by two assessors and minimal inter observer variation was found.

**Table 2.3: IHC antibodies analysed and their functions**

<b>Antibody</b>	<b>Target</b>	<b>Brain Region Analysed</b>	<b>Dilution</b>	<b>Species</b>	<b>Manufacturer</b>
APP (22C11)	Axonal injury	Corpus callosum	1:1000 Citrate	Anti mouse	Boehringer
Iba1	Total & activated microglia	Cortex, corpus callosum	1:2000 Citrate	Anti rabbit	Wako (019 19741)
GFAP	Astrocytes	Cortex, corpus callosum	1:40,000 Citrate	Anti rabbit	Dako (Z0334)

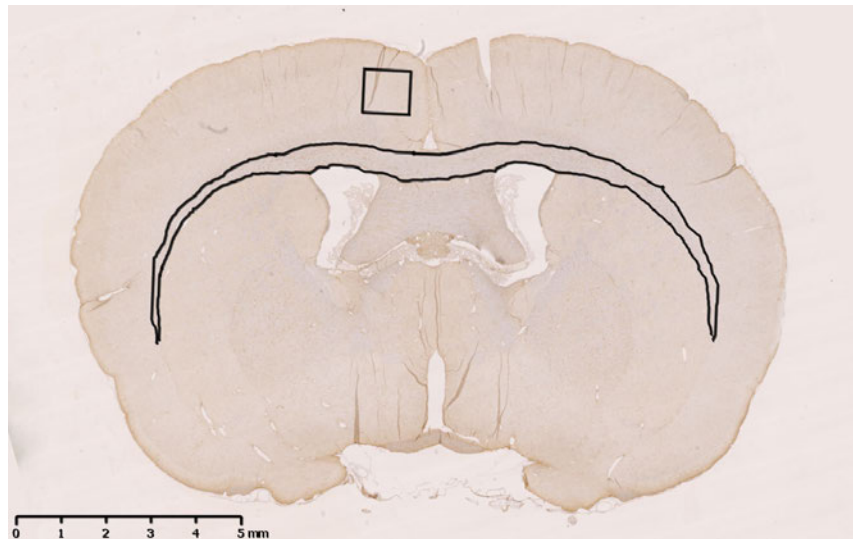


**Figure 2.8: Representative image demonstrating the regions of the cortex and corpus callosum that were used for IHC analysis.**

### **2.6.1 Axonal Injury**

APP is frequently used as a highly sensitive marker of DAI (Gentleman et al., 1993, Blumbergs et al., 1994). Damage and stretching of axons through injury results in localised intra axonal changes to the axolemma, disrupting fast axonal transport and facilitating accumulation of APP, which can be observed as early as 30 minutes following trauma (Finnie and Blumbergs,



2002). Consequently, APP accumulations or swellings can be observed at the site of damage, and are easily detectable via IHC (Gentleman et al., 1993, Blumbergs et al., 1994). The extent of DAI in these experiments was assessed by counting the number of APP immunopositive (APP+) lengths throughout the entire length of the corpus callosum (Figure 2.8).

### 2.6.2 Microglia

Both the total number as well as activated microglia were visualized using an Iba1 antibody. Iba1 immunoreactivity was determined by counting all microglia within a 1mm<sup>2</sup> area in cortex under the impact site, and throughout the entire length of the corpus callosum, to give an indication of total microglia present (Figure 2.8). This was followed by assessment of morphology to count the number of activated microglia within the same regions. Activated microglia can exhibit a number of different morphological characteristics, including changes to the size of the cell body and processes (Olah et al., 2011, Davis et al., 1994, Donat et al., 2017). Microglia demonstrating an increase in length, number and thickness of their processes were of most importance for this study (Figure 2.9).

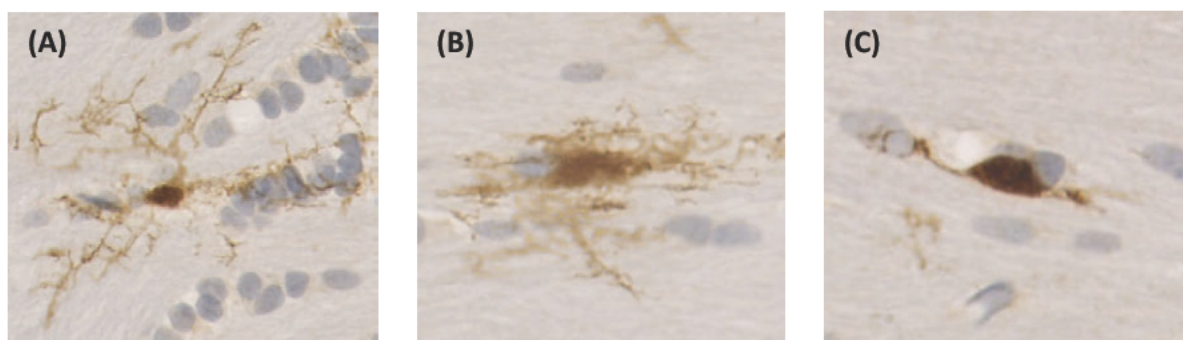


**Figure 2.9: Representative images demonstrating the morphological differences between microglia activation states. Image (A) demonstrates ramified resting microglia with long, thin processes, while images (B) and (C) demonstrate hyper-ramified activated microglia with retracted processes and enlarged cell bodies.**

### 2.6.3 Astrocytes

Reactive astrocytes were visualised using a GFAP antibody, as GFAP protein expression is increased in astrocytes as they become reactive (Karve et al., 2016). GFAP immunoreactivity was determined by assessing morphology and subsequently counting the number of reactive astrocytes within a  $1\text{mm}^2$  area in the cortex under the impact site, and throughout the entire length of the corpus callosum (Figure 2.8). Similar to microglia, astrocytes can exhibit changes in morphology between their unreactive and reactive states, including the presence of a halo like structure surrounding the nucleus, as well as changes in size and length of their processes (Karve et al., 2016). Astrocytes demonstrating a dark & thick halo like structure surrounding their nucleus, as well as an increase in thickness and retraction of their processes were of most importance for this study (Figure 2.10).

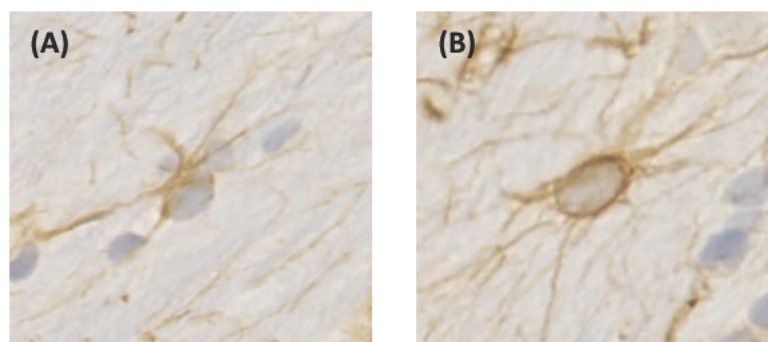


**Figure 2.10: Representative images demonstrating the morphological differences between astrocytes. Image (A) demonstrates an unreactive astrocyte with star-like processes, while image (B) demonstrates a reactive astrocyte with GFAP upregulation producing a hallmark 'halo' surrounding the cell body.**

## 2.7 Western Blot Analysis

Protein analysis of 30 day fresh snap frozen tissue in Chapter 6 was undertaken using Western Blot (WB) (Table 2.4). Protein from fresh tissue was extracted in standard RIPA buffer, with the protein concentration estimated with a Pierce BCA Protein Assay (Thermoscientific). Gel electrophoresis was performed using Bolt 4–12% Bis Tris Plus gels (Life Technologies) with 30µg of protein loaded per well. Gels were run at 100 volts for 2 hours, depending on the molecular weight of the protein of interest, and transferred to a PVDF membrane using the iBlot 2 Dry Blotting System in accordance with the manufacturer's instructions (Life Technologies). Membranes were stained with Ponceau S red solution (Fluka Analytical) for 2 minutes for visual inspection to ensure equal protein loading in each well. Membranes were then washed in 1X tris buffered saline with tween (TBST) (3 washes × 5 minutes) until adequate removal of Ponceau S solution. Membranes were then incubated in 5% skim milk solution (5g skim milk powder, 100mL TBST) for 30 minutes to block endogenous peroxidases, before application of the desired primary antibodies and housekeeper antibody. Membranes were then incubated in 2% skim milk solution (1g skim milk powder, 50mL TBST) overnight with the primary antibodies and housekeeper protein, which were used at individually optimized concentrations (refer to table 2.4). Overnight incubation was undertaken on a rotating device at 4° Celsius to ensure adequate coverage of the milk solution to the membranes.

The following day, membranes were washed 3 times in TBST (3 washes x 5 minutes), before incubation with the appropriate secondary antibodies in 2% skim milk solution for one hour

(refer to table 2.4). Membranes were covered with aluminum foil on a rotating device at room temperature.

Western Blots were imaged using an Odyssey Infrared Imaging System (model 9120; software version 3.0.21) (LI COR, Inc.) at a resolution of 169 $\mu$ m. Analysis was performed using ImageJ version 1.49 and Image Studio Lite version 5.2. The same control sample was run on each gel, with expression of protein normalized to the housekeeper and to this loading control. Analysis was done by a blinded observer with all protein extraction samples labelled with a code for loading onto gels until completion of analysis which (Collins Praino et al., 2018).

**Table 2.4: Western blot antibodies analysed and their functions**

<b>Antibody</b>	<b>Target</b>	<b>Brain Region</b>	<b>Dilution</b>	<b>Species</b>	<b>Manufacturer</b>
PSD 95	Dendrites	Cortex & hippocampus	1:1000	Anti mouse	Abcam (ab18258)
Synaptophysin	Synapses	Cortex & hippocampus	1:500	Anti rabbit	Abcam (ab32127)
Neurofilament (NFL)	Axonal cytoskeletal	Cortex & hippocampus	1:1000	Anti chicken	Abcam (ab72997)
Myelin basic protein (MBP)	Myelin	Cortex & hippocampus	1:1000	Anti mouse	Abcam (ab62631)
Tau 5	Total tau	Cortex & hippocampus	1:1000	Anti mouse	Calbiochem/Millipore (577801)
GAPDH	Housekeeper	Cortex & hippocampus	1:1000	Anti chicken	Abcam (ab83956)

## 2.8 Statistical Analysis

All data were analyzed using Graph Pad Prism software. All values are displayed as Mean  $\pm$  SEM, with a significance level of  $p < 0.05$ . All parametric data were assessed using analysis of variance (ANOVA): one or two way or repeated measures, as necessary, followed by Tukey's or Brown Fostythe post tests for multiple comparisons. Individual tests will be described in detail in the relevant chapters.

## **Chapter 3: Materials & Methods Part II: Troubleshooting**

### 3.1 Introduction

During the last 3 5 years, our laboratory has witnessed a gradual but noticeable decline in injury severity in Sprague Dawley (SD) rats following the Marmarou impact acceleration model of moderate severe TBI, as measured by functional outcome tests and histology. This lack of injury has been evident in a number of our unpublished results (Figure 3.1), with animals displaying noticeable reductions in motor deficits, and only minimal AI, similar to that seen following a mild moderate TBI (McAteer et al., 2016). Both significant motor deficits and widespread AI are hallmark features of rodent moderate severe diffuse TBI and are used as firm markers to assess the severity of injury, without which confident conclusions regarding treatment effects cannot be drawn.

The strain of species used in experimental models is often not considered during study design, but may ultimately be a confounding factor in experimental research (Brower et al., 2015). Due to the consistency of all other facets of our experimental procedure to induce TBI, it was hypothesized that the strain of SD and/or the breeding methods used may have been significantly impacting the severity of injury produced in our laboratory. As such, this chapter dealing with troubleshooting will discuss these issues in depth.

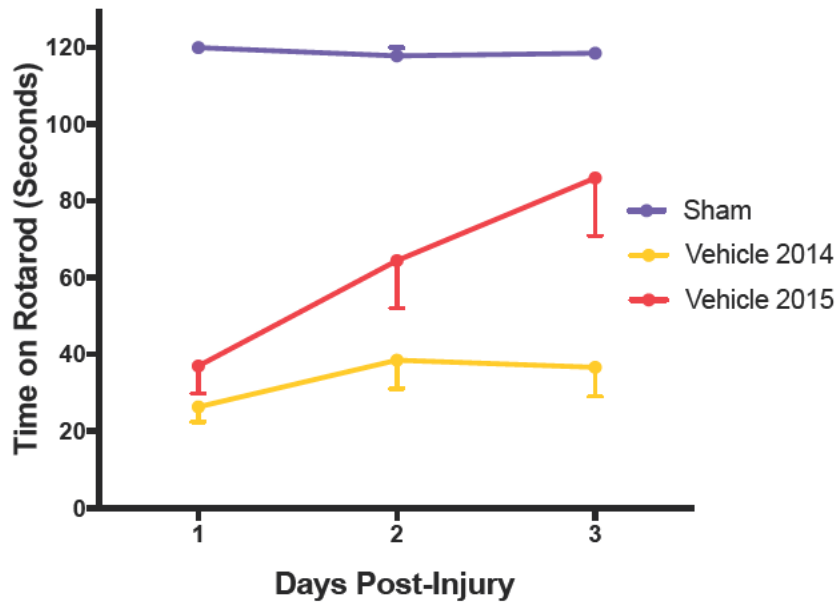


**Figure 3.1: A comparative image displaying the changes in motor outcome, and associated injury severity, over a period of 3 days over the course of the last 4 years in our laboratory. Image demonstrates 3 day motor performance between sham and vehicle control animals during 2014 and 2015.**

## 3.2 Animals

### 3.2.1 Sprague Dawley Rats

One of the most commonly used laboratory rats in experimental research is the SD rat, an albino outbred rat derived in the 1920s by breeding Wistar rats to hybrid rats of laboratory derived wild stocks (Brower et al., 2015). Over the years, a number of strains of SD rats have been developed with similar physical appearances, but subtle differences in anatomical and behavioural characteristics.



## **Harlan Strain**

Harlan strain SD rats were developed from the original SD stock in the 1980s by Harlan Laboratories, and have maintained their own SD stock since (Brower et al., 2015).

## **Charles River Strain**

The Charles River strain of SD rats were developed in the 1950s by Charles River Laboratories where original breeding pairs were re developed into a new breeding line, and believed to have superior microbial status due to caesarean derivation (Brower et al., 2015). While both the Charles River and Harlan strain SDs originated from the same stock, it is likely that these strains have drifted genetically over time due to differences in breeding practises (Brower et al., 2015). Studies have shown Charles River strain SDs to demonstrate a number of differences to other strains, in particular Harlan strain SDs. These differences include differences in growth rate and body composition, including a higher body fat mass, higher gross liver weight, lower testicular weight and lower cholesterol levels (Brower et al., 2015). Furthermore, a number of studies have demonstrated strain and sub strain differences between other laboratory rats like Wistars from different sources in a number of conditions including status epilepticus, and neurodegeneration (Honndorf et al., 2011, Langer et al., 2011). While these features are not directly relevant to the field of TBI research, it provides an insight into inter species genetic variability, and may ultimately affect experimental efficacy.

### **3.3 Pilot Study Examining Inter-Strain Differences Between Sprague Dawley Rats Following TBI**

A small study was carried out comparing Charles River strain SDs to our previously utilised Harlan strain SDs to examine the differences in response to TBI. Six male Charles River SDs were purchased from the Animal Resources Centre (ARC) in Perth, Australia weighing between 326 350g. Animals were group housed in a controlled temperature environment under a 12 hour light/dark cycle, with uninterrupted access to food and water.

Following a week acclimatization period following their arrival from Perth, and an additional week of pre training for motor assessments, animals were injured between 380 and 418g using the Marmarou impact acceleration model (previously described in Material & Methods Part I, section 2.3.2). Following TBI, animals were examined acutely post TBI to observe changes in both physical and motor outcome, with brain tissue examined to assess the extent of AI at 3 days post TBI. Outcomes from this study determined the most appropriate SD strain to use for the subsequent TBI studies.

### **3.4 Physical Outcome Prior to TBI**

The aforementioned discrepancies observed between Harlan and Charles River strain SDs in terms of body composition (Brower et al., 2015), meant it was essential that trauma with the injury device be re characterised with the new strain to ensure consistency and prevent premature death. Prior to trauma, Charles River strain SDs displayed a noticeable increase in age dependent body size compared to Harlan strain SD. Whilst both Harlan and Charles river

strain SDs were aged between 10-12 weeks for injury, their weights at this age differed considerably. Previously used Harlan strain rats weighed approximately 350-380g at this age, in contrast to Charles River strain SDs who weighed approximately 400-430g. These early observations are in keeping with findings that demonstrate significant differences in weekly mean body weight between Harlan and Charles River strain SDs at the same age (Brower et al., 2015). Indeed, the most significant increases in mean body weight in Charles River SDs occurred from approximately 10 weeks of age (Brower et al., 2015), highlighting differences between the two strains from the outset, before any experimental research even takes place.

### **3.5 Physical Appearances Following TBI**

A weight dependent effect on injury severity following TBI was observed in Charles River strain SDs, with a weight range of 380 – 418g used to induce moderate-severe TBI (Table 3.1). Following trauma, noticeable differences between the two strains remained evident. Charles River strain SDs displayed noticeable changes in their physical appearance, in keeping with that expected of a moderate-severe trauma, including substantial weight loss (averaging ~25g compared to ~18g with Harlan strain), the presence of a ruffled coat, hunched posture, stress marks, and hemiparesis (Figure 3.2). These features were rarely observed to this extent in Harlan strain SDs following trauma, with the absence of a ruffled coat and a lack of any stress marks or hemiparesis, highlighting differences not only in their response, but also the severity of injury they received.

**Table 3.1: Outcome of re-characterisation of optimal weights of SDs pre-injury to ensure consistency**

<b>Weight</b>	<b>Outcome Post-TBI</b>
380g	Brainstem bleed – Animal died
395g	Brainstem bleed – Animal died
413g	Weight loss, hunched posture, ruffled coat, paresis, stress marks
409g	Weight loss, hunched posture, ruffled coat, paresis, stress marks
418g	Weight loss, hunched posture, ruffled coat, paresis, stress marks
404g	Weight loss, hunched posture, ruffled coat, paresis, stress marks



**Figure 3.2: Injury severity of Charles-River SD 24 hours post TBI, as assessed by the clinical record sheet criteria. Image demonstrates evidence of severe hemiparesis and a ruffled coat, as expected following a genuine moderate-severe diffuse TBI.**

### 3.6 Motor Outcome Following TBI

Motor deficits post TBI were assessed using the rotarod, a sensitive test of motor ability following TBI (Hamm et al., 1994), which is routinely used in our laboratory (previously described in Materials & Methods Part I, section 2.4.1). Charles River SD rats demonstrated greater motor deficits when compared to Harlan strain SDs over the testing period, 27.7 seconds on day one and reaching 59.25 seconds by day 3. In contrast, Harlan strain SDs recorded 37 seconds on day one, reaching 86.25 seconds by day 3. Overall, the increased severity of injury seen in the Charles River SD rats compared to Harlan strain was reflected in the animals physical appearance, particularly the hemiparesis, that consequently produced greater motor deficits on the rotarod.

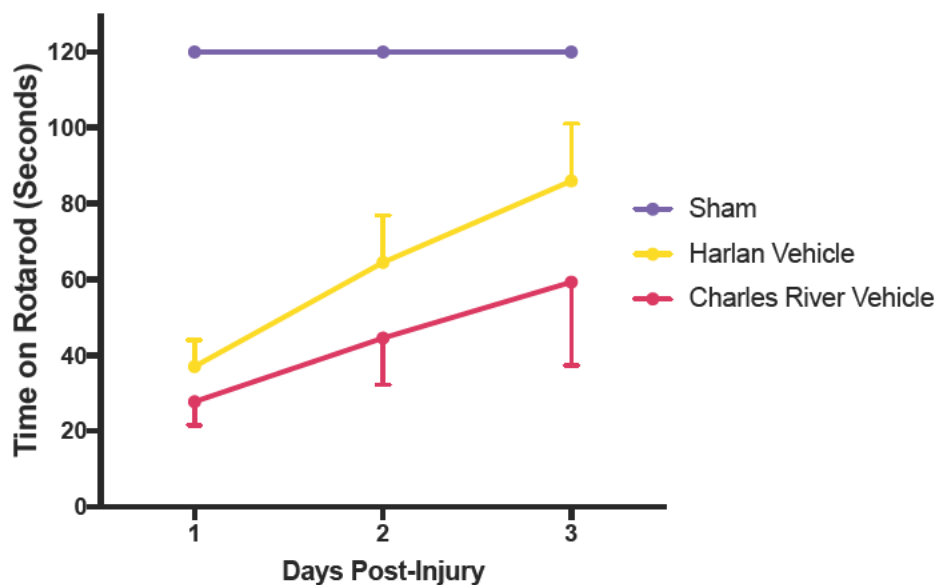


**Figure 3.3: 3 day motor outcome as assessed by the rotarod, illustrating the extent of injury severity post-TBI between Harlan strain and Charles-River strain SD rats. Sham animals are Harlan strain.**

### **3.7 Histological Outcome Following TBI**

While physical and motor outcomes are both key indications in injury severity post TBI, histological analysis of AI is fundamental, with motor performance previously shown to be associated with the extent of axonal injury post TBI (Thornton et al., 2006, Corrigan et al., 2012a). Histological analysis post TBI was assessed using IHC, with APP used as marker to indicate axonal injury (previously described in Materials & Methods Part I, section 2.6.1). Charles River strain SDs purchased directly from the supplier demonstrated considerably higher levels of AI compared to Harlan SDs, evident in both the absolute number of injured axons, as well as the distribution and spread throughout the corpus callosum (Figure 3.4).

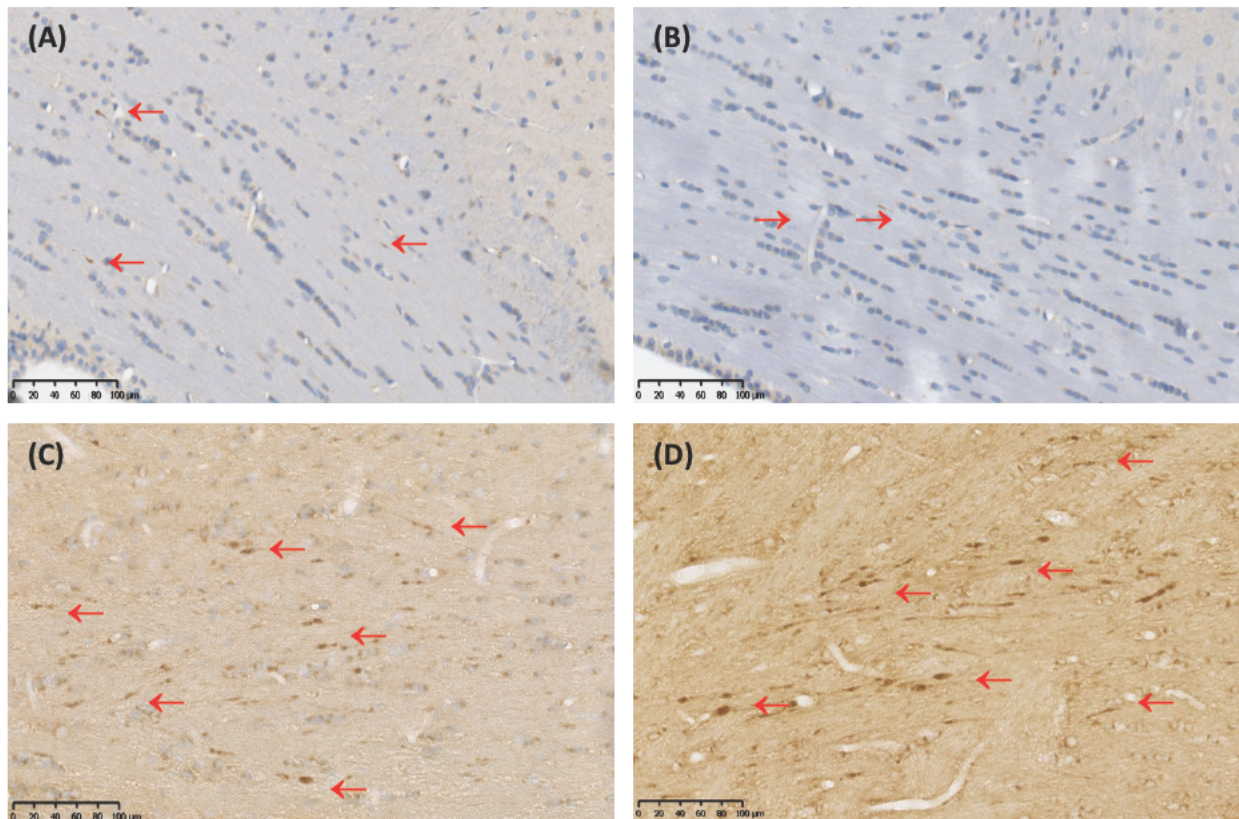


**Figure 3.4: Representative micrographs illustrating the extent of axonal injury in Harlan strain SDs post-TBI (A and B), compared with Charles River strain SDs (C and D). Scale = 40µm. Arrows indicate axonal injury. NB: Variation in background tissues A&B and C&D is due to batch variability.**

### 3.8 Establishment of a Charles River Strain Breeding Colony

The results from the aforementioned study clearly showed that Charles River strain SDS (at a weight of at least 400g) were needed to be used to obtain optimal levels of injury severity caused by the impact acceleration model of diffuse TBI. As such, a breeding colony for Charles River strain SDS was established at the University of Adelaide Animal House with rats bred through established breeding protocols. 12 breeding pairs were purchased from ARC in November 2015, and used to establish a colony using a modified outbred Poiley system. Both male and female breeders were randomly allocated to a colour group, with 3 breeding pairs per colour (Figure 3.5). This was critical to ensure that breeders were always matched with

an appropriate partner, ensuring the colony remained outbred. The first litter batches occurred in December 2015, with the first batch of animals ready for TBI at the age of 10-12 weeks. Fresh breeding pairs were purchased every 3-6 months to maintain the genetic line.

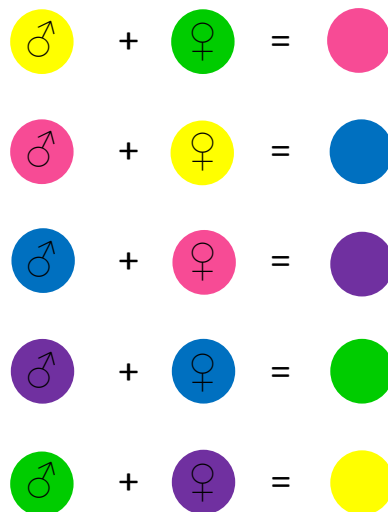


**Figure 3.5: The coloured protocol created for establishment of the modified outbred Poiley system.**

### **3.9 Long-term Efficacy of APP96-110 Following TBI in The Adelaide University Bred Charles-River Strain SD Rat**

Following the subsequent establishment of a Charles River SD breeding colony, a comprehensive study was undertaken that aimed to assess both the acute and long term efficacy of IV APP96-110 following a moderate-severe diffuse TBI. Animals were injured using the Marmarou impact acceleration model as previously described. At 5 hours post TBI, animals were treated with either saline vehicle control, 0.5mg/kg of an APP96-110 analogue (previously shown to show reduced efficacy post TBI) (Corrigan et al., 2014), 0.25mg/kg and



0.5mg/kg WT APP96 110, or 0.25mg/kg 3+APP96 110. Animals were euthanised at either 24 hours, 3 days, 7 days or 30 days post TBI (n=10 per treatment group, per timepoint), with brain tissue either perfusion fixed or fresh frozen. Rats participating in the long term efficacy study underwent both motor (Figure 3.6) and cognitive outcome testing (previously described in Materials & Methods Part I, section 2.4.2). Initially, physical and motor outcome of animals from the colony remained in keeping with that previously seen in the pilot study. However, over the course of the year, the outcome of the injured Charles River strain SDs appeared to improve, as injury severity declined (Figure 3.7). No differences in motor deficits were observed between vehicles and treatment groups over the 30 day testing period, with similar results seen across all cognitive tests undertaken (figures not shown).

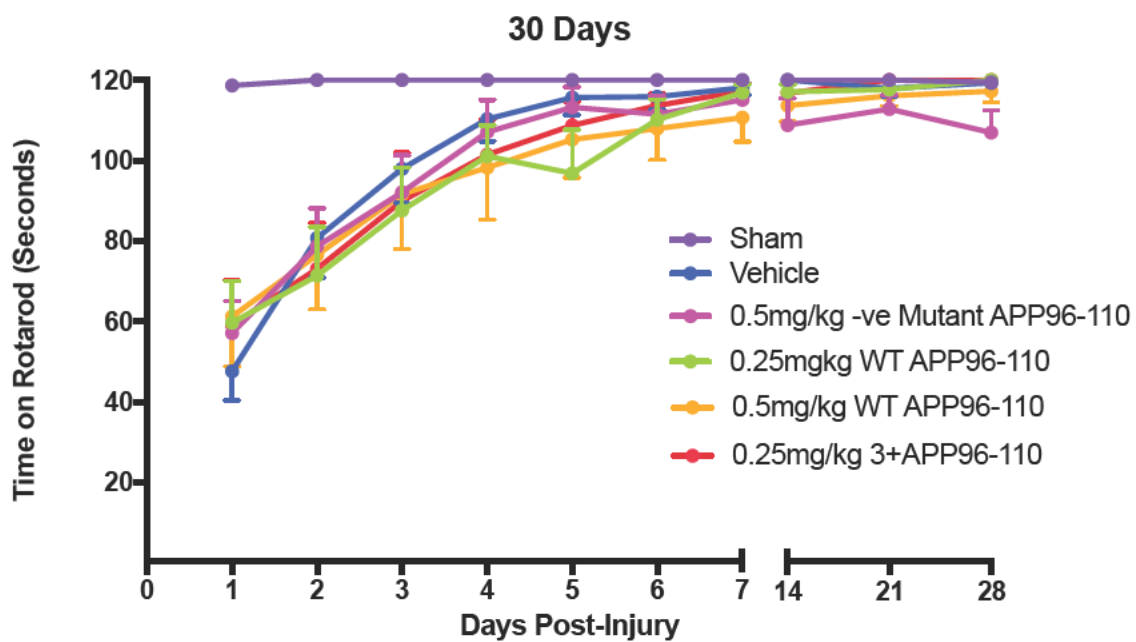


**Figure 3.6: 30 day motor outcome as assessed by the rotarod, illustrating the lack of motor deficits between all treatment groups with Charles River strain SDs bred from the established breeding colony in 2016. The lack of motor deficits between treatment groups is indicative of an insufficient moderate-severe TBI.**

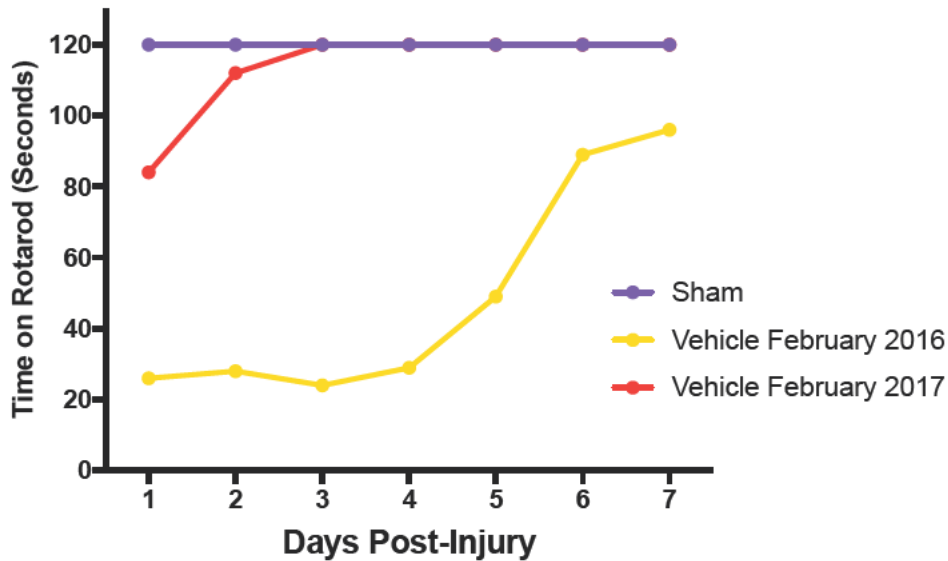


**Figure 3.7: 7 day motor outcome as assessed by the rotarod, illustrating the change in motor deficits, and therefore injury severity, over the course of one year following establishment of the Charles River breeding colony.**

### 3.10 Summary

The observations from these studies clearly demonstrate considerable differences between strains of SD rats post TBI, highlighting the critical role that the strain of rat used in TBI research can play in the success of experimental research. The exact causes of the inter strain differences in outcome seen during these studies is not understood. It may be that the individual breeding environment plays a critical role, influenced by factors including differences in diet and exposure to microbial pathogens, testing of which is beyond the scope of this thesis. Nonetheless, these studies have shown that Charles River strain SDs purchased directly from the supplier are required to produce the hallmark features of moderate severe diffuse TBI in our laboratory.

**Chapter 4: The Amyloid Precursor Protein Derivative,  
APP96-110, is Efficacious Following Intravenous  
Administration After Traumatic Brain Injury**

# Statement of Authorship

Title of Paper	The amyloid precursor protein derivative, APP96-110, is efficacious following intravenous administration after traumatic brain injury
Publication Status	<input type="checkbox"/> Published <input checked="" type="checkbox"/> Accepted for Publication As of 16/12/17 <input checked="" type="checkbox"/> Submitted for Publication <input type="checkbox"/> Unpublished and Unsubmitted work written in manuscript style
Publication Details	Plummer SL, Thornton E, Corrigan F, Woenig JA, Vink R, Cappai R and Van Den Heuvel C. (2017). The amyloid precursor protein derivative, APP96-110, is efficacious following intravenous administration after traumatic brain injury.

## Principal Author

Name of Principal Author (Candidate)	Stephanie L Plummer		
Contribution to the Paper	Conducted the entirety of experimental work, performed data analysis & interpretation, wrote the manuscript.		
Overall percentage (%)	80%		
Certification:	This paper reports on original research I conducted during the period of my Higher Degree by Research candidature and is not subject to any obligations or contractual agreements with a third party that would constrain its inclusion in this thesis. I am the primary author of this paper.		
Signature		Date	19/11/17

## Co-Author Contributions

By signing the Statement of Authorship, each author certifies that:

- i. the candidate's stated contribution to the publication is accurate (as detailed above);
- ii. permission is granted for the candidate to include the publication in the thesis; and
- iii. the sum of all co-author contributions is equal to 100% less the candidate's stated contribution.

Name of Co-Author	Dr Emma Thornton		
Contribution to the Paper	Conceptualisation of the work & research design, supervision of the work, assisted in data analysis & interpretation, and contributed to the writing of the manuscript.		
Signature		Date	26/11/17

Name of Co-Author	Dr Frances Corrigan		
Contribution to the Paper	Conceptualisation of the work & research design, supervision of the work, assisted in data analysis & interpretation, and contributed to the writing of the manuscript.		
Signature		Date	1/12/17

Name of Co-Author	Mr Joshua A Woenig		
Contribution to the Paper	Helped conduct experiments.		
Signature		Date	24/11/2017 ..

Name of Co-Author	Professor Robert Vink		
Contribution to the Paper	Helped conceptualise the work.		
Signature		Date	8/12/2017

Name of Co-Author	Professor Roberto Cappai		
Contribution to the Paper	Conceptualisation of the work & research design, assisted in data interpretation, and contributed to the writing of the manuscript.		
Signature		Date	3-Dec-2017

Name of Co-Author	A/Prof Corinna Van Den Heuvel		
Contribution to the Paper	Conceptualisation of the work & research design, supervision of the work, assisted in data analysis & interpretation, and contributed to the writing of the manuscript.		
Signature		Date	30/11/17

## 4.1 Abstract

Following traumatic brain injury (TBI) neurological damage is ongoing through a complex cascade of primary and secondary injury events in the ensuing minutes, days and weeks. The delayed nature of secondary injury provides a valuable window of opportunity to limit the consequences with a timely treatment. Recently, the amyloid precursor protein (APP) and its derivative APP96 110 have shown encouraging neuroprotective activity following TBI following an intracerebroventricular administration. Nevertheless, its broader clinical utility would be enhanced by an intravenous (IV) administration. This study assessed the efficacy of IV APP96 110, where a dose response for a single dose of 0.005mg/kg – 0.5mg/kg APP96 110 at either 30 minutes or 5 hours following moderate severe diffuse impact acceleration injury was performed. Male Sprague Dawley rats were assessed daily for 3 or 7 days on the rotarod to examine motor outcome, with a separate cohort of animals utilised for immunohistochemistry analysis 3 days post TBI to assess axonal injury and neuroinflammation. Animals treated with 0.05mg/kg or 0.5mg/kg APP96 110 after 30 minutes demonstrated significant improvements in motor outcome. This was accompanied by a reduction in axonal injury (AI) and neuroinflammation in the corpus callosum at 3 days post TBI, whereas 0.005mg/kg had no effect. In contrast, treatment with 0.005m/kg or 0.5mg/kg APP96 110 at 5 hours post TBI demonstrated significant improvements in motor outcome over 3 days, which was accompanied by a reduction in axonal injury in the corpus callosum. This demonstrates that APP96 110 remains efficacious for up to 5 hours post TBI when administered IV, and supports its development as a novel therapeutic compound following TBI.

## 4.2 Introduction

Traumatic brain injury (TBI) is a major public health concern, one which in industrialised countries leads to more deaths in people under the age of 45 than any other cause (Feigin et al., 2013). Following TBI, extensive neurological damage occurs through the initiation of multiple injury events, both immediately after and progressively from the initial injury. This delayed injury is a prolonged and deleterious cascade of cellular and biochemical events that often compound the existing injury including excitotoxicity, oxidative stress, irreversible cell injury and death, inflammation and blood brain barrier (BBB) disruption (Maas et al., 2008, Vink and Van Den Heuvel, 2004, Finnie and Blumbergs, 2002, Greve and Zink, 2009). Diffuse axonal injury (DAI), a significant feature of TBI, is the most common cause of coma and vegetative state following head trauma (Adams et al., 1989, Smith et al., 2003). Occurring as a result of rapid acceleration/deceleration forces, DAI causes considerable deformation of brain tissue through shearing forces and stretching, and currently lacks an efficacious pharmacological treatment. Many of these serious events could be reversed if targeted with an appropriate therapy, preventing serious complications and reducing the burden on society. Fortunately, the delayed onset and potentially reversible nature of these secondary events provides a novel window of opportunity for a therapy to reduce neuronal damage and help limit the associated morbidity and mortality of TBI (Vink and Van Den Heuvel, 2004). It has been proposed that upcoming therapeutic interventions should be multifactorial in nature and target multiple elements of the secondary injury cascade (Vink and Van Den Heuvel, 2004, Faden and Stoica, 2007, Vink and Nimmo, 2002). One frequently proposed approach is to emulate the brain's endogenous repair response.

It has been consistently demonstrated that the amyloid precursor protein (APP) and its derivatives are neuroprotective following experimental TBI (Thornton et al., 2006, Corrigan et al., 2011, Corrigan et al., 2012b, Corrigan et al., 2012a, Corrigan et al., 2014). Intracerebroventricular administration of APP was shown to ameliorate both motor and cognitive deficits, as well as attenuate cellular loss and inflammation following TBI *in vivo*. This makes APP a promising candidate to develop as a therapeutic treatment for TBI patients. APP undergoes distinct proteolytic events (Andrew et al., 2016), and the soluble APP $\alpha$  (sAPP $\alpha$ ) species, produced via proteolytic cleavage with  $\alpha$  secretase enzyme, is thought to be responsible for APP's neuroprotective properties following TBI, including protection against a range of cytotoxic insults, regulation of neurite outgrowth and synaptogenesis, and improvement in functional outcome *in vivo* (Bayer et al., 1999, Dawkins and Small, 2014, Plummer et al., 2016).

Domain mapping studies attributed the neuroprotective activity of sAPP $\alpha$  to the growth factor domains (Corrigan et al., 2011), with subsequent sequence activity studies able to localize the neuroprotective activity to the N terminal heparin binding region, encompassed by amino acid residues 96-110 (Corrigan et al., 2014). It was shown that APP96-110's neuroprotective activity correlated with its affinity for heparin (Clarris et al., 1997, Corrigan et al., 2011, Corrigan et al., 2014). Intracerebroventricular administration of APP96-110 was shown to not only restore motor and cognitive deficits, but also preserve cortical and hippocampal tissue in APP / mice, and reduce axonal injury in the corpus callosum following diffuse TBI in rats. This suggests that that APP96-110 could functionally substitute for native sAPP $\alpha$  (Corrigan et al., 2014).



Whilst these results using intracerebroventricular administration are promising and clinically relevant, the intravenous (IV) route of administration would provide a more tractable method of drug administration, especially in a paramedic setting where TBI victims will first encounter medical treatment. Accordingly, this study aimed to determine the efficacy of IV administered APP96 110, along with its therapeutic window, following moderate severe diffuse TBI. APP96 110 was firstly administered IV at 30 minutes after trauma, and its effects on motor outcome, the extent of DAI and neuroinflammation at 3 days were assessed. Secondly, delayed IV administration of APP96 110 at 5 hours post TBI was assessed to determine if APP96 110 would remain efficacious at a delayed but more clinically relevant time point.

## **4.3 Methods**

All studies were performed within the guidelines established by the National Health and Medical Research Committee of Australia and were approved by the Animal Ethics Committee of the University of Adelaide. All animals were purchased from the University of Adelaide breeding facility.

### **4.3.1 The APP96-110 Peptide**

The APP96 110 peptide, NWCKRGRKQCKTHPH, was synthesized by *Auspep* (Tullamarine, Victoria, Australia) and was N terminally acetylated and C terminally amidated. The peptide was dissolved into distilled water to produce a 1mM stock solution, and further diluted to produce doses of 0.005mg/kg, 0.05mg/kg and 0.5mg/kg APP96 110.

### **4.3.2 Evaluation of the Efficacy of IV APP96-110 Administered at 30 Minutes Following TBI**

#### **Injury Induction**

A total of 62 adult male Sprague Dawley rats weighing between 336g and 427g were group housed in a controlled temperature environment under a 12 hour light/dark cycle, with uninterrupted access to food and water. Animals were randomly assigned into 3 day histological and 7 day outcome groups, and each further assigned into sham, vehicle control, 0.005mg/kg, 0.05mg/kg and 0.5mg/kg APP96 110 treatment groups.

Animals were injured using the impact acceleration model of diffuse TBI (Marmarou et al., 1994). This injury model produces a range of injuries from moderate through to moderate–severe, and its heterogeneity provides a clinically relevant model to test neuroprotective therapeutics. Animals were anaesthetised with isoflurane and upon the absence of pain reflexes, a midline incision was made on the skull, a metallic disk (10mm in diameter and 3mm in depth) was adhered onto the skull centrally between lambda and bregma sutures. Animals were placed on a foam bed of 10cm height, and injured by releasing a 450g weight from 2 meters onto the metallic disk (Marmarou et al., 1994). The model of TBI is associated with a period of apnea. To regulate this and replicate what occurs clinically, animals were ventilated directly after injury whilst introducing a period of post traumatic hypoxia with 2L/min of nitrogen and 0.2L/min of oxygen (Hellewell et al., 2010). Post traumatic hypoxia has been previously shown to exacerbate both AI and inflammation, and can often be attributed to poor neurological outcome post TBI (Hellewell et al., 2010). Sham animals were surgically prepared but not injured and did not receive hypoxia. The use of general anaesthetics and

the absence of pain receptors in the brain means injury to the brain tissue is not painful for the animals. However, the initial skin incision on the scalp required to adhere the metallic disk can cause minor discomfort in the initial 24 hours post surgery. As such, all animals received 0.2mL subcutaneous Lignocaine under the incision site at the end of the procedure to minimize pain and discomfort.

At 30 minutes following TBI, animals were administered either saline, 0.005mg/kg, 0.05mg/kg or 0.5mg/kg APP96 110 intravenously via the tail vein by a blinded observer, and returned to their home cage to recover once normal behaviour was established. Intensive continuous monitoring of the animals was provided for the first 2 hours post procedure and animals were then checked at least hourly for the next 4 hours. If signs of clinical deterioration were evident, the frequency of monitoring was adjusted accordingly so that appropriate intervention could occur. Following this initial period, animals were monitored twice daily with clinical record sheets maintained to assess the following criteria: daily weight loss, appearance and texture of their coats, posture, changes in social behaviour, as well as the presence or absence of stress marks, circling behaviour, operation site swelling, and paresis. Weight loss of greater than 5 10% of their pre surgical body weight were treated with subcutaneous saline to prevent dehydration. Overall, 9 animals died shortly following the trauma, with a further 9 animals euthanized prior to the end of experiments in accordance with ethical guidelines.

### **Assessment of Motor Outcome**

Motor deficits post TBI were assessed using the rotarod, a sensitive test of motor ability following TBI (Hamm et al., 1994). Briefly, the rotarod comprises of 18 rotating metallic rods on which the animal is required to balance and walk. The speed of the rotarod is increased

from 6 to 36 rpm in intervals of by 3 rpm every 10 seconds. Animals were pre trained daily on the rotarod for 5 days until they could complete 120 seconds, and were then assessed daily for 7 days post injury. The length of time in seconds that animals were successfully able to walk on the rotarod post injury was recorded.

### **Histological Assessment**

At 3 days post TBI, animals were anaesthetised with isoflurane, and upon the absence of pain reflexes, were transcardially perfused with 10% formalin. Animals were perfused at 3 days rather than 7, as the most significant improvements in motor outcome were observed within the first 3 days following trauma. Fixed brains were sectioned into 2mm coronal slices and embedded in paraffin wax, before the brain region containing the area under the impact ( 0.40mm relative to Bregma) was further sectioned into 5µm coronal slices for representative serial sections. Immunohistochemistry was performed following standard procedure with sections stained for APP for axonal injury (22C11; Boéhringer, 1:1000), glial fibrillary acidic protein (GFAP; Dako, 1:40,000) and Iba1 (Wako, 1:10,000). Following overnight incubation with the primary antibody, slides were then incubated with the appropriate secondary antibody (1:250, Vector), before incubation with streptavidin peroxidase conjugate (SPC – 1:1000). This was followed by antigen detection with 3,3' Diaminobenzidine tetrahydrochloride (DAB) for 7 minutes, and sections counterstained with haematoxylin. Sections were digitally scanned using the Nanozoomer slide scanner (*Hamamatsu*, Hamamatusu City, Shizuoka, Japan), and the associated software (NDPview) used to view and analyze the images. The extent of DAI was assessed by counting the number of APP immunopositive (APP+) lengths in the entire length of the corpus callosum (from left to right)

of two consecutive brain sections per animal, where each animal represents a 10µm area of the corpus callosum. This area is directly under the impact site ( 0.40mm relative to Bregma), and was chosen as this region has previously demonstrated the highest degree of axonal injury.

GFAP and Iba1 immunoreactivity was determined by assessing morphology (previously described in Materials & Methods Part I, sections 2.6.2 & 2.6.3). The number of reactive astrocytes and activated microglia were counted within the same region of the corpus callosum of two consecutive brains sections per animal, as with APP histology. All histological counts were done blinded by two assessors using strict criteria, and minimal inter observer variation was found.

### **4.3.3 Evaluation of the Efficacy of IV APP96-110 Administered at 5 Hours Following TBI**

A total of 40 adult male Sprague Dawley rats weighing between 361g and 427g were randomly assigned into 3 day sham, vehicle control, 0.05mg/kg and 0.5mg/kg APP96 110 treatment groups. The APP96 110 peptide was manufactured as described above, and animals were again injured using the impact acceleration model of diffuse TBI as described above (Marmarou et al., 1994). 4 animals died shortly following the trauma, with the remaining animals monitored appropriately in accordance with ethical guidelines as previously described. Sham animals were surgically prepared but not injured. At 5 hours following TBI, animals were administered either saline, 0.05mg/kg or 0.5mg/kg APP96 110 intravenously via the tail vein by a blinded observer, before being returned to their home cage to recover once normal behaviour was established. Motor outcome and histological

assessments were carried out as previously described.

#### **4.3.4 Statistical Analysis**

All data were analyzed using Graph Pad Prism software. All values are displayed as Mean  $\pm$  SEM, with a significance level of  $p < 0.05$ . Motor outcome was assessed using a two way repeated measures ANOVA with Tukey's post test. DAI and the number of reactive astrocytes and activated microglia were by assessed using a one way ANOVA with Tukey's post test.

### **4.4 Results**

#### **4.4.1 Examining the Efficacy of IV APP96-110 Administered at 30 Minutes Following TBI**

##### **Administration of APP96-110 was Efficacious on Motor Outcome**

Motor outcome post TBI was assessed using the rotarod (Figure 4.1). Sham animals (n=7) demonstrated normal motor abilities over the testing period, recording 120 seconds on all 7 days post injury. In contrast, vehicle control animals showed significant motor deficits when compared to shams on days 1 to 3 post TBI ( $p < 0.01$ , n=9). Animals treated with 0.005mg/kg APP96 110 (n=9) performed similarly to vehicles, and were significantly different to shams on days 1 to 4 post injury ( $p < 0.05$ ). However, treatment with both 0.05mg/kg (n=9) and 0.5mg/kg (n=7) APP96 110 improved motor outcome over 7 days, as these animals only recorded significant motor deficits different to sham animals on days 1 and 2 post injury ( $p < 0.05$ ).

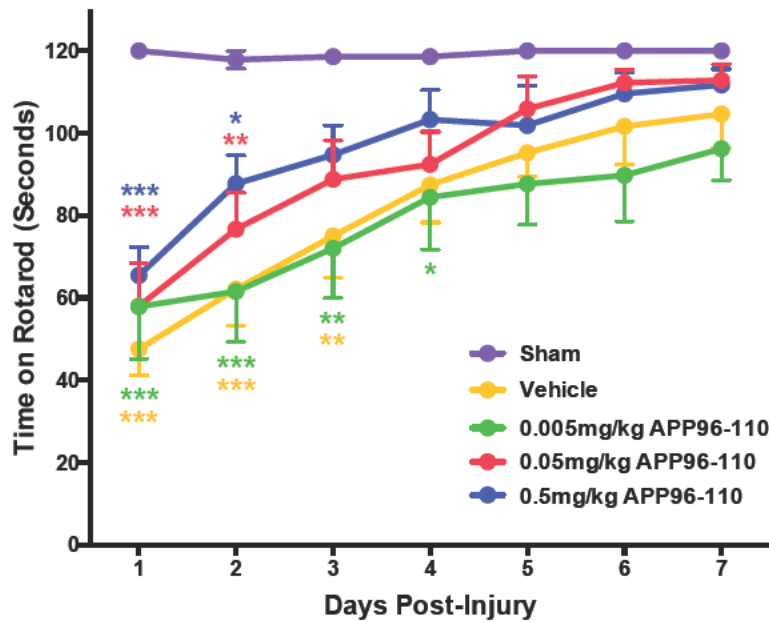


Figure 4.1: Motor outcome illustrating the effect of treatment with 0.005mg/kg, 0.05mg/kg and 0.5mg/kg APP96-110 IV at 30 minutes post-TBI. Data were assessed using a two-way repeated measures ANOVA with Tukey's post-test. (Sham n=7, vehicle n=9, 0.005mg/kg n=9, 0.05mg/kg n=9, 0.5mg/kg n=7, per group). (\*\*p<0.01, \*\*\*p<0.001, \*\*p<0.05, compared to sham animals).

#### APP96-110 Administration After TBI Reduced Axonal Injury

The finding that only the 0.05mg/kg and 0.5mg/kg doses of APP96 110 were able to significantly improve motor outcome, led us to analyze these doses in histological studies for AI and neuroinflammation at 3 days post TBI.

The extent of DAI was determined by counting the number of APP immunopositive lengths within the corpus callosum at 3 days post TBI (Figure 4.2). APP is a robust marker for assessing AI (Gentleman et al., 1993). A significant increase in APP immunoreactivity was observed in vehicle control animals at 3 days post TBI ( $161 \pm 19$ ,  $p < 0.001$ ,  $n = 4$ ) when compared to sham animals ( $p < 0.001$ ,  $n = 5$ ). Administration of both doses of APP96 110 showed a reduction in

DAI post TBI, however, a significant reduction compared to vehicle animals was only recorded in the 0.05mg/kg dose ( $79\pm 19$ ,  $p<0.05$ ,  $n=5$ ), and not the 0.5mg/kg dose ( $124\pm 21$ ,  $n=4$ ).



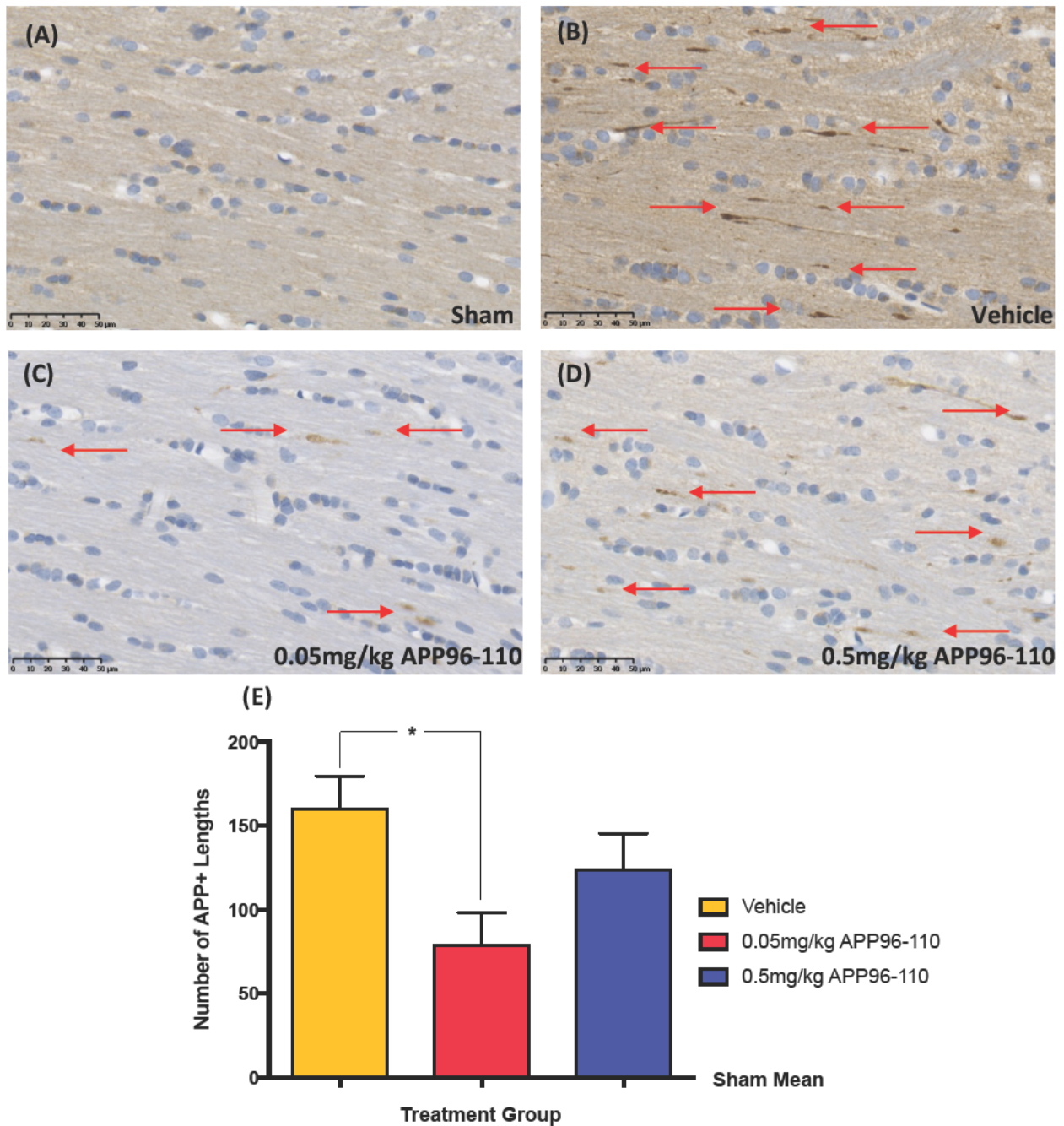


**Figure 4.2: Representative micrographs showing the degree of DAI in the corpus callosum at 3 days following diffuse TBI (A-D). 0.05mg/kg (C) and 0.5mg/kg (D) APP96-110 treated animals demonstrated a reduced number of APP immunopositive lengths in the corpus callosum at 3 days following injury, compared to vehicle treated animals (B), with 0.05mg/kg APP96-110 treated animals showing the most pronounced reduction. These observations were confirmed with counts of the number of APP immunopositive lengths (E). Data were assessed using a one-way ANOVA with Tukey's post-test. (Sham n=5, vehicle n=4, 0.05mg/kg n=5, 0.5mg/kg n=4) (\*p<0.05, compared to vehicle control animals).**

### **APP96-110 Administration after TBI Reduced Neuroinflammation**

Neuroinflammation was assessed by counting the number of reactive astrocytes and activated microglia within the corpus callosum at 3 days post TBI (Figures 4.3 & 4.4). GFAP immunoreactivity (Figure 4.3) demonstrated a significant increase in the number of reactive astrocytes within the corpus callosum in vehicle control animals ( $243\pm 11$ ,  $n=5$ ) at 3 days post TBI when compared to sham animals ( $174\pm 10$ ,  $p<0.01$ ,  $n=4$ ). Treatment with both 0.05mg/kg ( $n=5$ ) and 0.5mg/kg ( $n=4$ ) doses of APP96 110 demonstrated significant reductions in GFAP immunoreactivity ( $170\pm 9$  and  $172\pm 6$ , respectively), compared to vehicle control animals ( $p<0.001$ ), with levels similar to that seen in shams.

These astrocytic changes were mirrored by Iba1 immunoreactivity (Figure 4.4) where a significant increase in the number of microglia was observed in the corpus callosum of vehicle control animals ( $127\pm 7$ ,  $n=5$ ) at 3 days post TBI when compared to sham animals ( $85\pm 4$ ,  $p<0.01$ ,  $n=4$ ). Notably, animals treated with both the 0.05mg/kg ( $n=5$ ) and 0.5mg/kg ( $n=4$ ) doses of APP96 110 also demonstrated a return to sham level, with significant reductions in the number of activated microglia in both treatment groups,  $92\pm 4$  and  $82\pm 1$ , respectively ( $p<0.001$ ), when compared to vehicle control animals.

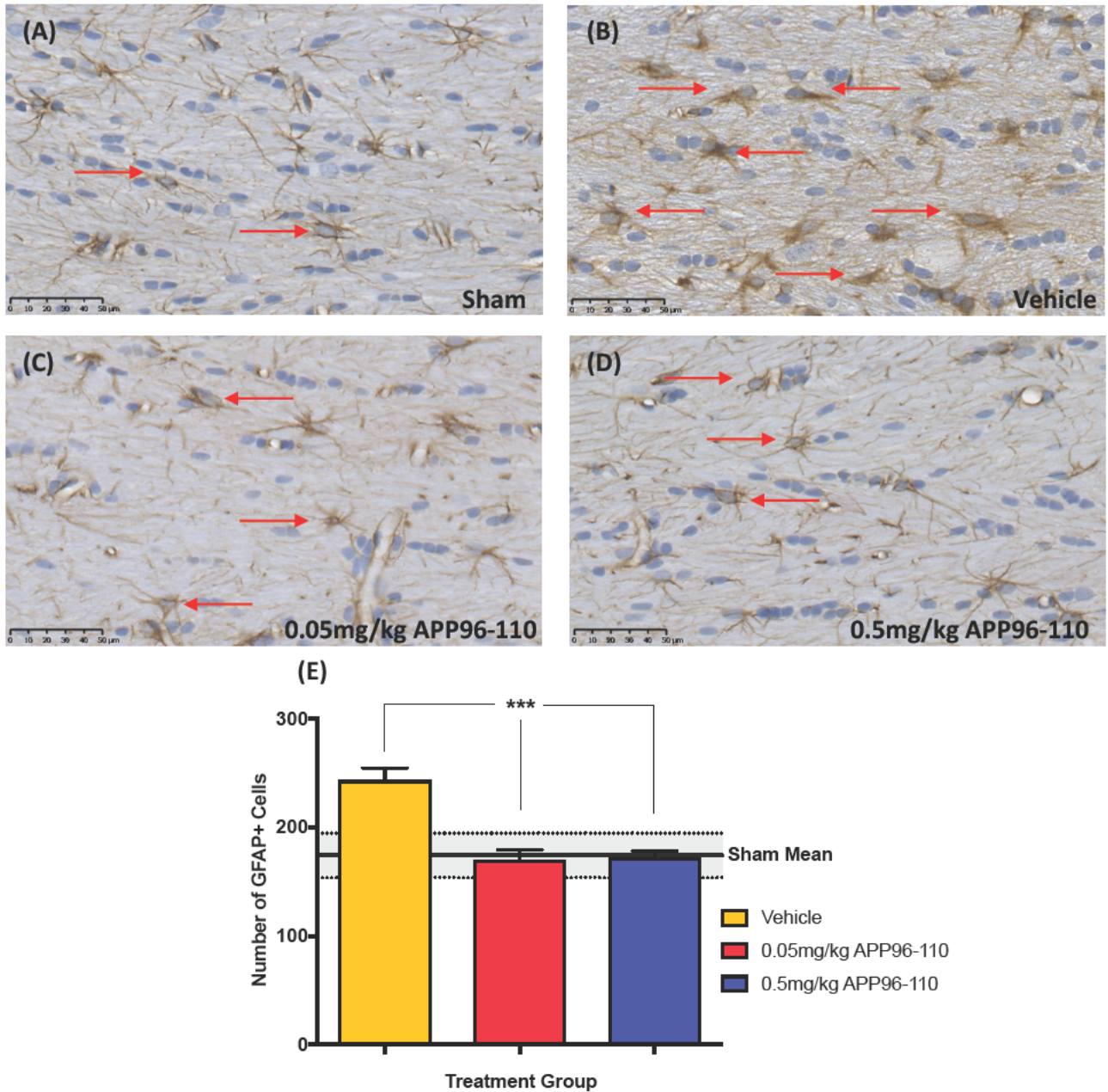


**Figure 4.3: Representative micrographs showing the degree of neuroinflammation in the corpus callosum at 3 days following diffuse TBI, as assessed by GFAP immunoreactivity (A-D). 0.05mg/kg (C) and 0.5mg/kg (D) APP96-110 treated animals demonstrated a clear reduction in the number of reactive astrocytes in the corpus callosum at 3 days following injury, compared to vehicle treated animals (B). These observations were confirmed with counts of the number of reactive astrocytes (E). Data were assessed using a one-way ANOVA with Tukey's post-test. (Sham n=4, vehicle n=5, 0.05mg/kg n=5, 0.5mg/kg n=4) (\*\*\*) $p < 0.001$ , compared to vehicle control animals).**

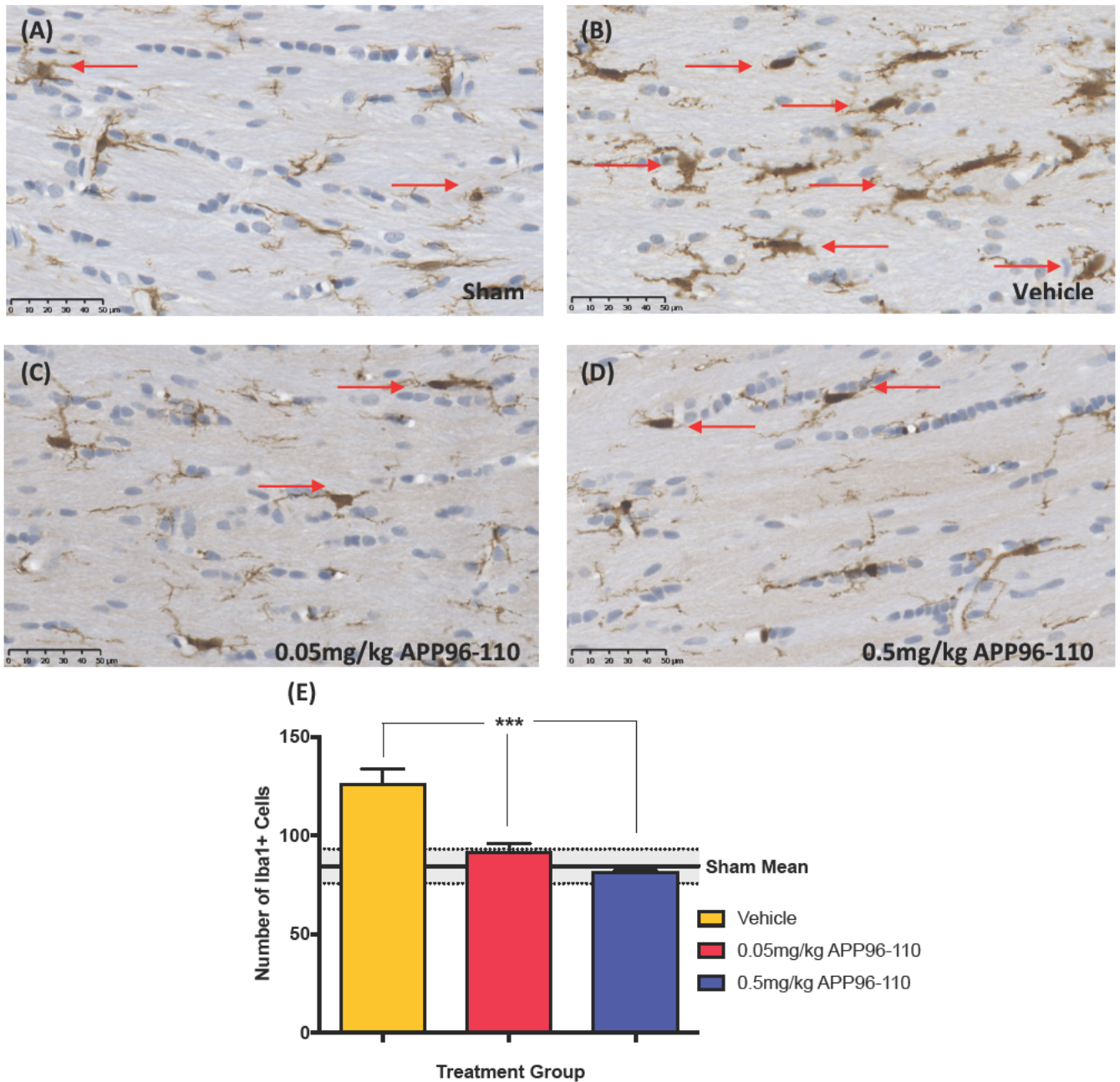


**Figure 4.4: Representative micrographs showing the degree of neuroinflammation in the corpus callosum at 3 days following diffuse TBI, as assessed by Iba1 immunoreactivity (A-D). 0.05mg/kg (C) and 0.5mg/kg (D) APP96-110 treated animals demonstrated a profound reduction in the number of activated microglia in the corpus callosum at 3 days following injury, compared to vehicle treated animals (B). These observations were confirmed with counts of the number of activated microglia (E). Data were assessed using a one-way ANOVA with Tukey's post-test. (Sham n=4, vehicle n=5, 0.05mg/kg n=5, 0.5mg/kg n=4) (\*\*\*) $p < 0.001$ , compared to vehicle control animals).**

#### **4.4.2 Evaluation of the Efficacy of IV APP96-110 Administered at 5 Hours Following TBI**

In order to determine whether IV APP96 110 would remain efficacious if delivered at a later and more clinically relevant time point, injured rats were injected 5 hours post TBI. Rats were treated with either 0.05mg/kg or 0.5mg/kg APP96 110, as these doses were efficacious as determined above.

##### **Delayed Administration of APP96-110 Remained Efficacious on Motor Outcome**

As motor deficits were most pronounced on days 1 to 3 post injury (Figure 4.1), motor outcome was assessed on these days (Figure 4.5). Sham animals (n=7) demonstrated normal motor abilities over the 3 day testing period, recording 120 seconds on all 3 days post injury, whereas vehicle control animals demonstrated significant motor deficits when compared to shams on all 3 assessment days ( $p < 0.001$ , n=9). In contrast, treatment with both doses of APP96 110 significantly improved motor ability. Animals treated with 0.05mg/kg APP96 110 ( $p < 0.01$ , n=10) or 0.5mg/kg APP96 110 ( $p < 0.001$ , n=10) demonstrated significant improvements in motor outcome compared to vehicle animals on all 3 days following TBI. ( $p < 0.01$ ). There were no significant differences between the two APP96 110 doses.

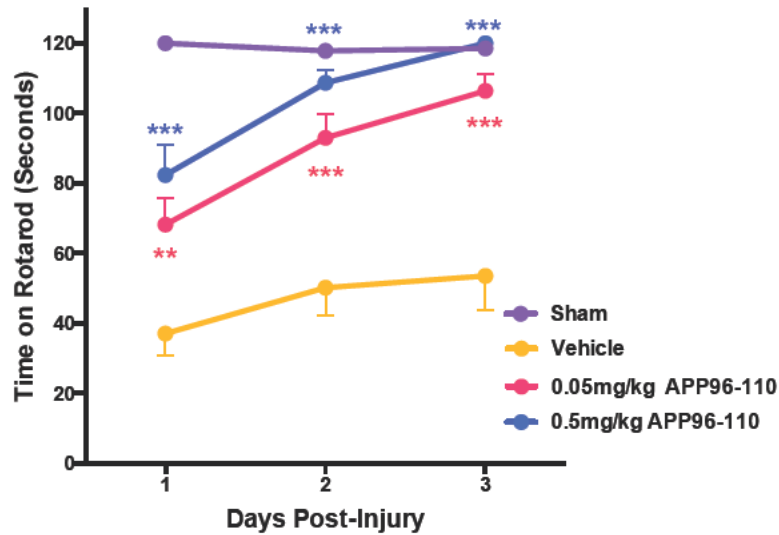
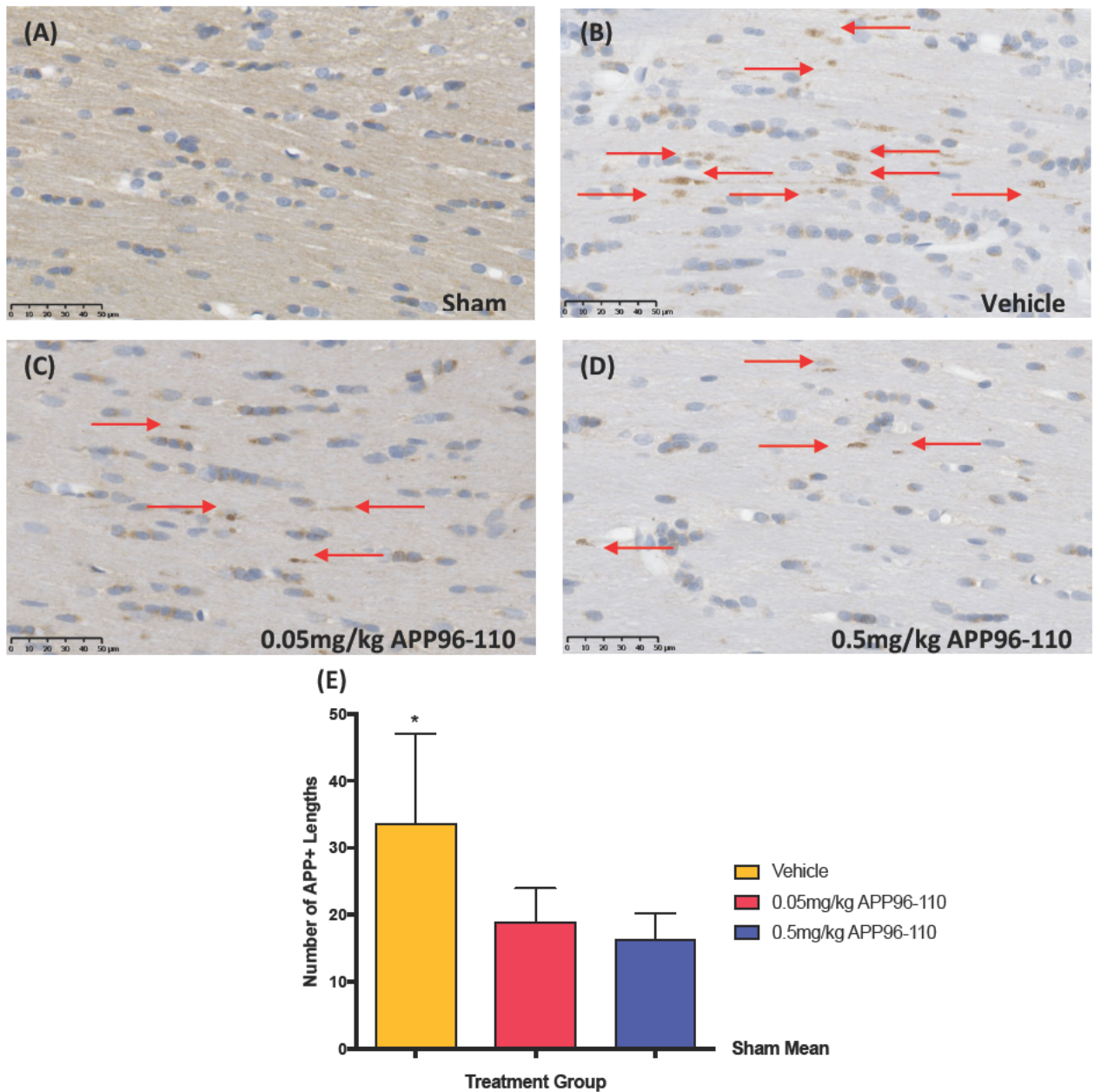


Figure 4.5: Motor outcome illustrating the effect of treatment with 0.05mg/kg and 0.5mg/kg APP96-110 IV at 5 hours post-TBI. Data were analysed using a two-way repeated measures ANOVA with Tukey's post-test. (Sham n=7, vehicle n=9, 0.05mg/kg n=10, 0.5mg/kg n=10, per group). (\*\*\*) $p < 0.001$ , (\*\*) $p < 0.01$ , compared to vehicle control animals).

### Delayed Administration of APP96-110 Remained Efficacious in Reducing Diffuse Axonal Injury

The extent of DAI was determined by counting the number of APP immunopositive lengths in the corpus callosum (Figure 4.6). Similar to the 30 minute treatment study, there was a significant increase in APP immunoreactivity observed in vehicle control animals at 3 days post TBI ( $34 \pm 11$ , n=8) compared to sham animals ( $p < 0.05$ , n=7). This delayed treatment with APP96 110 remained efficacious and reduced levels in both the 0.05mg/kg ( $19 \pm 11$ , n=9) and 0.5mg/kg ( $16 \pm 10$ , n=9) treatment groups, with DAI not significantly different to sham animals.



**Figure 4.6: Representative micrographs showing the degree of axonal injury in the corpus callosum at 3 days following diffuse TBI (A-D). 0.05mg/kg (C) and 0.5mg/kg (D) APP960110 treated animals demonstrated a reduced number of APP immunopositive lengths in the corpus callosum at 3 days following injury, compared to vehicle treated animals (B). These observations were confirmed with counts of the number of APP immunopositive lengths (E). Data were assessed using a one-way ANOVA with Tukey's post-test. (Sham n=7, vehicle n=8, 0.05mg/kg n=9, 0.5mg/kg n=9) (\*p<0.05, compared to sham animals).**

## 4.5 Discussion

Over recent years, a growing body of data has suggested that APP and its derivatives have a neuroprotective role following TBI (Van den Heuvel et al., 1999, Thornton et al., 2006, Corrigan et al., 2011, Corrigan et al., 2012b). This study is the first to examine the neuroprotective efficacy of APP96 110 following IV administration after TBI.

Posttraumatic administration of APP96 110 IV not only demonstrated noticeable improvements in motor outcome and reductions in AI and neuroinflammation, but importantly, that APP96 110 remains efficacious when injected up to 5 hours post TBI. Previous research has focused solely on intracerebroventricular administration, however, IV administration soon after trauma offers clear clinical advantages. Following trauma, ensuing secondary damage to the BBB facilitates a localized increase in permeability of blood contents into the brain parenchyma as early as 15 minutes after injury, lasting for up to four to six hours for large molecules. Permeability for smaller molecules, however, can last up to three to four days (Baskaya et al., 1997, Habgood et al., 2007). Whilst this permeability does contribute to the injury process, it also provides a window of opportunity through which therapeutics may gain entry to the brain (Habgood et al., 2007). A challenge for many IV drugs targeting brain injury is the inability to penetrate the BBB and reach the CNS. However, the ability of IV administered APP96 110 to produce neuroprotective effects *in vivo* that were comparable to intracerebroventricular administration, suggests that APP96 110 can enter the brain following injury in a functional state via the IV route. This has been confirmed by out laboratory with live animal luminescence studies, where APP96 110's ability to enter the brain was observed for up to 5 hours post TBI (unpublished data).



Over the years, a number of experimental therapies have shown promising neuroprotective efficacy in experimental settings, but subsequently fail to produce similar neuroprotective efficacy in humans (Vink and Nimmo, 2002, Maas et al., 2010). A therapeutic challenge often slowing bench to bedside progress for TBI is the choice of therapeutic administration time. Research often focuses on an immediate time point after injury, generally up to one hour post TBI (Vink and Van Den Heuvel, 2004, Faden and Stoica, 2007). However, in a clinical setting, the time frame between injury and arrival to a trauma unit can often far exceed one hour (Vink and Van Den Heuvel, 2004). Therefore, testing of more clinically relevant time frames is needed to develop TBI treatments which can be administered by paramedics at the place of injury. APP96 110 demonstrated clear efficacy for up to 5 hours post injury, a finding that significantly extends the therapeutic timeframe for treatment. Its therapeutic efficacy may in fact extend beyond the 5 hour window, and as such may form the basis of future dose and time response studies using APP96 110.

The results of this study strengthen previous findings that highlight the considerable neuroprotective functions of APP and its derivatives in TBI (Plummer et al., 2016). Following trauma, IV administration of APP96 110 at 30 minutes resulted in significant improvements in motor outcome over 7 days. Whilst the lowest 0.005mg/kg dose was ineffective, animals treated with the higher doses no longer displayed significant motor deficits compared to shams at two days after TBI. Moreover, these doses were able to reduce the currently untreatable DAI, with the 0.05mg/kg dose of APP96 110 producing a significant decrease in DAI compared to vehicle control animals at 3 days post TBI. Importantly, when APP96 110 was administered at 5 hours following injury, both the 0.05mg/kg and 0.5mg/kg doses remained efficacious at improving motor outcome, with animals significantly different to

vehicle control rats throughout the testing period. This improvement in outcome was also associated with a reduction in levels of DAI in the corpus callosum at day 3 post injury compared to vehicle control animals. DAI occurs as a result of a progressive secondary insult to axons, often leading to prolonged neurological damage (Heath and Vink, 1999, Povlishock, 1993, Maxwell et al., 1993). Primary injury often causes considerable axonal stretching, causing localized damage to the cytoskeleton and subsequent disruption to axoplasmic transport. However, much of the progression of DAI is secondary in nature, with the disruption of axoplasmic transport leading to axonal swelling and subsequent axonal disconnection (Povlishock, 1993, Buki and Povlishock, 2006), the disruption of sodium and calcium channels facilitating an influx of ions, and the production of deleterious phospholipases and proteases causing damage to mitochondria and complete axonal separation and eventually cell death (Smith et al., 2003, Buki and Povlishock, 2006). Injury to this extent is likely to be a major cause of functional deficits, and a key predictor of functional outcome following trauma, particularly in human CNS conditions. (Medana and Esiri, 2003)

The neuroprotective effects of APP96 110 on DAI, even when administered at the delayed time of 5 hours post TBI is important, as this suggests that APP96 110 may reduce overall injury severity by limiting the progression of axonal damage throughout the secondary injury cascade, and important finding given that current therapies targeting DAI are lacking.

Whilst AI is an important indicator of injury severity following TBI (Smith et al., 2003), it is not the sole factor. A hallmark feature of TBI is neuroinflammation, a significant part of the secondary injury cascade, which often leads to the prolonged and detrimental neurological injury and degeneration (Kumar and Loane, 2012). As important cells in the neuroinflammatory response, microglia and astrocytes play a key role in a number of both

beneficial and detrimental functions following CNS injury, including the release of neurotrophic factors, but also both pro and anti inflammatory cytokines (Kumar and Loane, 2012). The impact acceleration model of diffuse TBI produces wide spread axonal damage throughout the brain, particularly in white matter tracts, like the corpus callosum, where axons are abundant (Marmarou et al., 1994). Whilst neuroinflammation can often be observed in cortical regions, in this setting it was assessed within the corpus callosum, as this region corresponds to the largest area of damage seen following diffuse trauma. Administration of APP96 110 at 30 minutes post TBI prevented the profound neuroinflammation associated with TBI at all doses tested, with numbers of both reactive astrocytes and activated microglia significantly reduced following APP96 110 treatment. These findings could in part be explained by the associated reductions in DAI seen in APP96 110 treated animals, where the reduction in secondary injury events may reduce the need for neuroinflammation to occur. This is in contrast to vehicle control animals where secondary injury and DAI was more considerable. Furthermore, the reduction in acute neuroinflammation could represent a pathway in which APP96 110 treatment acts to ameliorate the motor deficits. As animals were assessed at day 3, these results only represent the acute neuroinflammatory response, and as such are not reflective of the long term progressive nature of posttraumatic neuroinflammation. As such, investigation into the mechanism through which APP96 110 is able to reduce neuroinflammatory events remains an important avenue for further research.

While the use of APP96 110 as a novel and clinically relevant therapeutic agent for TBI has been clearly demonstrated, the mechanism of action through which APP96 110 exerts these effects is yet to be fully understood. A key functional domain of sAPP $\alpha$ , of which APP96 110

is the active region, is its high structural similarity to growth factor like domains, and its strong affinity to heparin, particularly to heparin sulfate proteoglycans (HSPGs) (Narindrasorasak et al., 1991, Small et al., 1992, Rossjohn et al., 1999). The importance of APP96 110's affinity for heparin binding for its neuroprotective activity was demonstrated using an APP96 110 analogue with reduced heparin binding affinity, which in turn showed no neuroprotective effect *in vivo* after moderate severe diffuse TBI (Corrigan et al., 2014). It is thought that APP96 110 could bind to cell surface or extracellular matrix bound HSPGs to elicit a neuritogenic response (Clarris et al., 1997, Small et al., 1992, Small et al., 1994). The APP96 110 region contains a  $\beta$  hairpin loop constrained by a disulphide bond between cysteines 98 and 105 (Rossjohn et al., 1999, Small et al., 1994), which has been shown to be critical for promoting neurite outgrowth from central and peripheral neurons (Small et al., 1994, Williamson et al., 1995, Williamson et al., 1996, Young Pearse et al., 2008), as well as the activation of MAP kinase (Greenberg et al., 1995).

Irrespective of the mechanisms of neuroprotection, this study demonstrates that APP96 110 is efficacious by IV administration for up to 5 hours after TBI and strengthens its potential as a novel and multifactorial therapeutic agent following trauma. Important next steps for APP96 110 include enhancing our understanding of its pharmacokinetics to optimize its therapeutic activity, and also identifying its receptor and the signaling pathways it activates, which will help decipher the molecular mechanisms for APP96 110's activity. Testing the efficacy of APP96 110 in other neuronal injury models such as spinal cord injury and ischemia, where APP expression has been shown to be altered (Kobayashi et al., 2010, Badan et al., 2004), could broaden the therapeutic utility of APP9 110. As such, further development of APP96 110 as a therapeutic for TBI, and in particular DAI that currently lacks an efficacious

treatment, is warranted. Overall, APP96 110 shows promise as a novel and clinically relevant treatment option by offering substantial neuroprotective and neurotrophic effects towards reducing secondary injury and functional deficits associated with acute traumatic brain injury.

**Chapter 5: Enhanced Heparin Binding Affinity Of  
APP96-110 Results In Increased Neuroprotection  
Following Traumatic Brain Injury**

## 5.1 Introduction

Traumatic brain injury (TBI) is a major public health concern, yet despite extensive research no acceptable treatments currently exist. Over recent years, the Amyloid Precursor Protein (APP) has been shown to be a viable therapeutic option, with previous studies consistently demonstrating neuroprotective efficacy of APP and many of its derivatives, like sAPP $\alpha$  and APP96 110, following experimental TBI (Van den Heuvel et al., 1999, Thornton et al., 2006, Corrigan et al., 2011, Corrigan et al., 2012b, Corrigan et al., 2012a, Corrigan et al., 2014). APP96 110, in particular, has been shown to provide efficacy in both APP knockout ( / ) mice and in rats following diffuse TBI, observed through the restoration of functional deficits, the preservation of cortical and hippocampal tissue, as well as reductions in axonal injury in the corpus callosum (Corrigan et al., 2014). Furthermore, its neuroprotective ability has since been shown to extend for up to 5 hours post TBI, with intravenous administration shown to continue to improve motor outcome for up to 7 days, and reduce axonal injury and neuroinflammation (results previously discussed in chapter 4).

Over recent years, these neuroprotective actions of APP96 110 have gradually been attributed to two of APP's functional domains (Corrigan et al., 2011). The D1 domain in particular, of which APP96 110 is the active region, displays a high structural similarity to growth factor like domains, and exhibits a strong affinity to heparin, particularly to heparin sulfate proteoglycans (HSPGs) (Narindrasorasak et al., 1991, Small et al., 1992, Rossjohn et al., 1999). Whilst the exact mechanisms through which APP96 110 is able to exert its efficacy remains unclear, sufficient evidence supports that of a 'heparin binding hypothesis'. Through the process of mutating key residues in the APP96 110 amino acid sequence, an APP96 110

analogue with reduced heparin binding demonstrated no neuroprotective effect post TBI, with animals performing no differently to vehicle control animals (Corrigan et al., 2014). This suggests that that APP96 110 could functionally substitute for native sAPP $\alpha$ , highlighting that the neuroprotective activity of APP96 110 seems to correlate to its ability to bind heparin (Clarris et al., 1997, Corrigan et al., 2011, Corrigan et al., 2014).

Accordingly, the modulation of the heparin binding affinity of APP96 110 may prove beneficial in an attempt to increase its neuroprotective action. As such, this study aimed to examine whether mutation of key amino acid residues on APP96 110 would result in an increased binding affinity to heparin, and subsequently confer greater neuroprotective efficacy post TBI *in vivo*. Wildtype (WT) APP96 110 was assessed against two mutated APP96 110 peptides with either two or three amino acid mutations, and their ability to bind to heparin assessed via chromatography assay. Secondly, the peptide with the strongest affinity for heparin was then assessed *in vivo* following TBI, to determine whether the enhanced heparin binding affinity would confer greater levels of neuroprotection compared to the previously used WT APP96 110.

## 5.2 Methods

All studies were performed within the guidelines established by the National Health and Medical Research Council of Australia and were approved by the Animal Ethics Committee of the University of Adelaide (Ethics number: M 2014 131).



### 5.2.1 APP96-110 Peptides

The APP96 110 peptides were synthesized by *Auspep* (Tullamarine, Victoria, Australia) and were N terminally acetylated and C terminally amidated (previously outlined in Materials & Methods Part I, section 2.3.3). By combining multiple sequence and structural alignments of APP96 110 across different species, within the APP family as well as with other heparin binding proteins, it was hypothesised that mutation of key amino acid residues could enhance the heparin binding affinity of APP96 110. As such, WT APP96 110 was mutated in two ways: K99R, H100R (2+APP96 110) and N96R, K99R, H100R (3+APP96 110) (previously outlined in Materials & Methods Part I, section 2.3.3).

### 5.2.2 Chromatography Assay

Synthesised APP96 110 peptides were dissolved in phosphate buffered saline to produce a final concentration of 1mM. 10 µL of peptide was injected onto a 1 ml HiTrap Heparin column (GE Healthcare, Sydney, NSW, Australia), equilibrated in Buffer A (20mM Tris 7.5) and connected to an AKTA Purifier (GE Health care). The bound peptide was eluted from the column in a linear gradient of 0–1.2 M NaCl at a flow rate of 1 mL/min. Eluted peptide was detected by UV absorbance at 280 (mAU). The heparin binding affinity of each peptide was measured against WT APP96 110 on a Heparin Sepharose column.

### **5.2.3 In Vivo APP96-110 Preparation**

Prior to injury, each peptide was dissolved into distilled water to produce a 1mM stock solution, and further diluted to produce doses of 0.5mg/kg and 0.05mg/kg WT APP96 110, and 0.05mg/kg, 0.25mg/kg, 0.1mg/kg and 0.05mg/kg 3+APP96 110 for IV administration (refer to Figure 5.2 for justification for the choice of this mutant peptide).

### **5.2.4 Injury Induction**

A total of 45 adult male Sprague Dawley rats weighing between 357g and 409g were group housed in a controlled temperature environment under a 12 hour light/dark cycle, with uninterrupted access to food and water. Animals were randomly assigned into 3 day sham, vehicle control, 0.05mg/kg or 0.5mg/kg WT APP96 110, or 0.05mg/kg, 0.1mg/kg, 0.25mg/kg or 0.5mg/kg 3+APP96 110 treatment groups. Animals were injured using the Marmarou impact acceleration model of diffuse TBI (Marmarou et al., 1994) (previously described in Materials & Methods Part I, section 2.3.2). At 5 hours following TBI, animals were administered either saline vehicle control, 0.05mg/kg or 0.5mg/kg WT APP96 110, or 0.05mg/kg, 0.1mg/kg, 0.25mg/kg or 0.5mg/kg 3+APP96 110 IV via the tail vein by a blinded observer, and returned to their home cage to recover once normal behaviour was established.

### **5.2.5 Assessment of Motor Outcome**

Motor deficits post TBI were assessed using the rotarod, a sensitive test of motor ability

following TBI as previously described in Chapter 2 (Hamm et al., 1994) (previously described in Materials & Methods Part I, section 2.4.1). Animals were assessed daily for 3 days post injury.

### **5.2.6 Histological Assessment**

At 3 days post TBI, animals were transcardially perfused with 10% formalin (previously described in Materials & Methods Part I, section 2.5.1), with IHC performed to stain for AI with APP. The extent of DAI was assessed by counting the number of APP immunopositive (APP+) lengths in the entire length of the corpus callosum of three brain sections per animal.

### **5.2.7 Statistical Analysis**

All data were analysed using Graph Pad Prism software. All values are displayed as Mean  $\pm$  SEM, with a significance level of  $p < 0.05$ . Motor outcome was assessed using a two way repeated measures ANOVA with Tukey's post test, while DAI was assessed using a one way ANOVA with Tukey's post test.

## 5.3 Results

### 5.3.1 Design of APP96-110 Mutant Peptides

The experimental strategy was based on the hypothesis that the neuroprotective activity of APP96-110 correlates with its ability to bind to heparin. As such, analogues with increased heparin binding affinity were predicted to have greater neuroprotective activity. The crystal structure of APP96-110 within the D1 domain has been previously localised and solved for structure based analysis (Rossjohn et al., 1999) (Figure 5.1), with specific amino acid residues predicted to be involved with heparin binding. *In silico* analysis of APP96-110 identified a group of basic amino acid residues within the loop structure encompassing the peptide, which is consistent with the ionic nature of heparin binding, where side chain groups of basic amino acids on the protein bind to the negatively charged groups on heparin (Cardin et al., 1991, Montserret et al., 1999). As such, WT APP96-110 was mutated in two ways: K99R, H100R (2+APP96-110) and N96R, K99R, H100R (3+APP96-110) (previously outlined in Materials & Methods Part I, section 2.3.3).

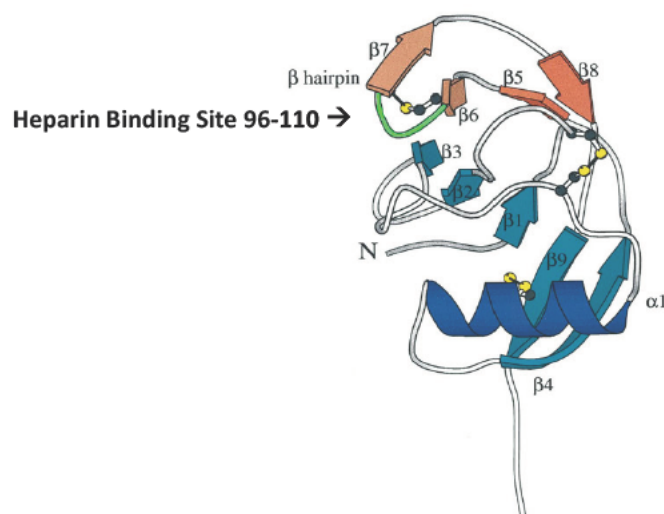


**Figure 5.1: The structural configuration of APP96-110, inclusive of the  $\beta$  hairpin loop constrained by a disulphide bond between cysteines 98 and 105**

### 5.3.2 Heparin Binding

The heparin binding affinity of various APP96 110 derivatives was assessed using chromatography assay on a heparin sepharose column (Figure 5.2). The salt concentration of WT APP96 110 was used as a baseline to compare the salt concentrations at which the mutated peptides, 2+APP96 110 and 3+APP96 110 eluted. WT APP96 110 eluted at 570mM NaCl, while the mutated peptides demonstrated an increased affinity for heparin, with 2+APP96 10 eluting at 650mM NaCl and 3+APP96 110 at 750mM NaCl.

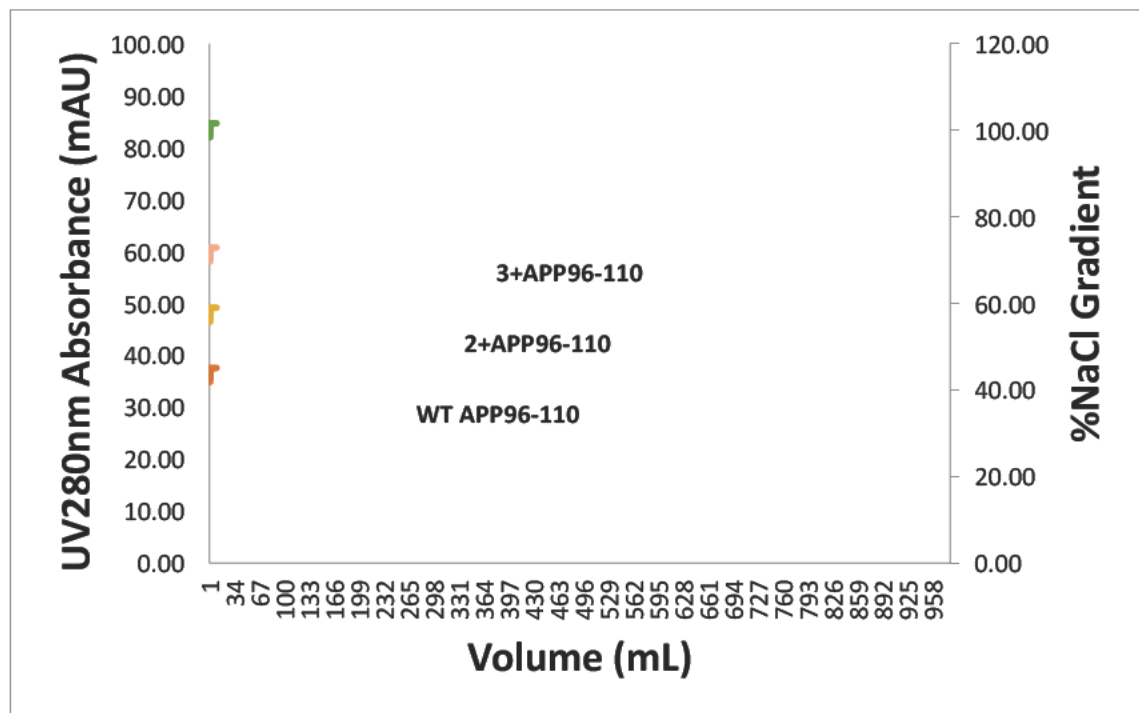


**Figure 5.2: Heparin affinity chromatography showing the heparin binding affinity of WT APP96-110, 2+APP96-110 and 3+APP96-110 at UV280 absorbance (mAU) eluting at 570mM, 650mM and 750mM salt concentrations, respectively. Green line is the NaCl gradient.**

### 5.3.3 Testing the Efficacy of the Mutant 3+APP96-110 Peptide Following TBI

Given the stronger heparin binding affinity displayed by 3+APP96 110 over the other analogue (2+APP96 110), this peptide was assessed *in vivo* following TBI, to determine whether the enhanced heparin binding affinity would translate to increased levels of neuroprotection compared to the previously used WT APP96 110. This was tested using the Marmarou impact acceleration model as previously described in this article.

### 5.3.4 Motor Outcome

Motor outcome post TBI was assessed using the rotarod (Figure 5.3). Sham animals demonstrated normal motor abilities over the testing period, recording 120 seconds on all 3 days post injury. In contrast, vehicle control animals showed significant motor deficits when compared to sham rats on all 3 days post TBI ( $p < 0.05$ ). Animals treated with WT APP96 110 demonstrated significant improvements in motor outcome over the testing period. 0.5mg/kg WT APP96 110 treated rats were significantly different to vehicle control animals on days 1 and 2 post TBI ( $p < 0.001$ ), and only significantly different to shams on day 1 post TBI ( $p < 0.01$ ). In contrast, 0.05mg/kg WT APP96 110 treated rats were only significantly different to shams on day 1 post TBI ( $p < 0.001$ ). Animals treated with mutated 3+APP96 110 demonstrated variable improvements in motor outcome. Animals treated with the highest dose of 3+APP96 110 (0.5mg/kg) demonstrated no improvement in motor outcome, with animals not significantly differently from vehicles, but were significantly different to shams on all 3 days post TBI ( $p < 0.001$ ), and significantly different to WT APP96 110 0.5mg/kg treated animals ( $p < 0.0001$ ). In contrast, treatment with 0.25mg/kg 3+APP96 110 demonstrated significant

improvements in motor outcome compared to vehicles ( $p < 0.001$ ), and on par with 0.5mg/kg WT APP96-110 treated animals.

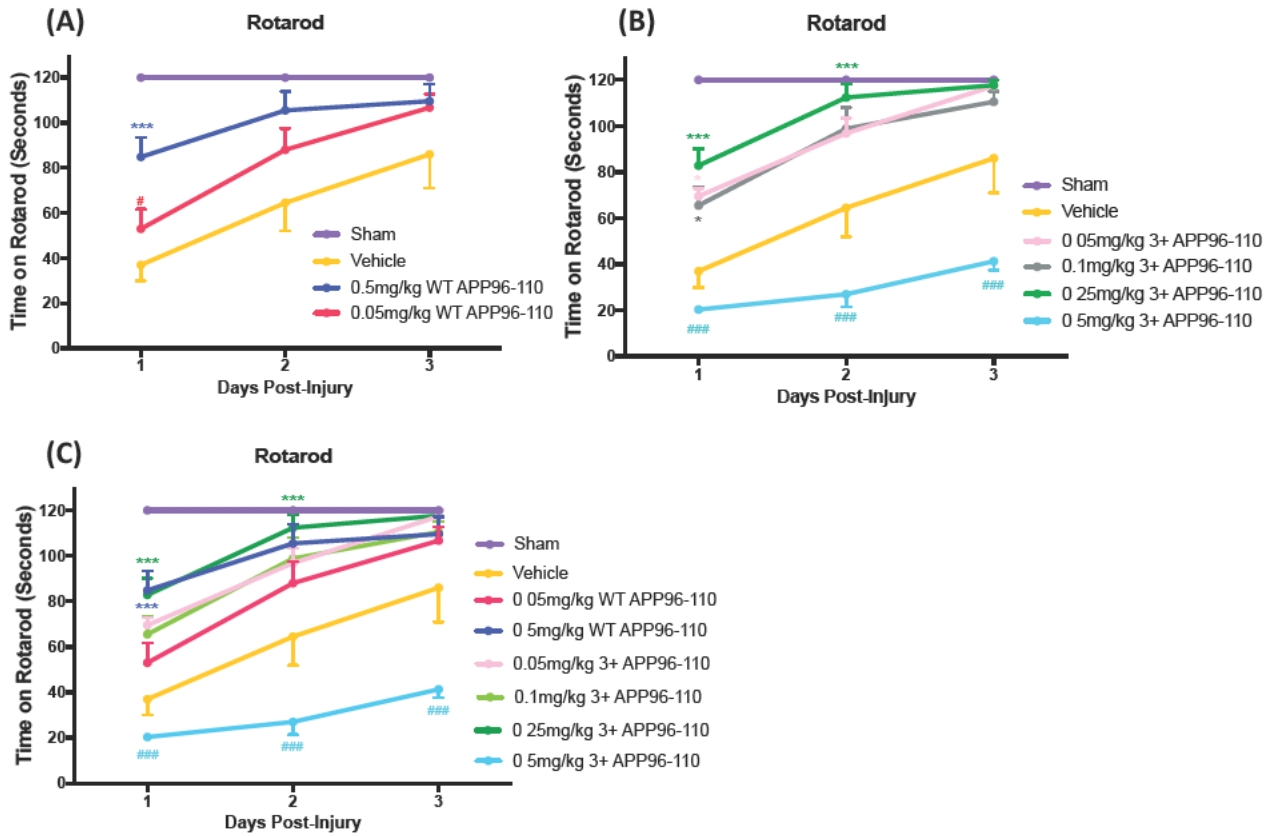


**Figure 5.3: Motor outcome illustrating the effect of treatment with doses of WT APP96-110 and 3+APP96-110 IV at 5 hours post-TBI. Image (A) demonstrates WT APP96-110 doses, (B) 3+APP96-110 doses, and (C) all doses combined. (Sham n=6, vehicle n=5, 0.05mg/kg WT APP96-110 n=6, 0.5mg/kg WT APP96-110 n=7, 0.05mg/kg 3+APP96-110 n=4, 0.1mg/kg 3+ APP96-110 n=5, 0.25mg/kg 3+APP96-110 n=4, 0.5mg/kg 3+APP96-110 n=3). Data were assessed with a two-way repeated measures ANOVA with Tukey's post-test. (\*\*\*) $p < 0.001$ , \* $p < 0.05$ , compared to vehicle control animals, #### $p < 0.001$  compared to 0.5mg/kg WT APP96-110 treated animals).**

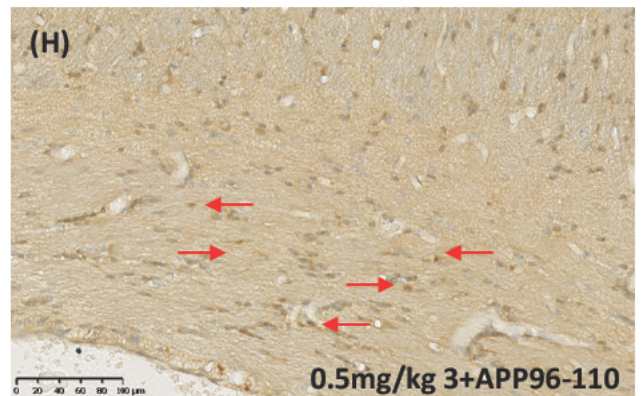
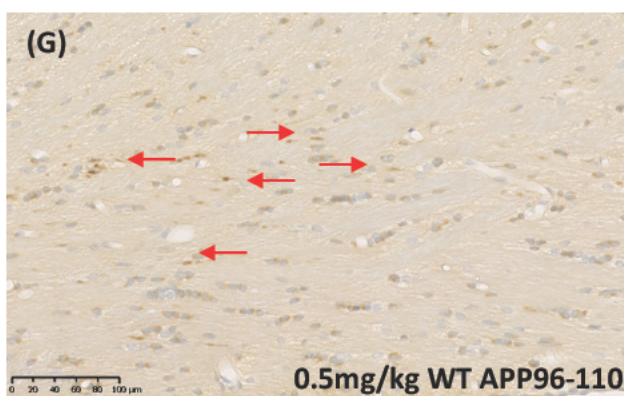
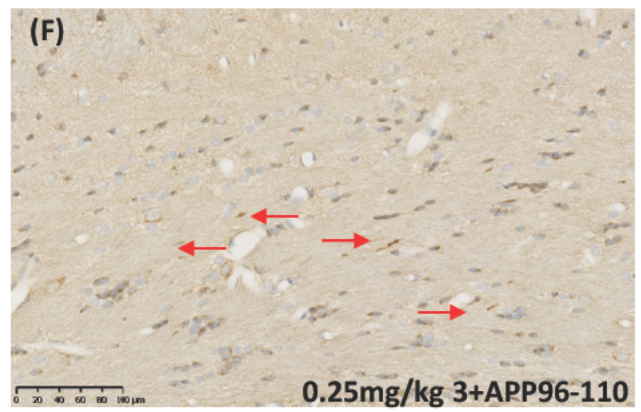
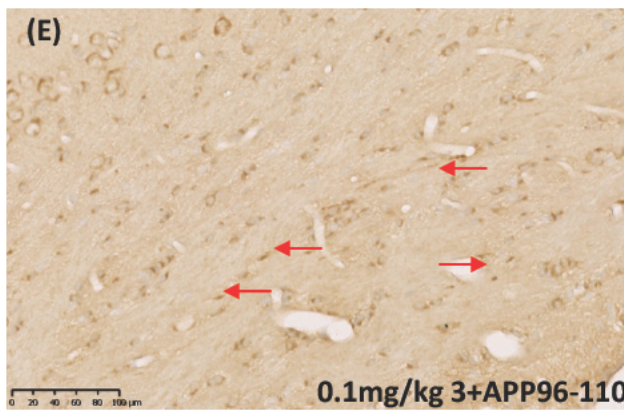
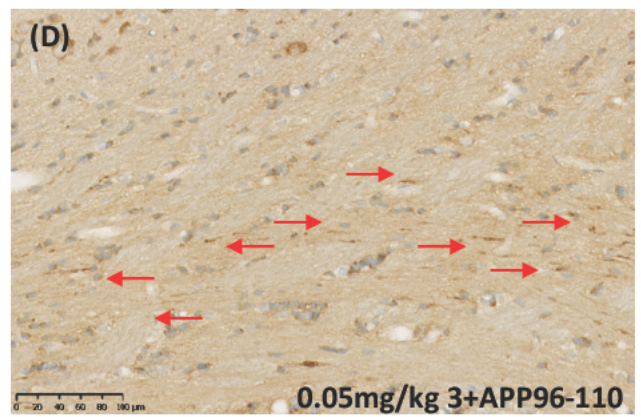
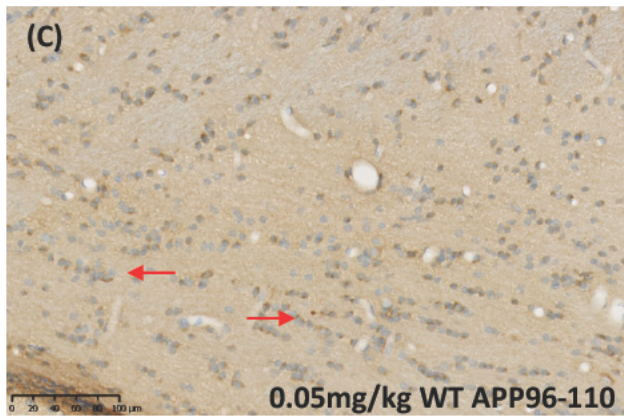
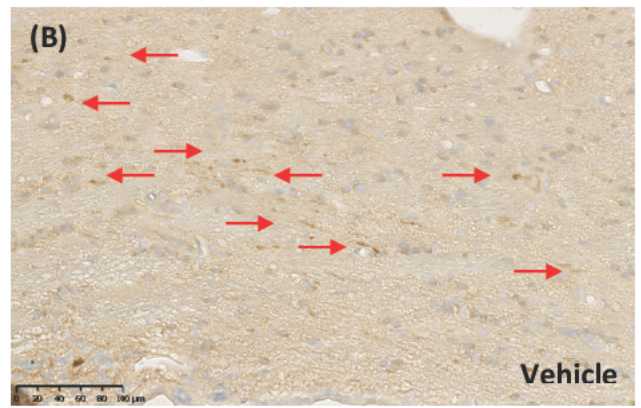
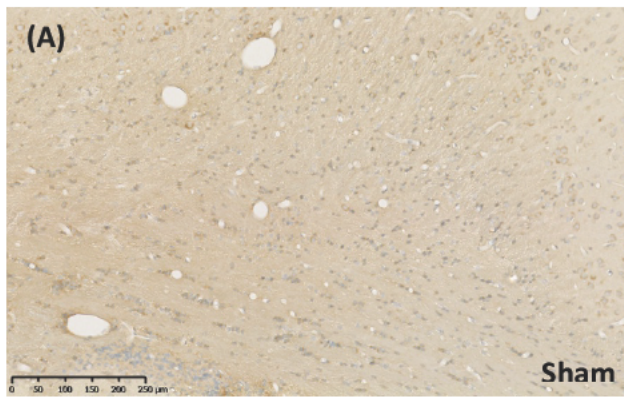
### 5.3.5 Diffuse Axonal Injury

To examine whether the changes seen in motor outcome were associated with any injury to axons, the number of APP positive lengths within the corpus callosum were counted (Figure 5.4). A significant increase in APP immunoreactivity was observed in vehicle control animals at 3 days post TBI ( $43.06 \pm 11.98$ ,  $n=5$ ) when compared to sham animals ( $p < 0.05$ ,  $n=5$ ). Overall however, there were no significant differences observed between WT APP96 110 and 3+APP96 110 doses, when compared to vehicle control rats.

Firstly, when assessing the WT APP96 110, treatment with 0.05mg/kg WT APP96 110 demonstrated reductions in Ai compared to vehicle control rats ( $32.9 \pm 11.47$ ,  $n=6$ ), however this was not significant ( $p=0.99$ ). Furthermore, treatment with 0.5mg/kg WT APP96 110 demonstrated significant increases in the extent of AI compared to sham animals ( $39.83 \pm 11.09$ ,  $n=7$ ) ( $p=0.02$ ).

Variable AI results were seen with 3+APP96 110 treatment doses. Treatment with both 0.1mg/kg 3+APP96 110 ( $n=5$ ) and 0.25mg/kg 3+APP96 110 ( $n=4$ ) demonstrated reductions in AI compared to vehicle control animals, however, this decrease was not significant ( $p=0.97$  and  $0.99$ , respectively). No significant differences were seen between these doses compared to sham animals ( $31.32 \pm 11.98$  and  $39.4 \pm 12.7$ , respectively). In contrast, treatment with both 0.05mg/kg and 0.5mg/kg 3+APP96 110 demonstrated significant increases in AI compared to sham animals ( $49.65 \pm 12.7$ ,  $n=4$  ( $p < 0.01$ )) and  $51.53 \pm 13.83$ ,  $n=3$  ( $p < 0.05$ )), respectively.





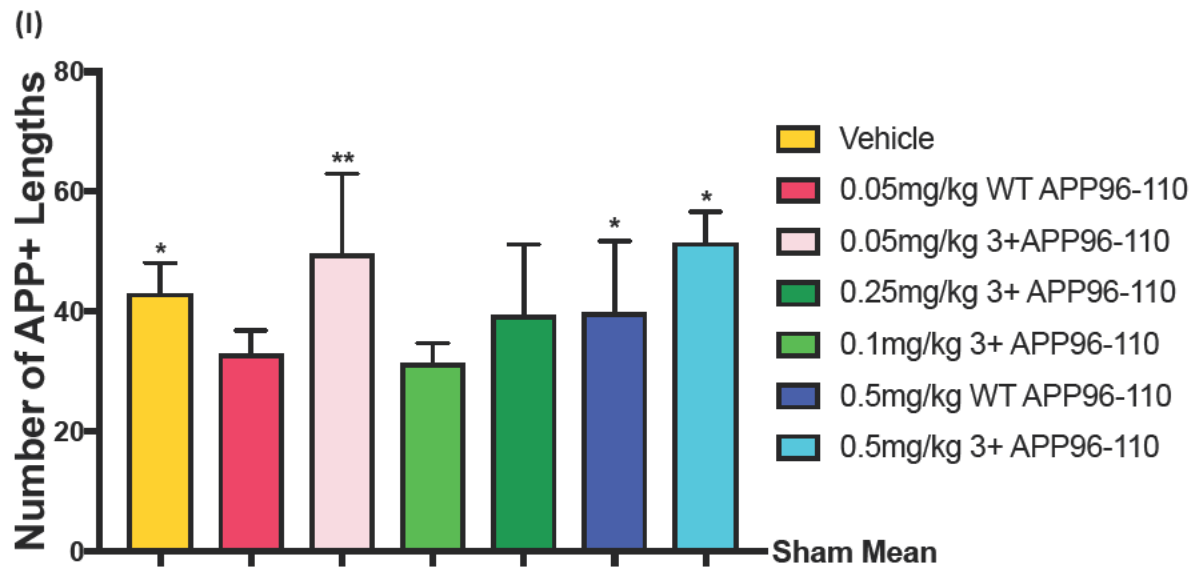


**Figure 5.4: Representative micrographs showing the degree of DAI in the corpus callosum at 3 days following diffuse TBI (A-H). These observations were confirmed with counts of the number of APP immunopositive lengths (I). Arrows indicate AI. (Sham n=5, vehicle n=5, 0.05mg/kg WTAPP96-110 n=6, 0.05mg/kg 3+APP96-110 n=4, 0.25mg/kg 3+APP96-110 n=4, 0.1mg/kg 3+ APP96-110 n=5, 0.5mg/kg WTAPP96-110 n=7, 0.5mg/kg 3+APP96-110 n=3. Data were assessed using a one-way ANOVA with Tukey's post-test. (\*\*p<0.01, \*p<0.05, compared to sham animals).**

## 5.4 Discussion

The APP derivative peptide APP96 110 has been consistently shown to offer neuroprotective benefits following TBI (Corrigan et al., 2014) (previously discussed in Chapter 4), however, its mechanism of action remains uncertain. As such, this study is important to determine if the neuroprotective activity of APP96 110 correlates to its heparin binding activity, and if increasing its heparin binding affinity will enhance its neuroprotective activity.

The mutation of key amino acid residues within the APP96 110 sequence was shown through a heparin chromatography assay to increase the affinity of each of these peptides to bind to heparin. When assessed *in vivo* following TBI, these peptides demonstrated a dose dependent improvement in motor outcome, with lower doses of the enhanced peptide improving motor outcome equal to higher doses of the wildtype peptide. These improvements in outcome were associated with variable decreases in AI throughout the corpus callosum, predominantly following treatment with the 0.1mg/kg and 0.25mg/kg 3+APP96 110 doses.

The ability to selectively mutate a protein based on its amino acid sequence, and subsequently design and generate analogues to APP96 110 is an exciting prospect for the development of novel therapeutic agents for conditions like TBI. The crystal structure of APP96 110 within the D1 domain has been solved (Rossjohn et al., 1999), and specific amino acid residues predicted to be involved with heparin binding identified. Using this structural information, together with sequence homology analysis, the generation of two APP96 110 analogues, 2+APP96 110 and 3+APP96 110, occurred. It was anticipated that the two

mutated APP96 110 peptides would have a stronger affinity to bind to heparin. As expected, these analogues did demonstrate an increased affinity for heparin, with 2+APP96 110 eluting at 650mM and 3+APP96 110 possessing greater affinity and eluting at 750mM, when compared to 570mM for WT APP96 110. The increased heparin binding affinity evident in these peptides helps to support the rationale that *in silico* based methods can be employed to successfully design APP96 110 analogues, based on protein structure.

Whilst the ability of the APP96 110 analogues to show an increased affinity to heparin was the initial step in exploring the 'heparin binding hypothesis', it was crucial to establish the efficacy of these peptides in an *in vivo* TBI model. Animals treated with both doses of WT APP96 110 demonstrated considerable improvements in motor outcome post TBI compared to vehicle control rats, which is in line with previous our findings (Thornton et al., 2006, Corrigan et al., 2012b, Corrigan et al., 2014) (results previously described in Chapter 4). The enhancement of heparin binding affinity in the APP96 110 peptide produced widespread improvement of motor performance. Rats treated with 0.25mg/kg of mutated 3+APP96 110 showed significantly improved motor performance post TBI when compared to vehicle control rats; reaching a similar level as the 0.5mg/kg WT APP96 110 treatment. Similar statistically significant differences were seen between other doses of mutated 3+APP96 110 and WT APP96 110 peptides, where lower doses of mutated 3+APP96 110 showed improved motor outcome on a par with higher doses of WT APP96 110. However, these effects were not entirely mirrored following histological examination of AI. Only selective doses of 3+APP96 110, the 0.25mg/kg and 0.1mg/kg 3+APP96 110 doses, were able to reduce AI compared to vehicle control animals. Unexpectedly, treatment with the highest 0.5mg/kg dose of 3+APP96 110 was unable to improve motor outcome, with animals performing

considerably worse compared to vehicle controls and any other APP96 110 treatment group. This treatment group also demonstrated considerably elevated levels of AI following TBI. The sample size in this group (n=3) compared to the other groups (n=6) may explain the substantial lack of neuroprotective efficacy of this dose, and suggests that a therapeutic threshold has been reached, beyond which any neuroprotective benefits can be achieved. Overall, these motor and histological observations indicate the ability of the mutated 3+APP96 110 peptides to improve motor outcome and reduce AI occurring in a dose dependent fashion, with lower doses of mutated 3+APP96 110 peptides conferring equal neuroprotective efficacy compared to higher doses of WT APP96 110. This may be through its enhanced ability to bind to heparin, and lends further weight to the heparin binding hypothesis for its mechanism of action.

Taken together, the findings of this study support heparin binding activity being at least a strong correlate of APP96 110's neuroprotective activity, and a number of studies over recent decades have suggested this. The structure of APP96 110 contains a  $\beta$  hairpin loop constrained by a disulphide bond between cysteines 98 and 105 (Rossjohn et al., 1999, Small et al., 1994), the presence of which has been shown to be critical for promoting neurite outgrowth from central and peripheral neurons (Young Pearse et al., 2008), as well as the activation of MAP kinase (Greenberg and Kosik, 1995). Indeed, the binding of this region to HSPGs can promote neurite outgrowth from central and peripheral neurons (Small et al., 1994, Williamson et al., 1995, Williamson et al., 1996). Further evidence has shown that the D1 domain of sAPP $\alpha$ , of which APP96 110 is the active region, displays a high structural similarity to growth factor like domains, and exhibits a strong affinity to heparin, particularly to heparin sulfate proteoglycans (HSPGs) (Narindrasorasak et al., 1991, Small et al., 1992,

Rossjohn et al., 1999). HSPGs can act as either receptors or co receptors (Sarrazin et al., 2011), and it is thought that APP96 110 may bind to cell surface or extracellular matrix bound HSPGs to elicit a neurotogenic response (Small et al., 1992, Small et al., 1994, Clarris et al., 1997). Indeed, heparin sulfates are recognized as playing an important role in regulating processes (Zhang et al., 2014). The binding of sAPP $\alpha$ , through APP96 110, is proposed to lead to key physiological changes such as the regulation of cell adhesion, synaptogenesis, cell signalling and neurite outgrowth (Small et al., 1994, Clarris et al., 1997, Rossjohn et al., 1999) all of which are important steps in promoting neuroplasticity and subsequent neurogenesis following TBI. Since HSPGs such as glypican and perlecan can inhibit the ability of APP to stimulate neurite outgrowth (Williamson et al., 1996), there may be an interplay between APP and different HSPGs for it to mediate its neuroprotective effects.

Interestingly, it is also possible that HSPGs are not the neuroprotective receptor for sAPP $\alpha$  or APP96 110, and that a more conventional protein receptor may be the target for these metabolites. As such, the identification of the definitive APP neuroprotective ligand remains an important goal to understanding its mechanism of action in TBI.

In summary, this study demonstrated that mutating the amino acid sequence of APP96 110 to generate analogues with an increased affinity for heparin can result in increased neuroprotective action of these peptides *in vivo* following TBI. Results suggest that lower doses of mutated 3+APP96 110 may confer equal neuroprotective efficacy to higher doses of WT APP96 110, with this finding potentially having considerable impacts from both a manufacturing and clinical viewpoint. In deciding upon the most efficacious dose of either WT or 3+APP96 110 to pursue for further comprehensive studies, motor outcomes were

balanced with the extent of AI observed at 3 days post TBI, with the 0.25mg/kg 3+APP96 110 dose ultimately chosen due to its ability to improve motor outcome, and the associated decrease in AI compared to vehicle control animals. The observations that the enhancement of heparin binding activity can improve the neuroprotective action of APP96 110 *in vivo* highlights that further investigation of these mutated analogues as novel therapeutic agents following TBI is warranted.

## **Chapter 6: The Long-Term Efficacy of APP96-110 Peptides Following TBI**



## 6.1 Introduction

The Amyloid Precursor Protein (APP) and its various derivatives like APP96 110 have consistently demonstrated neuroprotective efficacy when administered following experimental TBI (Van den Heuvel et al., 1999, Thornton et al., 2006, Corrigan et al., 2011, Corrigan et al., 2012b, Corrigan et al., 2012a, Corrigan et al., 2014). This efficacy has been shown to extend for up to 5 hours post TBI when administered intravenously, with the improvement of motor outcome and reduction of AI and neuroinflammation. The preclinical development of APP96 110 and its various analogues is critical for the progression of the APP story (results previously discussed in Chapter 4).

However, as previously discussed in Chapter 5, the exact mechanisms through which APP96 110 is able to exert its effect remains unclear. The mutation of key amino acid residues in the APP96 110 sequence has been shown to enhance its heparin binding affinity (previously discussed in Chapter 5), and following *in vivo* administration post TBI, resulted in greater neuroprotective action compared to WT APP96 110. In particular, treatment with 0.25mg/kg 3+APP96 110 appeared to confer equal neuroprotective activity compared to 0.5mg/kg WT APP96 110, highlighting that smaller doses of 3+APP96 110 could confer similar neuroprotective benefits to higher doses of WTAPP96 110 following trauma.

The next logical step in the progression of APP96 110 derivatives as novel therapeutic agents is the investigation of their long term efficacy. Until this point, research has only assessed the efficacy of these peptides up to 7 days post TBI. While acute time points enable clear examination of the immediate ability of a therapy to provide neuroprotective benefits, as well

as the ability to examine its molecular effects acutely within the secondary injury cascade, the long term effects of administration cannot be assessed. The long term efficacy of APP96 110 derivatives following TBI has never been investigated, with long term behavioural, cognitive and molecular changes still to be examined. As such, the aim of this study was to examine the long term efficacy of IV APP96 110 administration and the effects on functional outcome, neuroinflammation and neurodegeneration.

## **6.2 Methods**

All studies were performed within the guidelines established by the National Health and Medical Research Council of Australia and were approved by the Animal Ethics Committee of the University of Adelaide (Ethics number: M 2014 131).

### **6.2.1 APP96-110 Peptides**

For this study, two APP96 110 peptides were used: WT APP96 110 and 3+APP96 110. As previously outlined in Materials & Methods part I, section 2.3.3 the APP peptides were custom synthesized by *Auspep* (Tullamarine, Victoria, Australia) and were all N terminally acetylated and C terminally amidated. Peptides were received as lyophilized powder and dissolved in distilled water to produce 1mM stock solutions, before diluted accordingly to the required concentrations. As determined in Chapter 5, 0.25mg/kg 3+APP96 110 was the best performing dose to elicit both improvements in motor outcome and reductions in AI, and so for this study, this dose was compared to 0.25mg/kg WT APP96 110.

## **6.2.2 Animals**

Due to the inter strain differences seen in outcome and histology previously discussed (Material & Methods Part II), Charles River strain SDs were used in this study and all were purchased directly from the supplier (ARC in Perth, Australia).

## **6.2.3 Injury Induction**

A total of 40 adult male Sprague Dawley rats weighing between 382 and 424g were group housed in a controlled temperature environment under a 12 hour light/dark cycle, with uninterrupted access to food and water. Animals were randomly assigned into 24 hour or 30 day outcome groups, and each further assigned into sham, vehicle control, 0.25mg/kg WT APP96 110 or 0.25mg/kg 3+APP96 110 treatment groups. Animals were injured using the Marmarou impact acceleration model of diffuse TBI (Marmarou et al., 1994) (previously described in Materials & methods Part 1, section 2.3.2). Sham animals were surgically prepared but not injured and did not receive hypoxia. At 5 hours following TBI, animals were administered either IV saline vehicle control, 0.25mg/kg WT APP96 110 or 0.25mg/kg 3+APP96 110 by a blinded observer, and returned to their home cage to recover once normal behaviour was established.

#### **6.2.4 Assessment of Motor Outcome**

Motor deficits post TBI were assessed using the rotarod, a sensitive test of motor ability that assesses a rat's locomotion, balance and grip strength (Hamm et al., 1994) (previously described in Materials & Methods Part I, section 2.4.1).

#### **6.2.5 Assessment of Functional Outcome**

Functional deficits post TBI were assessed using a number of mazes and tests, as previously described in Materials & Methods Part I, section 2.4.2). Mazes included the Elevated Plus Maze, Y Maze and Barnes Maze. Open Field and the Forced Swim Test were also undertaken. All tests were performed in order of least stressful to most stressful to ensure animals were given sufficient time to recover from the already stressful injury, and to minimize pre existing stress from impact the cognitive testing (refer to Table 2.2 for the schedule for the functional mazes and tests).

### **6.2.6 Histological Assessment**

At 30 days post TBI animals were humanly euthanised, with half of the brain tissue perfused fixed with formalin, whilst the other half was fresh snap frozen in liquid nitrogen (previously described in detail in Materials & Methods Part I, sections 2.5.1 & 2.5.2, respectively). Formalin fixed tissue was prepared accordingly for IHC analysis with the following antibodies: Iba1 for microglia and GFAP for astrocytes (previously outlined in detail in Materials & Methods, Part I, section 2.6).

### **6.2.7 Western Blot Analysis**

Protein was extracted from the 30 day fresh snap frozen tissue as previously described in Materials & Methods, Part I, section 2.7, with analysis of PSD 95, synaptophysin, MBP, NFL and tau markers by western blot.

### **6.2.8 Statistical Analysis**

All data were analysed using Graph Pad Prism software. With all values displayed as Mean  $\pm$  SEM with a significance level of  $p < 0.05$ . Motor outcome was assessed using a two way repeated measures ANOVA with Tukey's post test. Results from the Barnes Maze were assessed using a two way ANOVA with Tukey's post test, while results from the Forced Swim Test were assessed using a one way ANOVA with Tukey's post test. Both IHC and WB analyses were performed using a one way ANOVA with Tukey's post test.

## 6.3 Results

### 6.3.1 Motor Outcome

Motor outcome was assessed using the rotarod (Figure 6.1). Sham animals demonstrated normal motor abilities over the testing period, recording a 120 seconds on all days post TBI. In contrast, vehicle treated animals demonstrated significant motor deficits on all 3 days post TBI ( $p < 0.01$ ), returning to a score of 108 seconds by 7 days post injury, and maintaining around this level of performance for the rest of the testing period. Rats treated with 0.25mg/kg WT APP96 110 showed significant differences compared to sham animals on all 3 days post TBI ( $p < 0.05$ ), with no differences compared to vehicle control treated animals. In contrast, motor ability was rescued following treatment with 0.25mg/kg of 3+APP96 110, with significantly improved motor outcome over the first 3 days compared to vehicle control rats ( $p < 0.05$ ), with these animals only significantly different from shams on day 1 post TBI ( $p < 0.001$ ). These animals recovered to sham level by day 3 4 post injury. In contrast, neither vehicle control or 0.25mg/kg WT APP96 110 treated animals recovered to sham level over the 30 day testing period. No significant differences were observed between treatment groups beyond 14 days post TBI ( $p = 0.62$ ).

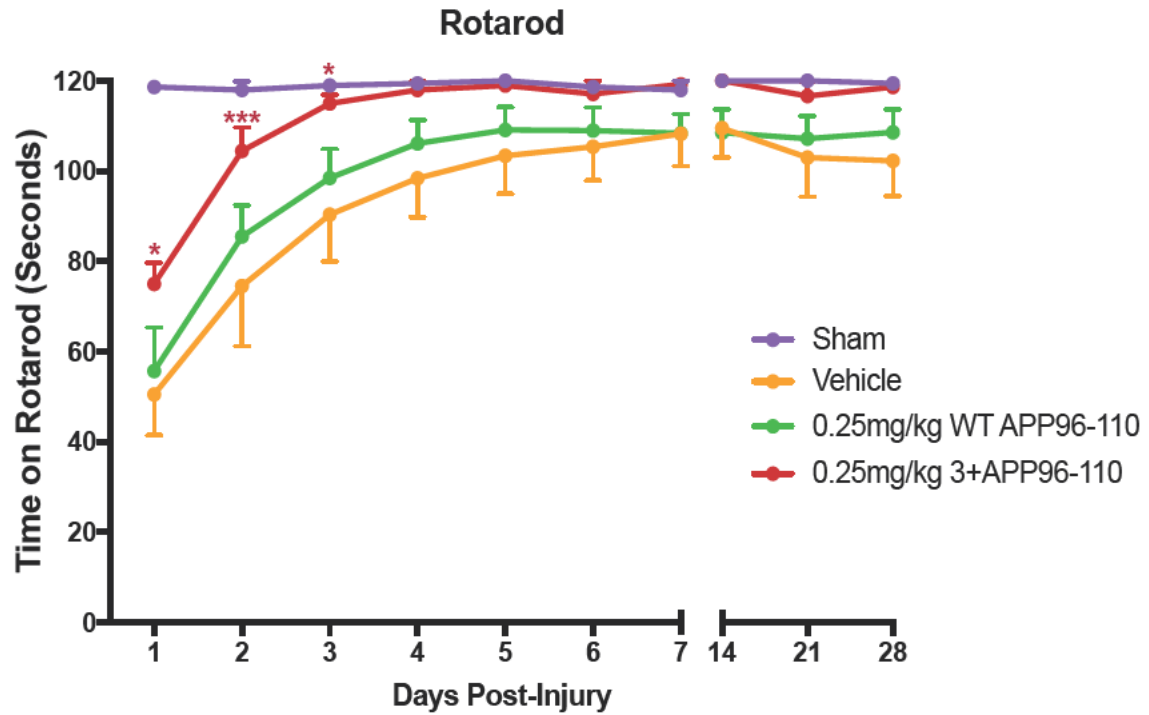


Figure 6.1: Motor outcome illustrating the effect of treatment with IV 0.25mg/kg of WTAPP906-110 and 3APP96-110 at 5 hour post-TBI over a 30 day period. (Sham = 9, vehicle = 8, 0.25mg/kg WTAPP96-110 = 10 and 0.25mg/kg 3+APP96-110 = 9.) Data were analysed with a two-way repeated measures ANOVA with Tukey's post-test. (\*\*\*) $p < 0.001$ , (\*) $p < 0.05$ , compared to vehicle control animals).

### **6.3.2 Functional Outcome**

No injury or treatment effects were observed in the Open Field, Elevated Plus Maze or Y Maze tests (Figure 6.2).

#### **Open Field**

In the Open Field, rats demonstrating locomotor deficits are likely to spend less time in the inner zone of the field. Vehicle control animals spent the greatest amount of time in the inner zone of any treatment group at 7 days post TBI, whilst at 21 days, vehicle control and 0.25mg/kg 3+APP96 110 treatment animals spent the least amount of time.

#### **Elevated Plus Maze**

In the Elevated Plus Maze, rats demonstrating increased levels of anxiety are likely to spend more time in the enclosed arms, rather than the open arms. Vehicle control animals spent an increased amount of time in the open arms on both days 6 and 22 post TBI compared to sham animals, indicating lower levels of anxiety compared to sham animals.

#### **Y-Maze**

In the Y Maze, rats displaying deficits in spatial and recognition memory are likely to preference the start or other arms, spending more time in these arms compared to the novel arm. Despite spending a reduced amount of time in the novel arm compared to the start and other arms, vehicle control animals appeared, nonetheless, to still preference the novel arm



over the other the start and other arms on days 5 and 23 post TBI, and did not spend significant less time in the novel arm versus the start or other arms.

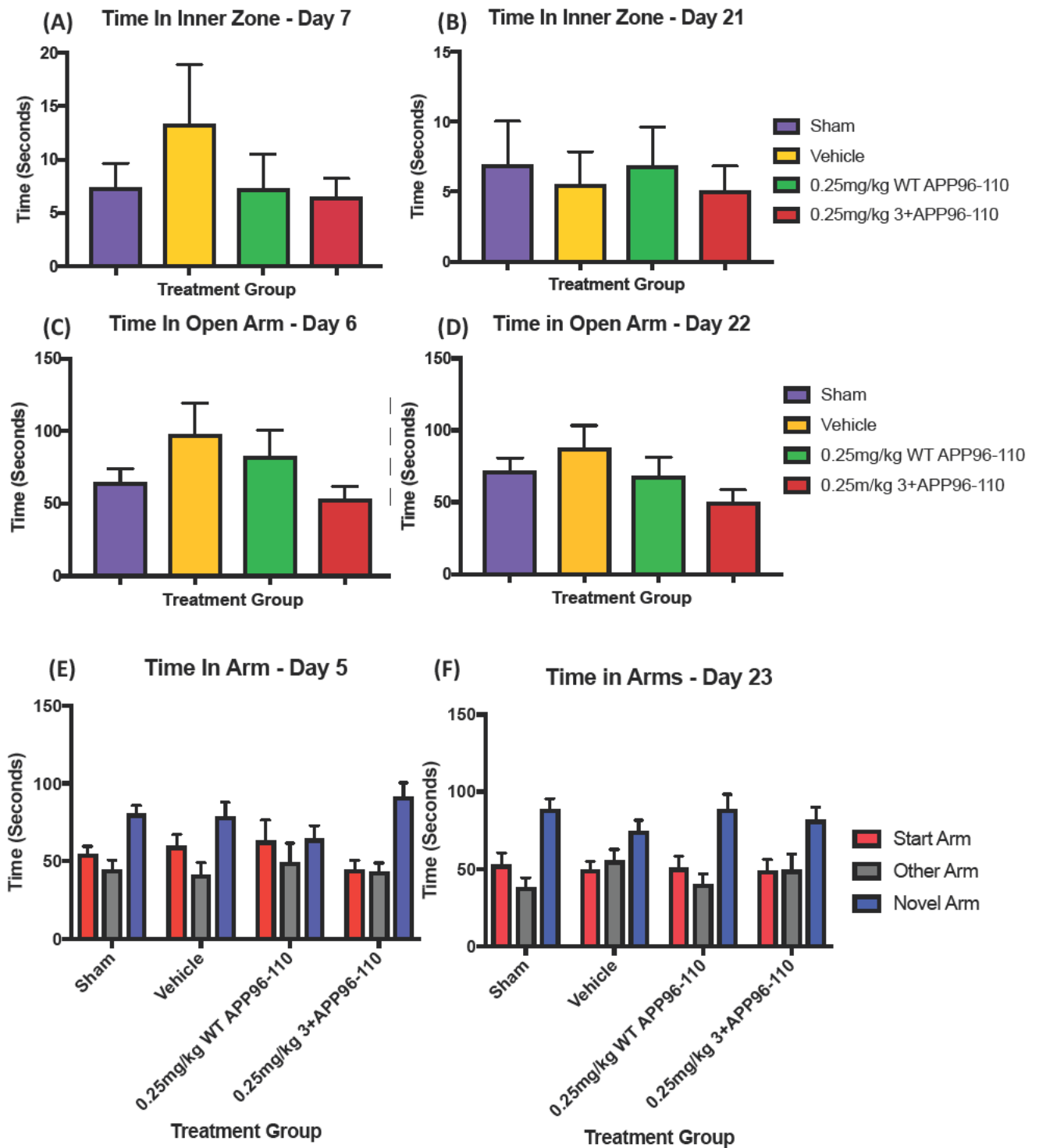


**Figure 6.2: Non-significant functional outcome results from the Open Field on day 7 (A) and 21 (B) post-TBI, from the Elevated Plus Maze on day 6 (C) and day 22 (D) post-TBI, and from the Y-Maze on day 5 (E) and day 23 (F) post-TBI. n= 8-10 per group.**

## Barnes Maze

The Barnes Maze aims to assess learning and memory (previously described in Materials & Methods Part I, section 2.4.2). On the first day of training, vehicle control animals showed significant impairments in their ability to locate the escape box ( $84.4 \pm 8.79$ ,  $p < 0.01$ ), when compared to sham animals ( $51.4 \pm 8.79$ ). Rats treated with  $0.25 \text{ mg/kg}$  WT APP96 110 showed a reduced amount to time required to locate the escape box, averaging  $68.7 \pm 8.5$  seconds. In contrast, animals treated with  $0.25 \text{ mg/kg}$  3+APP96 110 displayed similar abilities to sham rats, averaging  $47.9 \pm 8.79$  seconds to locate the escape box, performing significantly different to vehicle control animals ( $p < 0.01$ ). By day 2 of training, animals in all treatment groups showered improvements in their abilities in locating the escape box, a trend replicated on day 3, with sham animals averaging  $12.2 \pm 8.8$  seconds and vehicles averaging  $23.7 \pm 8.8$  seconds.

On day 5 of Barnes Maze, a probe trial was conducted where the location of the escape box was moved, and the time taken to find both the old box as well as the new box was recorded. Vehicle control animals spent an average of  $15.51 \pm 4.7$  seconds finding the location of the old box ( $p = 0.055$ ) compared to sham animals ( $3.1 \pm 4.7$ ). Treatment with both WT APP96 110 and 3+APP96 110 reduced the time spent for treated animals to find the old box, with  $0.25 \text{ mg/kg}$  WT APP96 110 animals taking  $3.29 \pm 4.4$  seconds ( $p = 0.081$ ), while  $0.25 \text{ mg/kg}$  3+APP96 110 animals taking  $2.6 \pm 4.5$  seconds ( $p = 0.068$ ), respectively. No significant differences were observed between treatment groups in the time it took for animals to find the location of the new escape box over two trials ( $p = 0.26$ ). In the first trial, vehicle control animals averaged  $69.3 \pm 11.7$  seconds finding the new escape box, compared to sham animals  $42.46 \pm 11.7$ . Animals treated with WT and 3+APP96 110 averaged  $37.4 \pm 10.1$ , and  $51.5 \pm 11.3$ , respectively.

By the second trial however, animals across treatment groups all performed similarly, averaging between 19.9 – 21.8±10.9 – 11.8 seconds.

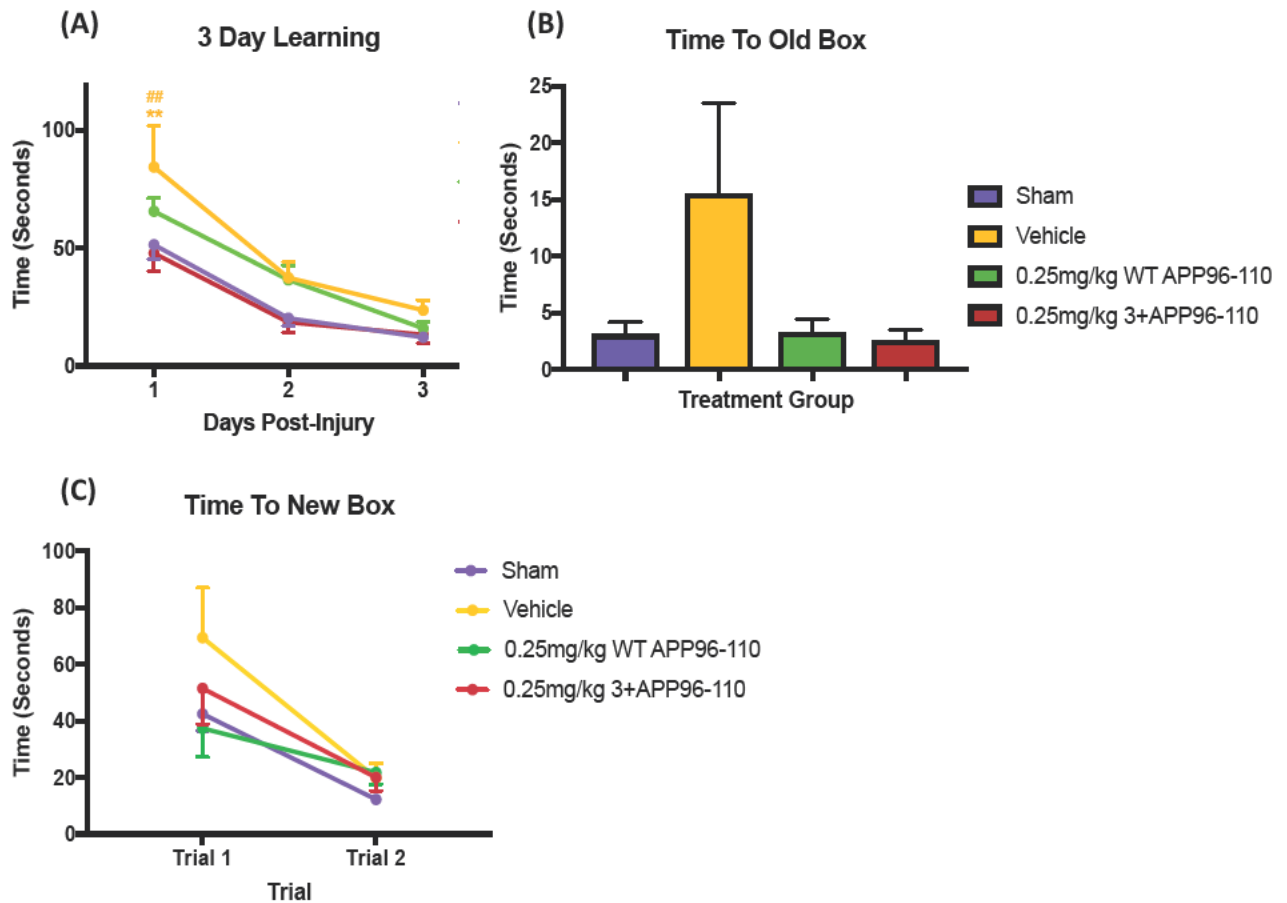


**Figure 6.3: Performance in the Barnes Maze.** Image (A) demonstrates the 3 day learning of animals across treatment groups, whilst the time required to find the old escape box (B) and new escape box (C) is demonstrated. n=8-10 per group. \*\*= $p < 0.01$ , compared to sham animals, ##= $p < 0.01$ , compared to vehicle control animals. 3 day learning data were analysed using a repeated measures two-way ANOVA with Dunnett's post-test, the time to the old box using a one-way ANOVA with Tukey's post-test, and time to the new box using a repeated measures two-way ANOVA with Tukey's post-test.

## Forced Swim Test

The Forced Swim Test aims to measure depressive like behaviour (previously described in Materials & Methods Part I, section 2.4.2). Rats displaying an increase in depressive like behaviour are likely to spend more time immobile throughout the test. No significant difference were noted ( $p=0.12$ ), with sham animals spending  $108.3\pm 13.89$  seconds immobile, vehicle control animals  $133.4\pm 13.898$ ,  $0.25\text{mg/kg}$  WT APP96 110 treated animals  $134.3\pm 13.41$ , and  $0.25\text{mg/kg}$  3+APP96 110 treated animals  $111.3\pm 13.41$  seconds, respectively.

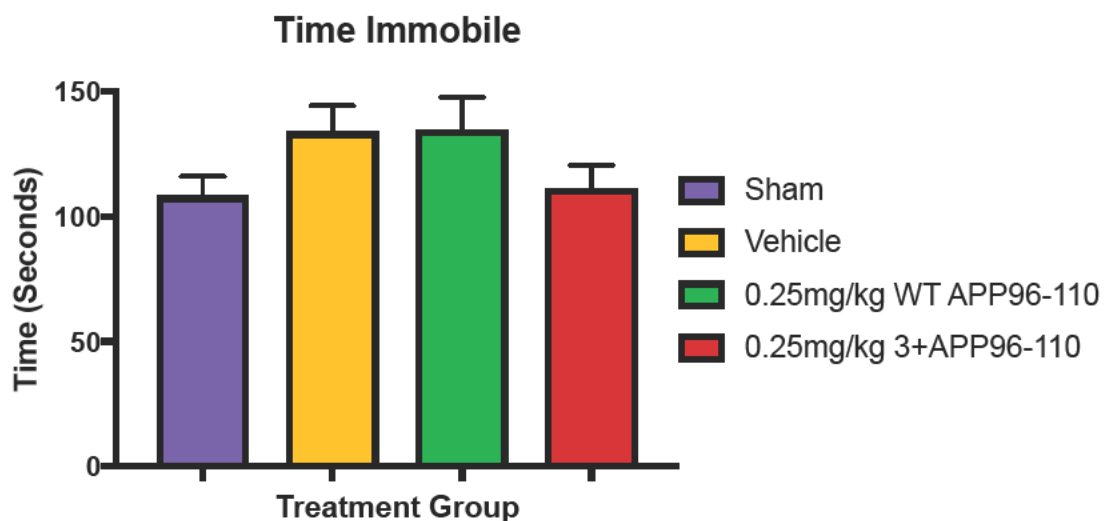


**Figure 6.4: Time spent immobile throughout the Forced Swim Test.  $n=8-12$  per group. Data were analysed using a one-way ANOVA with Tukey's post-test.**

### 6.3.3 Histological Analysis

#### Microglia

Both the total number and the number of activated microglia in the cortex and corpus callosum were examined using an Iba1 antibody (previously described in Materials & Methods Part I, section 2.6.2). The number of activated microglia in each region were divided by the total number counted to produce the percentage of activated microglia (Figure 6.5).

No significant differences were noted in the percentage of activated microglia within the cortex ( $p=0.73$ ). Sham animals had a percentage of  $25.19\pm 3.05\%$  activated microglia, vehicle control animals  $27.96\pm 3.05\%$ ,  $0.25\text{mg/kg}$  WT APP96 110  $27.12\pm 2.875\%$  and  $0.25\text{mg/kg}$  3+APP96 110  $25.03\pm 3.05\%$ . However, in the corpus callosum there were significantly different numbers of activated microglia ( $p=0.027$ ). Here, vehicle control animals demonstrated significant increases in the percentage of activated microglia ( $31.33\pm 3.01\%$ ) compared to sham animals ( $21.92\pm 3.01\%$ ,  $p<0.05$ ). In contrast, treatment with WT APP96 110 significantly reduced the percentage of activated microglia compared to vehicle control rats ( $22.14\pm 3.12\%$ ,  $p<0.05$ ). A trend towards significance was also observed in the 3+APP96 210 treated animals when compared to vehicle controls ( $22.97\pm 29\%$ ,  $p=0.09$ ).

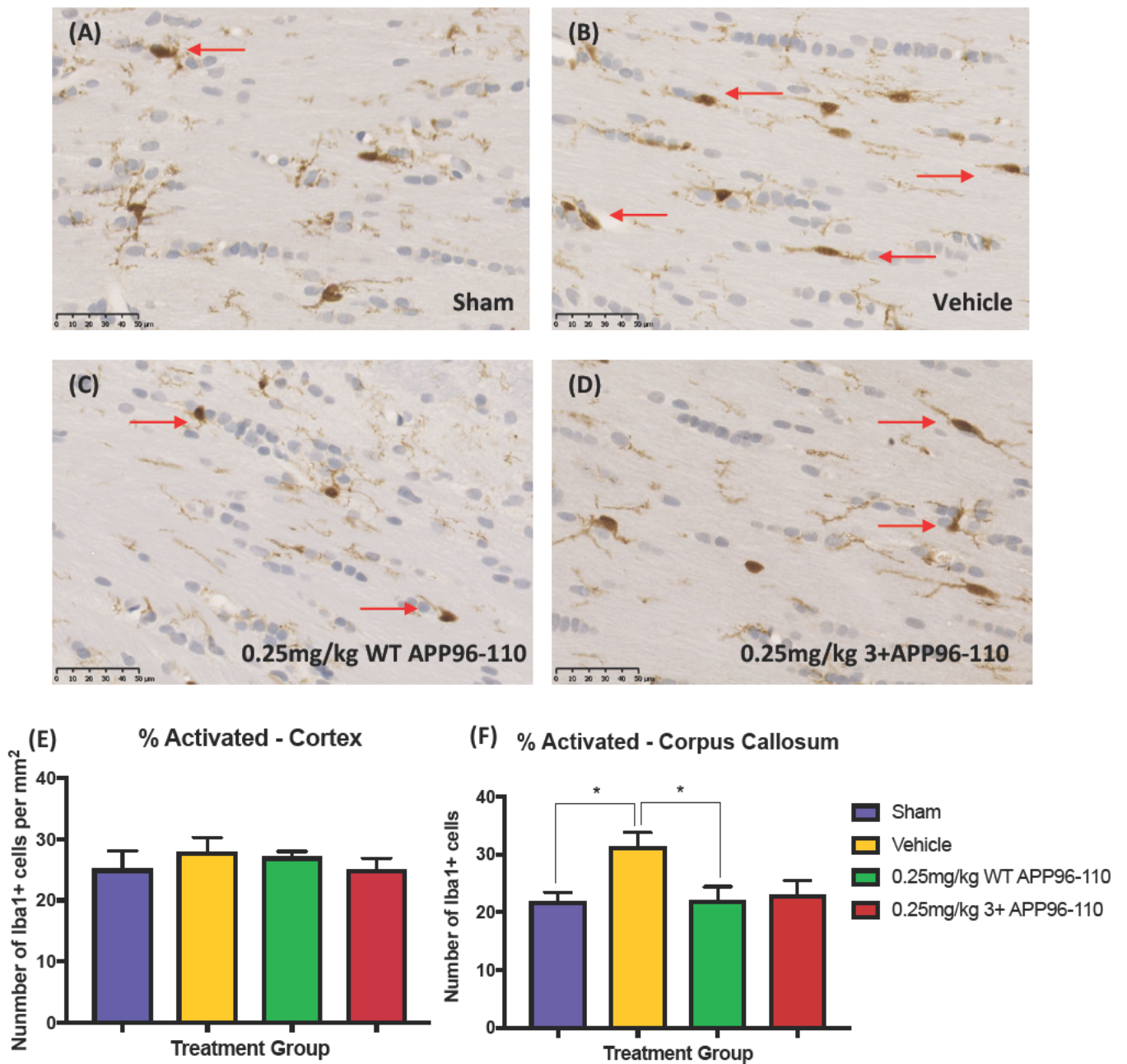


**Figure 6.5: Representative micrographs demonstrating the percentage of activated microglia in the corpus callosum following TBI (A-D). Scale = 50µm. Arrows indicate activated microglial based on morphological assessment. These observations were supported by counting the percentage of activated microglia in both the cortex and corpus callosum (E-F). Data were assessed using a one-way ANOVA with Tukey's post-test. \*= $p < 0.05$ .**

## Astrocytes

The absolute number of reactive astrocytes in the cortex and the corpus callosum were assessed using a GFAP antibody (previously described in Materials & Methods Part I, section 2.6.3). No significant differences in the absolute number of reactive astrocytes were observed between any of the treatment groups in either the cortex or corpus callosum at 30 days following TBI ( $p=0.28$ ,  $p=0.92$ , Figure 6.6). In the cortex, sham animals had a higher number of GFAP+ cells ( $50.73\pm 6.754$ ), compared to vehicle control animals ( $41.5\pm 6.754$ ), whilst WT APP96 110 and 3+APP96 120 treated animals demonstrated similar numbers shams ( $40.43\pm 6.368$  and  $38.42\pm 7.754$  GFAP+ve cells, respectively). Within the corpus callosum, all animals had similar numbers of GFAP+ve cells, with shams demonstrating  $217.1\pm 26.47$ , vehicle controls  $226\pm 26.47$ , WT APP96 110  $210.2\pm 25.12$ , and 3+APP96 110  $223.3\pm 26.47$  GFAP+ cells, respectively.



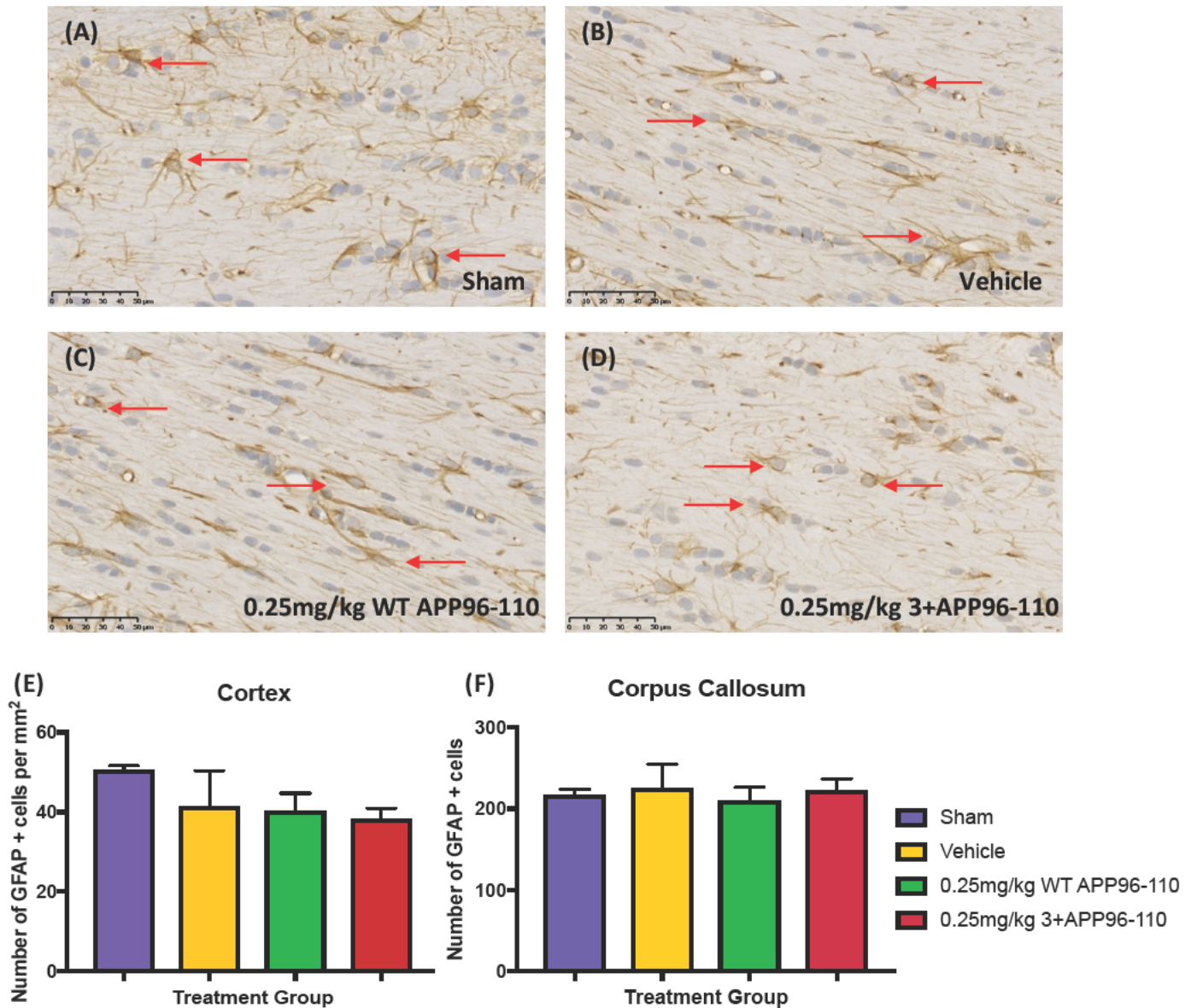


**Figure 6.6:** Representative micrographs demonstrating the number of reactive astrocytes in the corpus callosum following TBI (A-D). Scale = 50 $\mu$ m. Arrows indicate reactive astrocytes based on morphological assessment. These observations were supported by counting the number of GFAP+ cells in both the cortex and corpus callosum (E-F). Data were assessed using a one-way ANOVA with Tukey's post-test.

### 6.3.4 Western Blot Analysis

Western Blot analysis was used to examine effects of APP96 110 administration on the relative expression of proteins related to changes to synapses, dendrites, myelination, axonal structure and the accumulation of proteins associated with neurodegenerative disease.

#### PSD-95

PSD 95 is a post synaptic scaffolding protein used to examine the post synaptic density of neurons following TBI (Figure 6.7). No significant differences were noted within either the cortex ( $p=0.57$ ), or hippocampus ( $p=0.35$ ). However, within the cortex, vehicle control animals demonstrated a lower PSD 95 relative density ( $16079\pm4294$ ) compared to sham animals ( $22057\pm4294$ ). Animals treated with APP96 110 had slightly higher levels, with WT APP96 110 treated animals recording a PSD 95 relative density of  $19783\pm4463$  and 3+APP96 110 treated animals recording a PSD 95 relative density of  $20789\pm4294$ . In the hippocampus, vehicle control animals demonstrated no differences in PSD 95 relative density ( $25075\pm3115$ ), compared to sham animals ( $25294\pm3115$ ). In contrast, treatment with 0.25mg/kg WT APP96 110 reduced the PSD 95 relative density to  $20889\pm3115$ , while treatment with 0.25mg/kg 3+APP96 110 increased the PSD 95 relative density to  $24113\pm2668$ , compared to WT APP96 110.

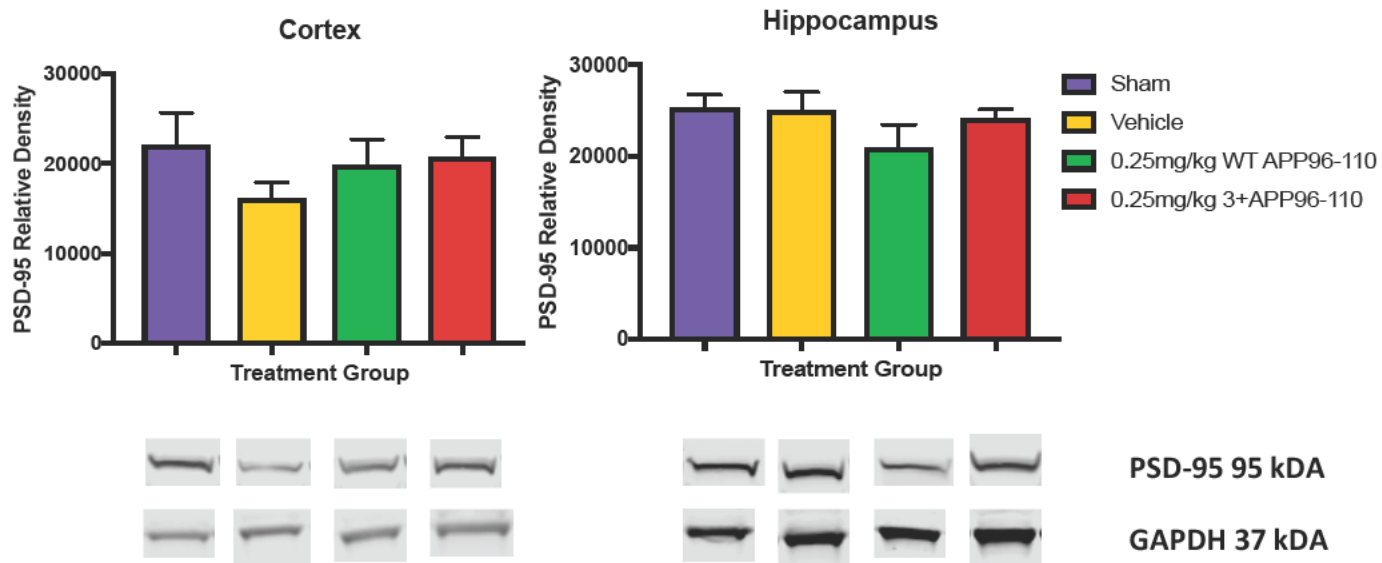


**Figure 6.7: Analysis of PSD-95 relative density within the cortex and hippocampus at 30 days following TBI. n=3-5 per group. Data were assessed using a one-way ANOVA with Tukey's post-test.**

## Synaptophysin

Like PSD 95, synaptophysin is a key protein involved in synaptic plasticity (Figure 6.8). In the cortex, significant differences were noted ( $p=0.04$ ). This was driven by a significant difference in the 0.25mg/kg WT APP96 110 treated animals ( $18722\pm747.7$ ,  $p<0.05$ ), compared to sham animals ( $16544\pm828.3$ ). Vehicle control animals ( $18719\pm828.3$ ) and 0.25mg/kg 3+APP96 110 treated animals ( $18179\pm781$ ) had similar levels to WT APP96 1 animals. In the hippocampus, no significant differences were noted ( $p=0.49$ ), with sham animals cording a relative density of  $22592\pm3538$ , vehicle control animals  $20302\pm3538$ , 0.25mg/kg WT APP96 110  $18648\pm3030$  and 0.25mg/kg 3+APP96 110  $18466\pm2889$  in synaptophysin relative density, respectively.

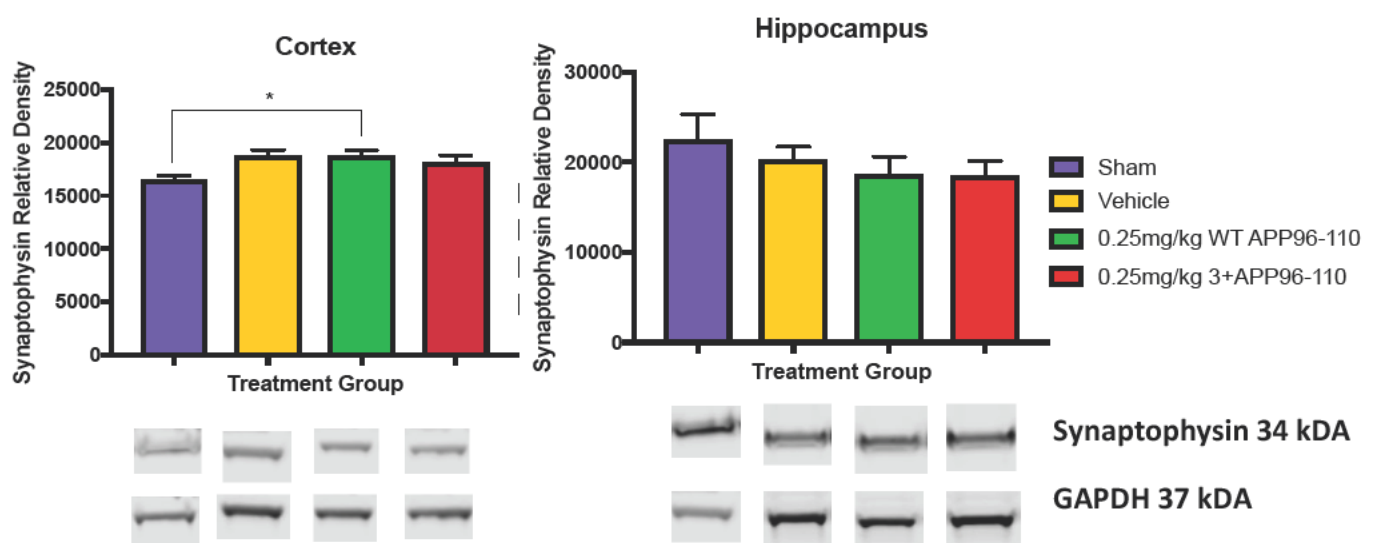


**Figure 6.8:** Analysis of synaptophysin relative density within the cortex and hippocampus at 30 days following TBI.  $n=3-5$  per group. Data were assessed using a one-way ANOVA with Tukey's post-test.  $*=p<0.05$ . compared to sham animals.

## Neurofilament (light)

NF L is a key axonal cytoskeletal protein, with an antibody used to assess proteins associated with axonal structure (Figure 6.9). No significant differences were noted in either the cortex ( $p=0.55$ ) or the hippocampus ( $p=0.60$ ). However, in the cortex, vehicle animals demonstrated an increase in NF L relative density ( $23497\pm3362$ ), compared to sham animals ( $20122\pm3362$ ). Treatment with  $0.25\text{mg/kg}$  WT APP96 110 was able to reduce NF L relative density to sham level ( $20044\pm3453$ ), while treatment with  $0.25\text{mg/kg}$  3+APP96 110 further reduce NF L relative density to  $18412\pm5086$ . In the hippocampus, vehicle control animals demonstrated an increase in NF L relative density ( $22207\pm4852$ ), compared to sham animals ( $17459\pm4852$ ). Treatment with both  $0.25\text{mg/kg}$  WT APP96 110 and  $0.25\text{mg/kg}$  3+APP96 110 demonstrated NF L relative density level similar to vehicle control animals ( $21903\pm4852$ , and  $22207\pm5011$ , respectively).

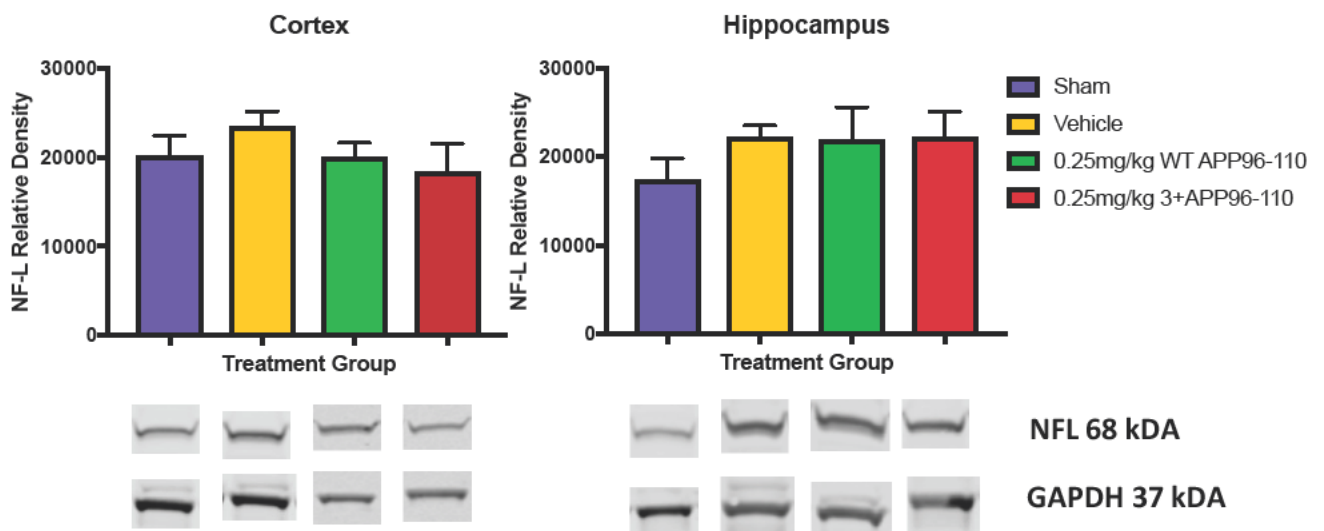


**Figure 6.9: Analysis of NF-L relative density within the cortex and hippocampus at 30 days following TBI.  $n=3-5$  per group. Data were assessed using a one-way ANOVA with Tukey's post-test.**

## Myelin Basic Protein

MBP is a key protein associated with normal myelination, and like NF L, provides insight into axonal cytoskeletal structure (Figure 6.10). No significant differences were noted in either the cortex ( $p=0.79$ ), or the hippocampus ( $p=0.41$ ). However, in the cortex, vehicle control animals demonstrated slightly elevated levels of MBP relative density ( $7643\pm 2047$ ), compared to sham animals to sham animals ( $6710\pm 2047$ ). Treatment with 0.25mg/kg WT APP96 110 resulted in an MBP relative density of  $7179\pm 1671$ , similar to shams, while treatment with 0.25mg/kg 3+APP96 110 slightly increased MBP relative density levels to  $8435\pm 1753$ . In the hippocampus, vehicle control animals demonstrated a decrease in MBP relative density ( $16656\pm 5380$ ), compared to sham animals ( $21178\pm 5389$ ). Treatment with 0.25mg/kg WT APP96 110 reduced MBP relative density to  $11302\pm 4615$ , while treatment with 0.25mg/kg 3+APP96 110 slightly increased MBP relative density to  $16308\pm 4615$ , when compared to treatment with WT APP96 110.

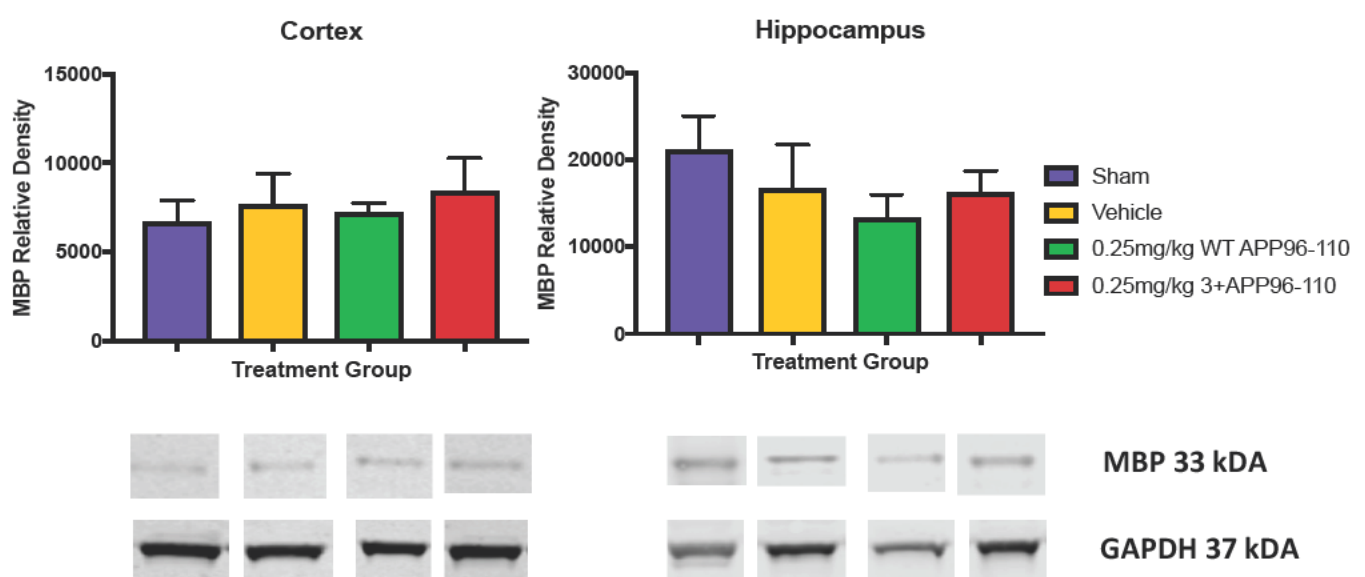


**Figure 6.10: Analysis of MBP relative density within the cortex and hippocampus at 30 days following TBI.  $n=3-5$  per group. Data were assessed using a one-way ANOVA with Tukey's post-test.**

## Tau 5

Tau proteins are involved with the stabilization of microtubules within neurons, with Tau 5 being a measure of the total amount of tau present (Figure 6.11). No significant differences were noted in the cortex ( $p=0.93$ ), or the hippocampus ( $p=0.25$ ). In the cortex, vehicle control animals demonstrated a small decrease in tau 5 relative density ( $42320\pm5211$ ), compared to sham animals ( $45628\pm5211$ ). Treatment with APP96 110 returned these levels to sham levels, with 0.25mg/kg WT APP96 110 reaching  $45234\pm4868$  in tau 5 relative density, while 0.25mg/kg 3+APP96 110 reached  $45135\pm4868$  in tau 5 relative density. In the hippocampus, vehicle control animals demonstrated a small decrease in tau 5 relative density ( $37261\pm5792$ ), compared to sham animals ( $44622\pm5792$ ). Treatment with 0.25mg/kg WT APP96 110 resulted in similar levels of tau 5 relative density ( $37166\pm4914$ ), whilst treatment with 0.25mg/kg 3+APP96 110 resulted in an increase to sham level in tau 5 relative density ( $46227\pm4914$ ).

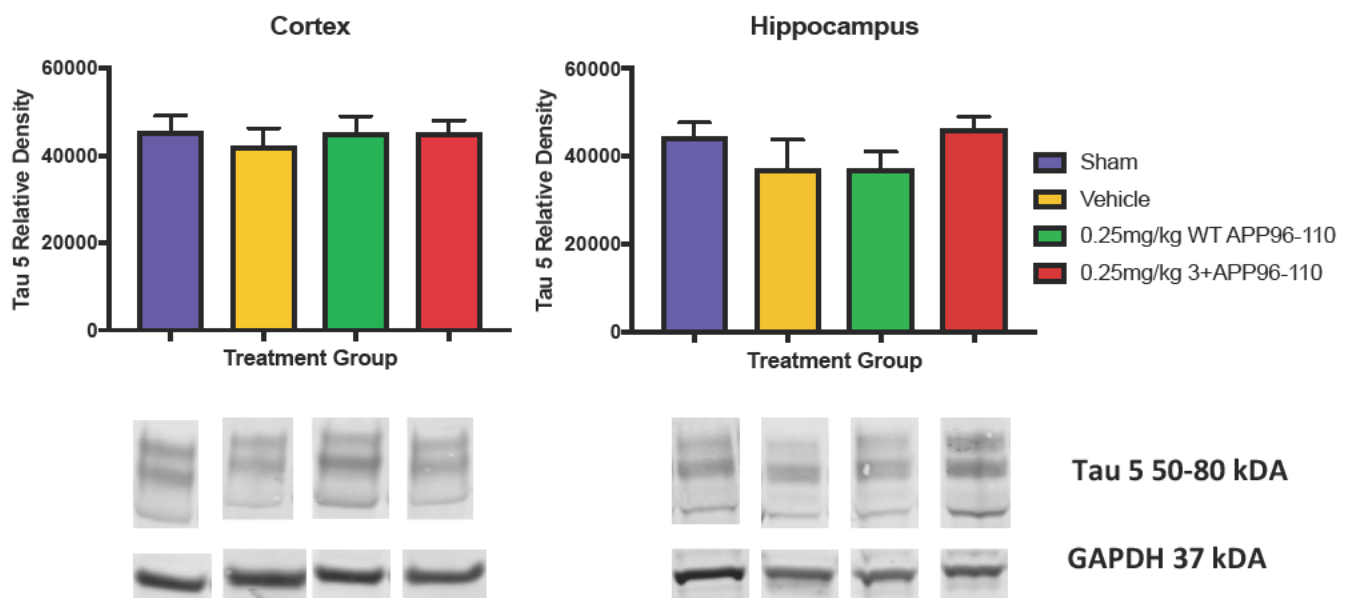


**Figure 6.11: Analysis of Tau 5 relative density within the cortex and hippocampus at 30 days following TBI. n=3-5 per group. Data were assessed using a one-way ANOVA with Tukey's post-test.**

## 6.4 Discussion

Until this point, research assessing the neuroprotective efficacy of APP96 110 peptides following TBI has only been assessed acutely following trauma. As such, this is the first study to examine the long term efficacy of IV APP96 110 derivatives following TBI, and forms the logical next step in the progression and development of APP96 110 derivatives as novel therapeutic agents following TBI.

Treatment with the enhanced 0.25mg/kg 3+APP96 110 peptide resulted in significant improvements in motor outcome early, with animals returning to sham level by day 5 and maintained this level throughout the 30 day testing period. Importantly, treatment with either WT or 3+APP96 110 did not produce any physical signs of long term toxicity over 30 days. The 3+APP96 110 peptide also produced significant effects in learning and memory ability of the rats. This was associated with a significant reduction in microglial activation in the corpus callosum with WT APP96 110 treatment, with a trend towards significance with the 3+APP96 110 treatment. However, no changes in astrocyte reactivity were observed. Overall there were no significant differences between treatment groups following examination of the relative expression of proteins related to changes to synapses, dendrites, myelination, axonal structure and phosphorylation of neurodegenerative proteins, as determined by Western Blot analysis.

The administration of 0.25mg/kg WT APP96 110 and 0.25mg/kg 3+APP96 110 (as determined and discussed in Chapter 5), saw considerable improvements in motor outcome over the 30 day testing period, with treatment with 0.25mg/kg 3+APP96 110 demonstrating significant



differences from vehicle control animals on days 1-3 post TBI. This acute improvement is consistent with previous findings, where the greatest deficits in motor outcome have been observed initially following TBI lasting up to 3-5 days, after which animals show improvement towards sham level (refer to previously discussed motor performance in Chapters 4 and 5). While there were no significant differences in motor outcome between treatment groups beyond 14 days post TBI, continuous observation over the 30 day timepoint did not highlight any long term changes in motor performance, with animals' performance remaining consistent amongst their respective treatment groups with their earlier performance. The slight drop in the performance of vehicle control animals over days 14-28 is most likely due to the repetitive nature of daily, followed by weekly rotarod testing where animals appear to struggle for motivation to complete the task. Overall, these findings suggest that a singular administration of APP96-110 up to 5 hours post TBI may be sufficient to exert its neuroprotective properties long term, without any physical signs of long term toxicity or deterioration.

Whilst motor outcome has consistently shown to be a highly sensitive indicator of both injury severity and effectiveness of treatment, changes in cognitive outcome over time present an equally important story. In a human setting of TBI, patients that survive are often left with long term cognitive and personality changes (Rabinowitz and Levin, 2014). These changes are usually slow to develop and include issues like depression and anxiety, loss of spatial awareness, memory loss, as well as the loss of the ability to learn quickly and to form new memories (Rabinowitz and Levin, 2014). The mazes used in this study are all well established rodent mazes and were all aimed at assessing these changes following APP96-110 treatment in a clinically relevant way following rodent TBI. The Barnes Maze and Forced Swim Test both

demonstrated differences between vehicle control and APP96 110 treated animals. On day one of the Barnes Maze, 0.25mg/kg 3+APP96 110 treated animals showed a significant decrease in the time spent to learn the location of the escape box compared to vehicle control animals, performing on a par with sham animals. This continued for the remaining two days, indicative of no loss of ability to learn new tasks or with the acquisition of short term memory. On the fifth day, animals in both APP96 110 treatment groups displayed a substantial reduction in the time taken to find the old box when compared to vehicle control animals, on a par with sham animals. In the forced swim test, 0.25mg/kg 3+APP96 110 treated animals demonstrated a reduced, although not significant, amount of time spent immobile, on a par with sham level, indicative of lower depressive like tendencies.

In contrast to the Barnes Maze and Forced Swim Test, there were neither injury or treatment effects observed with the Open Field, Elevated Plus Maze or the Y Maze. In the Elevated Plus Maze, vehicle control animals did not display the levels of anxiety anticipated in injured animals. A lack of anxiety 6 weeks following TBI has been noted previously, with rats displaying memory disruptions, but a lack of anxiety, as assessed with this maze, following focal TBI at a similar age to the rats used in this study (Amoros Aguilar et al., 2015). Consequently, no conclusions about the effect of treatment on long term anxiety post TBI could be drawn. While the mazes chosen are all well established for rodent cognitive and behavioural testing, it is possible that the tests are not sensitive enough to detect subtle deficits like anxiety and hippocampal dependent spatial awareness and memory loss. As such, the use of more sensitive cognition testing like the use of rodent i pad based operant boxes may be required in the future to examine more subtle cognitive deficits. It is also possible that the 30 day time point may not be long enough post TBI for some of these more subtle deficits

to reach detectable level. Some cognitive impairments following diffuse TBI can develop at least a month after diffuse TBI before they become detectable (Muccigrosso et al., 2016), and as such, some of the more subtle cognitive deficits in this study may have been missed due to the 30 day endpoint. Accordingly, the examination of cognitive deficits at a later timepoint like 3 months following severe diffuse TBI may be worth further investigation.

Whilst the functional outcome tells an important story into the efficacy of these APP96 110 peptides post TBI, their efficacy molecularly helps to paint a bigger picture. No differences in the percentage of activated microglia, or the number of reactive astrocytes were observed in the cortex following TBI. While this area lies directly under the impact site of the trauma, this is not the location where the majority of damage seems to occur. The diffuse nature of this injury model produces widespread axonal damage throughout white matter tracts like the corpus callosum (Marmarou et al., 1994), where acute AI has been consistently observed and examined (Chapters 4 and 5). It stands to reason that, given some of the many roles of activated microglia and reactive astrocytes to migrate to the site of damage, that they will have an increased presence at the site of injury throughout the corpus callosum over other regions (Johnson et al., 2013). In the corpus callosum, the percentage of activated microglia were significantly elevated in vehicle control animals at 30 days, in line with findings showing a heightened inflammatory profile of microglia 30 days following diffuse TBI (Muccigrosso et al., 2016). In Chapter 4, microglial activation was shown to be increased at 3 days post TBI in vehicle control animals, with WT APP96 110 treatment able to return these levels to sham level. The paralleled observation at 30 days suggests that an acute inflammatory response may be initiated shortly following TBI, which was able to progress into a sustained chronic inflammatory state 30 days later, as has been seen clinically (Johnson et al., 2013,

Ramlackhansingh et al., 2011). In this study, the ability of both WT and 3+APP96 110 to again return these levels to sham level, suggests that treatment with APP96 110 is able to reduce the initial injury severity immediately following TBI compared to untreated animals, resulting in less physical damage to neurons and axons, consequently halting the progression of the secondary injury cascade to impede a chronic microglial response. In contrast, the long term astrocytic response to injury in the corpus callosum was unremarkable. Neither qualitative increases in overall astrocyte number, nor differences in the levels of reactive astrocytes between treatment groups were seen in the corpus callosum at 30 days. While this may be due to the differences in the method of assessment between the two cell types, the similar observations as with activated microglia, where reactive astrocytes were elevated at 3 days post TBI, with a lack of differences noted at 30 days, suggests that unlike microglia, a chronic astrocytic response to injury did not persist, with the astrocytic response seen at 3 days perhaps remaining acute. It is well established that astrocytes can play both a beneficial and detrimental role both acutely and chronically following TBI (Pekny et al., 2014, Laird et al., 2008). The diffuse nature of this TBI with an absence of a glial scar renders the precise role of the astrocytic responses in this study unclear, and warrants further investigation.

The immunohistological findings in this study were supplemented by Western Blot analysis looking to assess the long term effects of APP96 110 treatment on the density of dendrites and synapses, axonal structure and the beginnings of neurodegeneration through tau proteins. With the exception of 0.25mg/kg WT APP966 10 significantly increasing the synaptophysin relative density compared to sham animals in the cortex, no significant differences were seen between treatment groups with any of the other protein assessments. Whilst the finding of increased synaptogenesis in the cortex initially suggests a positive effect

of APP96 110 treatment on the density of synapses and suggestive of neurotrophic effects, the minute differences seen between the other TBI groups like vehicle controls and 3+APP96 110, in conjunction with a lack of similar trend seen in the hippocampus, suggests that a more in depth investigation is warranted. The lack of differences observed in both total and phosphorylated tau suggests in part, that the 30 day time point may be too early to look in depth at long term neurodegeneration following APP966 110 treatment post TBI.

Taken together, the results from this study demonstrate that IV administration of various APP96 110 derivatives produces long term neuroprotective effects that remain up to 30 days following TBI. There were no physical signs of long term toxicity following administration, and whilst WT and 3+APP96 110 produced similar results molecularly, treatment with 3+APP96 110 outperformed WT APP96 110 in terms of functional outcome. Whilst the 30 day time point in this study may lie on the cusp of displaying the beginnings of long term neurodegeneration and neuroinflammation, it provides a first look at the longer term performance and outcome of rats following treatment with APP96 110 peptides. The novel window of opportunity that exists between primary injury and the initiation of the secondary injury cascade following TBI provides a novel window of opportunity for a therapeutic intervention to be able to halt the progression of many of the deleterious secondary injury events like chronic inflammation. Together, the results of this study lend weight to support that APP96 110 derivatives can exert their neuroprotective action in the window of opportunity to halt the progression of the disease, rather than treating the consequences as they arise. As such the neuroprotective efficacy of APP96 110 derivatives should continue to be exploited in the quest to develop novel therapeutic agents for conditions like TBI.

## **Chapter 7: Summary & Future Directions**

TBI is a life threatening injury, and yet despite its serious nature, there are currently no effective therapeutic agents to treat the condition. The experiments within this thesis have further consolidated the neuroprotective role of the APP derivative APP96 110 following TBI, with an emphasis on progressing the pre clinical development of this peptide as a novel therapeutic agent. As such, the optimal dose, route and timepoint of administration for this peptide was determined in the acute phase post TBI. It was hypothesized that the neuroprotective properties of APP96 110 following TBI are linked to its heparin binding sites, and these specific regions are therefore responsible for APP protecting against neuronal injury and improving neurological outcome following TBI. Accordingly, novel APP96 110 analogues with enhanced heparin binding action were developed, with administration of these analogues tested for efficacy of improvement in long term outcome, neuroinflammation and neurodegeneration.

Currently following TBI, patients are only able to receive symptomatic relief with osmotherapies or the surgically invasive decompressive craniotomy. To date, DAI remains untreatable, and is the leading cause of coma and vegetative state following TBI (Smith et al., 2003, Adams et al., 1989). This highlights the need for the development of clinically relevant neuroprotective therapeutic options that prevent the ongoing damage associated with diffuse TBI like DAI. A challenge for many drugs targeting brain trauma is the inability to penetrate the BBB and reach the CNS. The first aim of this study was to determine whether APP966 110 would remain efficacious when administered via IV, with the transition from ICV to IV route of administration offering clear clinical advantages. The ability of IV APP96 110 in this study to produce neuroprotective benefits in functional outcome and neuronal damage

that were comparable to those seen following ICV administration, suggests that APP96 110 is able to enter the brain in a functional state via the IV route following injury. Furthermore, the finding that IV APP96 110 can remain effective up to 5 hours post TBI is clinically important, and significantly extends its therapeutic time frame for treatment. In a clinical setting, the time frame between injury and arrival to a trauma unit can often far exceed an hour, by which point the delayed, but inevitable, secondary injury events like cell death and neuroinflammation will have begun. As such, the ability to administer APP96 110 IV up to several hours following TBI in an effort to slow the progression of the secondary injury events is crucial in advancing bench to bedside progress.

While the clinical relevance of APP96 110 as a potential therapy for TBI has been clearly demonstrated, the mechanism of action through which these effects occur is yet to be fully understood. The ability of APP96 110 to have a strong affinity to bind to heparin is currently the strongest hypothesis for its mechanism of action. Indeed, the structure of APP96 110 itself is thought to play a crucial role in its mechanism. All APP96 110 analogues contain a  $\beta$  hairpin loop constrained by a disulphide bond between cysteines 98 and 105 (Small et al., 1994, Rossjohn et al., 1999). The presence of this loop has been previously shown to be critical for promoting neurite outgrowth from central and peripheral neurons (Young Pearse et al., 2008), the activation of MAP kinase (Greenberg and Kosik, 1995), as well as maintaining the physical structure of the peptide. Further evidence has highlighted that the D1 domain of sAPP $\alpha$ , of which APP96 110 is the active region, displays a high structural similarity to growth factor like domains, and exhibits a strong affinity to heparin, particularly to HSPGs (Narindrasorasak et al., 1991, Small et al., 1992, Rossjohn et al., 1999). HSPGs can act as either receptors or co receptors (Sarrazin et al., 2011), and it is thought that APP96 110 may bind,



through the region encompassing the  $\beta$  hairpin loop, to cell surface or extracellular matrix bound HSPGs to elicit a number of key physiological changes such as the regulation of cell adhesion, synaptogenesis, cell signalling and neurite outgrowth (Small et al., 1994, Clarris et al., 1997, Rossjohn et al., 1999), all of which are important steps in promoting neuroplasticity and subsequent neurogenesis following TBI. However, it is also possible that HSPGs are not the precise neuroprotective receptor for APP96 110, and that a more conventional protein receptor may be the target for these metabolites.

This research has demonstrated that the ability to selectively mutate a protein based on its amino acid sequence, and subsequently design and generate analogues to APP96 110, is an exciting prospect for the pre clinical development of therapeutic agents for conditions like TBI. As such, the second aim of this study was to determine whether the neuroprotective activity of APP96 110 correlates to its heparin binding activity, and if increasing its binding activity would enhance its neuroprotective activity *in vivo*. The mutation of key amino acid residues in the APP96 110 sequence was shown through a heparin chromatography assay to enhance the affinity of APP96 110 to bind to heparin. When the enhanced 3+APP96 110 peptide was administered at the same dose to WT APP96 110 *in vivo* following TBI, it resulted in greater neuroprotective action, highlighting that smaller doses of 3+APP96 110 could confer similar neuroprotective benefits to higher doses of WT APP96 110 following trauma.

Up until this point, research assessing the neuroprotective efficacy of APP96 110 peptides following TBI had as only been assessed acutely following trauma. The ability of APP96 110 derivatives to improve outcome in the long term forms the logical next step in the progression and development of APP96 110 derivatives as novel therapeutic agents following

TBI. Many patients who survive a TBI are typically left with lasting impairments, including motor difficulties, as well as long term issues like anxiety, depression, learning difficulties and memory loss (Rabinowitz and Levin, 2014). As such, the third aim of this study was to examine the long term efficacy of IV APP96 110 administration and the effects on functional outcome, neuroinflammation and neurodegeneration up to 30 days following TBI. IV administration of various APP96 110 derivatives appears to produce long term neuroprotective effects, with no physical signs of long term toxicity following administration. Whilst WT and 3+APP96 110 produced similar protection for neuroinflammation, axonal structure, myelination, synaptogenesis and neurodegeneration, treatment with 3+APP96 110 significantly outperformed WT APP96 110 in its ability to improve functional outcome. Whilst the 30 day time point in this study may lie on the cusp of displaying the beginnings of long term neurodegeneration and neuroinflammation, it provides a first look at the longer term performance and outcome of rats following treatment with APP96 110 peptides. The novel window of opportunity that exists between primary injury and the initiation of the secondary injury cascade following TBI provides a novel window of opportunity for a therapeutic intervention to be able to halt the progression of many of the deleterious secondary injury events like chronic inflammation.

## **7.1 Future directions**

The findings within this thesis continue to highlight the substantial neuroprotective benefits that APP96 110 offers following TBI. This work has been fundamental in laying the groundwork for two National Health & Medical Research Council (NHMRC) grants awarded in 2016 and 2017. The first grant aims to decipher the relationships between APLP2 and sAPP $\alpha$ .

in TBI, by testing the response of APLP knockout ( / ) mice to TBI, assessing whether this response is gender dependent, determining if APLP2's neuroprotective activity is mediated by sAPP $\alpha$ , and examining the molecular and cellular pathways that mediate the neuroprotective activity of sAPP $\alpha$ /APLP2 in TBI. The second grant aims to progress this important pre clinical research seen in this thesis into an ovine model of moderate severe diffuse TBI, through examining the effects of APP96 110 treatment on axonal injury, neuroinflammation, cell death and functional outcome. This ovine model of diffuse TBI has proven to be a superior model for TBI with highly relevant clinical features (Lewis et al., 1996). Importantly, treatments that were successful in rodent experimental TBI, but subsequently failed when assessed in the clinic, were also shown to be ineffective in this larger animal models in our laboratory (unpublished data), and as such, these upcoming studies should improve the clinical translation of APP96 110. Due to the gyrencephalic structure of the sheep brain, it is important to re assess the therapeutic window, investigating the optimal treatment regime through pharmacokinetic evaluation and determining the effect of treatment on gene expression patterns following moderate TBI in sheep.

Nonetheless, a considerable gap in our understanding of the precise mechanisms of action of this peptide following trauma remains. Our findings give a cursory overview of the neuroinflammatory and neurodegenerative changes long term following TBI, but highlight the need for a more comprehensive exploration of these changes. Indeed, more comprehensive molecular neuroinflammatory assessments on our tissue have already begun, and the very preliminary ongoing observations can be found in the Appendix. Furthermore, we are also in the process of undertaking more Western Blot analyses for neurodegeneration

antibodies like tau and  $\alpha$  synuclein, which due to ongoing issues that were unable to be rectified in due course, will be fully explored in the near future. The findings from this research also suggest a considerable influence of heparin binding in the mechanism of action of APP96 110, with a much more detailed investigation required to understand this fully. The identification of the receptor, and the subsequent signaling pathways that this activates, will help to decipher the molecular mechanisms for APP96 110's activity. Further exploration of the pharmacokinetic properties of APP96 110 is also vital. This is a key aim of one of the recently awarded NHMRC grants, and will help to further optimise the therapeutic activity of APP96 110 after TBI, with knowledge of its behaviour throughout the body providing a promising avenue for therapeutic exploitation. Furthermore, the evaluation of whether the current 5 hour therapeutic window of opportunity of APP96 110 treatment has reached its limit, or whether it may in fact extend beyond this time frame is also an important avenue to consider.

In conclusion, the neuroprotective benefits of APP96 110 demonstrated by the findings in this thesis support that APP96 110 derivatives can exert their neuroprotective action in the window of opportunity to halt the progression of the disease, whilst also targeting multiple elements of the secondary injury cascade as has been previously suggested. They also highlight the need for continued progression and development of APP96 110 as a therapeutic intervention for TBI, and in particular DAI, that currently lacks an efficacious treatment. It is hoped that a treatment like this could ultimately be administered by paramedics at the scene of a TBI, rather than requiring transfer to a trauma unit for treatment. This would ultimately slow the progression of the deleterious secondary injury early after trauma to minimize

functional deficits. Overall, APP96 110 shows promise as a novel and clinically relevant treatment option by offering substantial neuroprotective and neurotrophic effects that reduce secondary injury and functional deficits associated with acute traumatic brain injury.

## References

- ADAMS, J. H., DOYLE, D., FORD, I., GENNARELLI, T. A., GRAHAM, D. I. & MCLELLAN, D. R. 1989. Diffuse axonal injury in head injury: definition, diagnosis and grading. *Histopathology*, 15, 49 59.
- AMOROS AGUILAR, L., PORTELL CORTES, I., COSTA MISERACHS, D., TORRAS GARCIA, M. & COLL ANDREU, M. 2015. Traumatic brain injury in late adolescent rats: effects on adulthood memory and anxiety. *Behav Neurosci*, 129, 149 59.
- ANDREW, R. J., KELLETT, K. A., THINAKARAN, G. & HOOPER, N. M. 2016. A Greek Tragedy: The Growing Complexity of Alzheimer Amyloid Precursor Protein Proteolysis. *J Biol Chem*, 291, 19235 44.
- BADAN, I., DINCA, I., BUCHHOLD, B., SUOFU, Y., WALKER, L., GRATZ, M., PLATT, D., KESSLER, C. H. & POPA WAGNER, A. 2004. Accelerated accumulation of N and C terminal beta APP fragments and delayed recovery of microtubule associated protein 1B expression following stroke in aged rats. *Eur J Neurosci*, 19, 2270 80.
- BARNES, C. A. 1979. Memory deficits associated with senescence: a neurophysiological and behavioral study in the rat. *J Comp Physiol Psychol*, 93, 74 104.
- BASKAYA, M. K., RAO, A. M., DOGAN, A., DONALDSON, D. & DEMPSEY, R. J. 1997. The biphasic opening of the blood brain barrier in the cortex and hippocampus after traumatic brain injury in rats. *Neurosci Lett*, 226, 33 6.
- BAYER, T. A., CAPPAL, R., MASTERS, C. L., BEYREUTHER, K. & MULTHAUP, G. 1999. It all sticks together the APP related family of proteins and Alzheimer's disease. *Mol Psychiatry*, 4, 524 8.
- BLUMBERGS, P. C., SCOTT, G., MANAVIS, J., WAINWRIGHT, H., SIMPSON, D. A. & MCLEAN, A. J. 1994. Staining of amyloid precursor protein to study axonal damage in mild head injury. *Lancet*, 344, 1055 6.
- BROWER, M., GRACE, M., KOTZ, C. M. & KOYA, V. 2015. Comparative analysis of growth characteristics of Sprague Dawley rats obtained from different sources. *Lab Anim Res*, 31, 166 73.
- BUKI, A. & POVLISHOCK, J. T. 2006. All roads lead to disconnection? Traumatic axonal injury revisited. *Acta Neurochir (Wien)*, 148, 181 93; discussion 193 4.
- CARDIN, A. D., DEMETER, D. A., WEINTRAUB, H. J. & JACKSON, R. L. 1991. Molecular design and modeling of protein heparin interactions. *Methods Enzymol*, 203, 556 83.
- CLARRIS, H. J., CAPPAL, R., HEFFERNAN, D., BEYREUTHER, K., MASTERS, C. L. & SMALL, D. H. 1997. Identification of heparin binding domains in the amyloid precursor protein of Alzheimer's disease by deletion mutagenesis and peptide mapping. *J Neurochem*, 68, 1164 72.
- COLLINS PRAINO, L. E., ARULSAMY, A., KATHARESAN, V. & CORRIGAN, F. 2018. The effect of an acute systemic inflammatory insult on the chronic effects of a single mild traumatic brain injury. *Behav Brain Res*, 336, 22 31.
- CONRAD, C. D., GALEA, L. A., KURODA, Y. & MCEWEN, B. S. 1996. Chronic stress impairs rat spatial memory on the Y maze, and this effect is blocked by tianeptine pretreatment. *Behav Neurosci*, 110, 1321 34.
- CORRIGAN, F., PHAM, C. L., VINK, R., BLUMBERGS, P. C., MASTERS, C. L., VAN DEN HEUVEL, C. & CAPPAL, R. 2011. The neuroprotective domains of the amyloid precursor protein, in

- traumatic brain injury, are located in the two growth factor domains. *Brain Res*, 1378, 137 43.
- CORRIGAN, F., THORNTON, E., ROISMAN, L. C., LEONARD, A. V., VINK, R., BLUMBERGS, P. C., VAN DEN HEUVEL, C. & CAPPAL, R. 2014. The neuroprotective activity of the amyloid precursor protein against traumatic brain injury is mediated via the heparin binding site in residues 96 110. *J Neurochem*, 128, 196 204.
- CORRIGAN, F., VINK, R., BLUMBERGS, P. C., MASTERS, C. L., CAPPAL, R. & VAN DEN HEUVEL, C. 2012a. Characterisation of the effect of knockout of the amyloid precursor protein on outcome following mild traumatic brain injury. *Brain Res*, 1451, 87 99.
- CORRIGAN, F., VINK, R., BLUMBERGS, P. C., MASTERS, C. L., CAPPAL, R. & VAN DEN HEUVEL, C. 2012b. sAPPalpha rescues deficits in amyloid precursor protein knockout mice following focal traumatic brain injury. *J Neurochem*, 122, 208 20.
- DAVIS, E. J., FOSTER, T. D. & THOMAS, W. E. 1994. Cellular forms and functions of brain microglia. *Brain Res Bull*, 34, 73 8.
- DAWKINS, E. & SMALL, D. H. 2014. Insights into the physiological function of the beta amyloid precursor protein: beyond Alzheimer's disease. *J Neurochem*, 129, 756 69.
- DONAT, C. K., SCOTT, G., GENTLEMAN, S. M. & SASTRE, M. 2017. Microglial Activation in Traumatic Brain Injury. *Front Aging Neurosci*, 9, 208.
- DURAIYAN, J., GOVINDARAJAN, R., KALIYAPPAN, K. & PALANISAMY, M. 2012. Applications of immunohistochemistry. *J Pharm Bioallied Sci*, 4, S307 9.
- FADEN, A. I. & STOICA, B. 2007. Neuroprotection: challenges and opportunities. *Arch Neurol*, 64, 794 800.
- FEIGIN, V. L., THEADOM, A., BARKER COLLO, S., STARKEY, N. J., MCPHERSON, K., KAHAN, M., DOWELL, A., BROWN, P., PARAG, V., KYDD, R., JONES, K., JONES, A. & AMERATUNGA, S. 2013. Incidence of traumatic brain injury in New Zealand: a population based study. *Lancet Neurol*, 12, 53 64.
- FINNIE, J. W. & BLUMBERGS, P. C. 2002. Traumatic brain injury. *Vet Pathol*, 39, 679 89.
- GENTLEMAN, S. M., NASH, M. J., SWEETING, C. J., GRAHAM, D. I. & ROBERTS, G. W. 1993. Beta amyloid precursor protein (beta APP) as a marker for axonal injury after head injury. *Neurosci Lett*, 160, 139 44.
- GREENBERG, S. M. & KOSIK, K. S. 1995. Secreted beta APP stimulates MAP kinase and phosphorylation of tau in neurons. *Neurobiol Aging*, 16, 403 7; discussion 407 8.
- GREENBERG, S. M., QIU, W. Q., SELKOE, D. J., BEN ITZHAK, A. & KOSIK, K. S. 1995. Amino terminal region of the beta amyloid precursor protein activates mitogen activated protein kinase. *Neurosci Lett*, 198, 52 6.
- GREVE, M. W. & ZINK, B. J. 2009. Pathophysiology of traumatic brain injury. *Mt Sinai J Med*, 76, 97 104.
- HABGOOD, M. D., BYE, N., DZIEGIELEWSKA, K. M., EK, C. J., LANE, M. A., POTTER, A., MORGANTI KOSSMANN, C. & SAUNDERS, N. R. 2007. Changes in blood brain barrier permeability to large and small molecules following traumatic brain injury in mice. *Eur J Neurosci*, 25, 231 8.
- HAMM, R. J., PIKE, B. R., O'DELL, D. M., LYETH, B. G. & JENKINS, L. W. 1994. The rotarod test: an evaluation of its effectiveness in assessing motor deficits following traumatic brain injury. *J Neurotrauma*, 11, 187 96.
- HEATH, D. L. & VINK, R. 1999. Improved motor outcome in response to magnesium therapy received up to 24 hours after traumatic diffuse axonal brain injury in rats. *J Neurosurg*, 90, 504 9.

- HELLEWELL, S. C., YAN, E. B., AGYAPOMAA, D. A., BYE, N. & MORGANTI KOSSMANN, M. C. 2010. Post traumatic hypoxia exacerbates brain tissue damage: analysis of axonal injury and glial responses. *J Neurotrauma*, 27, 1997 2010.
- HONNDORF, S., LINDEMANN, C., TOLLNER, K. & GERNERT, M. 2011. Female Wistar rats obtained from different breeders vary in anxiety like behavior and epileptogenesis. *Epilepsy Res*, 94, 26 38.
- JOHNSON, V. E., STEWART, J. E., BEGBIE, F. D., TROJANOWSKI, J. Q., SMITH, D. H. & STEWART, W. 2013. Inflammation and white matter degeneration persist for years after a single traumatic brain injury. *Brain*, 136, 28 42.
- KARVE, I. P., TAYLOR, J. M. & CRACK, P. J. 2016. The contribution of astrocytes and microglia to traumatic brain injury. *Br J Pharmacol*, 173, 692 702.
- KOBAYASHI, S., SASAKI, T., KATAYAMA, T., HASEGAWA, T., NAGANO, A. & SATO, K. 2010. Temporal spatial expression of presenilin 1 and the production of amyloid beta after acute spinal cord injury in adult rat. *Neurochem Int*, 56, 387 93.
- KUMAR, A. & LOANE, D. J. 2012. Neuroinflammation after traumatic brain injury: opportunities for therapeutic intervention. *Brain Behav Immun*, 26, 1191 201.
- LAIRD, M. D., VENDER, J. R. & DHANDAPANI, K. M. 2008. Opposing roles for reactive astrocytes following traumatic brain injury. *Neurosignals*, 16, 154 64.
- LANGER, M., BRANDT, C. & LOSCHER, W. 2011. Marked strain and substrain differences in induction of status epilepticus and subsequent development of neurodegeneration, epilepsy, and behavioral alterations in rats. [corrected]. *Epilepsy Res*, 96, 207 24.
- LEWIS, S. B., FINNIE, J. W., BLUMBERGS, P. C., SCOTT, G., MANAVIS, J., BROWN, C., REILLY, P. L., JONES, N. R. & MCLEAN, A. J. 1996. A head impact model of early axonal injury in the sheep. *J Neurotrauma*, 13, 505 14.
- MAAS, A. I., ROOZENBEEK, B. & MANLEY, G. T. 2010. Clinical trials in traumatic brain injury: past experience and current developments. *Neurotherapeutics*, 7, 115 26.
- MAAS, A. I., STOCCHETTI, N. & BULLOCK, R. 2008. Moderate and severe traumatic brain injury in adults. *Lancet Neurol*, 7, 728 41.
- MARMAROU, A., FODA, M. A., VAN DEN BRINK, W., CAMPBELL, J., KITA, H. & DEMETRIADOU, K. 1994. A new model of diffuse brain injury in rats. Part I: Pathophysiology and biomechanics. *J Neurosurg*, 80, 291 300.
- MAXWELL, W. L., WATT, C., GRAHAM, D. I. & GENNARELLI, T. A. 1993. Ultrastructural evidence of axonal shearing as a result of lateral acceleration of the head in non human primates. *Acta Neuropathol*, 86, 136 44.
- MCATEER, K. M., CORRIGAN, F., THORNTON, E., TURNER, R. J. & VINK, R. 2016. Short and Long Term Behavioral and Pathological Changes in a Novel Rodent Model of Repetitive Mild Traumatic Brain Injury. *PLoS One*, 11, e0160220.
- MEDANA, I. M. & ESIRI, M. M. 2003. Axonal damage: a key predictor of outcome in human CNS diseases. *Brain*, 126, 515 30.
- MONTSERRET, R., AUBERT FOUCHER, E., MCLEISH, M. J., HILL, J. M., FICHEUX, D., JAQUINOD, M., VAN DER REST, M., DELEAGE, G. & PENIN, F. 1999. Structural analysis of the heparin binding site of the NC1 domain of collagen XIV by CD and NMR. *Biochemistry*, 38, 6479 88.
- MUCCIGROSSO, M. M., FORD, J., BENNER, B., MOUSSA, D., BURNSIDES, C., FENN, A. M., POPOVICH, P. G., LIFSHITZ, J., WALKER, F. R., EIFERMAN, D. S. & GODBOUT, J. P. 2016. Cognitive deficits develop 1month after diffuse brain injury and are exaggerated by



- microglia associated reactivity to peripheral immune challenge. *Brain Behav Immun*, 54, 95 109.
- NARINDRASORASAK, S., LOWERY, D., GONZALEZ DEWHITT, P., POORMAN, R. A., GREENBERG, B. & KISILEVSKY, R. 1991. High affinity interactions between the Alzheimer's beta amyloid precursor proteins and the basement membrane form of heparan sulfate proteoglycan. *J Biol Chem*, 266, 12878 83.
- OLAH, M., BIBER, K., VINET, J. & BODDEKE, H. W. 2011. Microglia phenotype diversity. *CNS Neurol Disord Drug Targets*, 10, 108 18.
- PEKNY, M., WILHELMSSON, U. & PEKNA, M. 2014. The dual role of astrocyte activation and reactive gliosis. *Neurosci Lett*, 565, 30 8.
- PELLOW, S., CHOPIN, P., FILE, S. E. & BRILEY, M. 1985. Validation of open:closed arm entries in an elevated plus maze as a measure of anxiety in the rat. *J Neurosci Methods*, 14, 149 67.
- PLUMMER, S., VAN DEN HEUVEL, C., THORNTON, E., CORRIGAN, F. & CAPPAL, R. 2016. The Neuroprotective Properties of the Amyloid Precursor Protein Following Traumatic Brain Injury. *Aging Dis*, 7, 163 79.
- POVLISHOCK, J. T. 1993. Pathobiology of traumatically induced axonal injury in animals and man. *Ann Emerg Med*, 22, 980 6.
- RABINOWITZ, A. R. & LEVIN, H. S. 2014. Cognitive sequelae of traumatic brain injury. *Psychiatr Clin North Am*, 37, 1 11.
- RAMLACKHANSINGH, A. F., BROOKS, D. J., GREENWOOD, R. J., BOSE, S. K., TURKHEIMER, F. E., KINNUNEN, K. M., GENTLEMAN, S., HECKEMANN, R. A., GUNANAYAGAM, K., GELOSA, G. & SHARP, D. J. 2011. Inflammation after trauma: microglial activation and traumatic brain injury. *Ann Neurol*, 70, 374 83.
- ROSSJOHN, J., CAPPAL, R., FEIL, S. C., HENRY, A., MCKINSTRY, W. J., GALATIS, D., HESSE, L., MULTHAUP, G., BEYREUTHER, K., MASTERS, C. L. & PARKER, M. W. 1999. Crystal structure of the N terminal, growth factor like domain of Alzheimer amyloid precursor protein. *Nat Struct Biol*, 6, 327 31.
- SARRAZIN, S., LAMANNA, W. C. & ESKO, J. D. 2011. Heparan sulfate proteoglycans. *Cold Spring Harb Perspect Biol*, 3.
- SMALL, D. H., NURCOMBE, V., MOIR, R., MICHAELSON, S., MONARD, D., BEYREUTHER, K. & MASTERS, C. L. 1992. Association and release of the amyloid protein precursor of Alzheimer's disease from chick brain extracellular matrix. *J Neurosci*, 12, 4143 50.
- SMALL, D. H., NURCOMBE, V., REED, G., CLARRIS, H., MOIR, R., BEYREUTHER, K. & MASTERS, C. L. 1994. A heparin binding domain in the amyloid protein precursor of Alzheimer's disease is involved in the regulation of neurite outgrowth. *J Neurosci*, 14, 2117 27.
- SMITH, D. H., MEANEY, D. F. & SHULL, W. H. 2003. Diffuse axonal injury in head trauma. *J Head Trauma Rehabil*, 18, 307 16.
- THORNTON, E., VINK, R., BLUMBERGS, P. C. & VAN DEN HEUVEL, C. 2006. Soluble amyloid precursor protein alpha reduces neuronal injury and improves functional outcome following diffuse traumatic brain injury in rats. *Brain Res*, 1094, 38 46.
- VAN DEN HEUVEL, C., BLUMBERGS, P. C., FINNIE, J. W., MANAVIS, J., JONES, N. R., REILLY, P. L. & PEREIRA, R. A. 1999. Upregulation of amyloid precursor protein messenger RNA in response to traumatic brain injury: an ovine head impact model. *Exp Neurol*, 159, 441 50.
- VINK, R. & NIMMO, A. J. 2002. Novel therapies in development for the treatment of traumatic brain injury. *Expert Opin Investig Drugs*, 11, 1375 86.

- VINK, R. & VAN DEN HEUVEL, C. 2004. Recent advances in the development of multifactorial therapies for the treatment of traumatic brain injury. *Expert Opin Investig Drugs*, 13, 1263-74.
- WILLIAMSON, T. G., MOK, S. S., HENRY, A., CAPPAL, R., LANDER, A. D., NURCOMBE, V., BEYREUTHER, K., MASTERS, C. L. & SMALL, D. H. 1996. Secreted glypican binds to the amyloid precursor protein of Alzheimer's disease (APP) and inhibits APP induced neurite outgrowth. *J Biol Chem*, 271, 31215-21.
- WILLIAMSON, T. G., NURCOMBE, V., BEYREUTHER, K., MASTERS, C. L. & SMALL, D. H. 1995. Affinity purification of proteoglycans that bind to the amyloid protein precursor of Alzheimer's disease. *J Neurochem*, 65, 2201-8.
- YANKELEVITCH YAHAV, R., FRANKO, M., HULY, A. & DORON, R. 2015. The forced swim test as a model of depressive like behavior. *J Vis Exp*.
- YOUNG PEARSE, T. L., CHEN, A. C., CHANG, R., MARQUEZ, C. & SELKOE, D. J. 2008. Secreted APP regulates the function of full length APP in neurite outgrowth through interaction with integrin beta1. *Neural Dev*, 3, 15.
- ZHANG, X., WANG, B. & LI, J. P. 2014. Implications of heparan sulfate and heparanase in neuroinflammation. *Matrix Biol*, 35, 174-81.

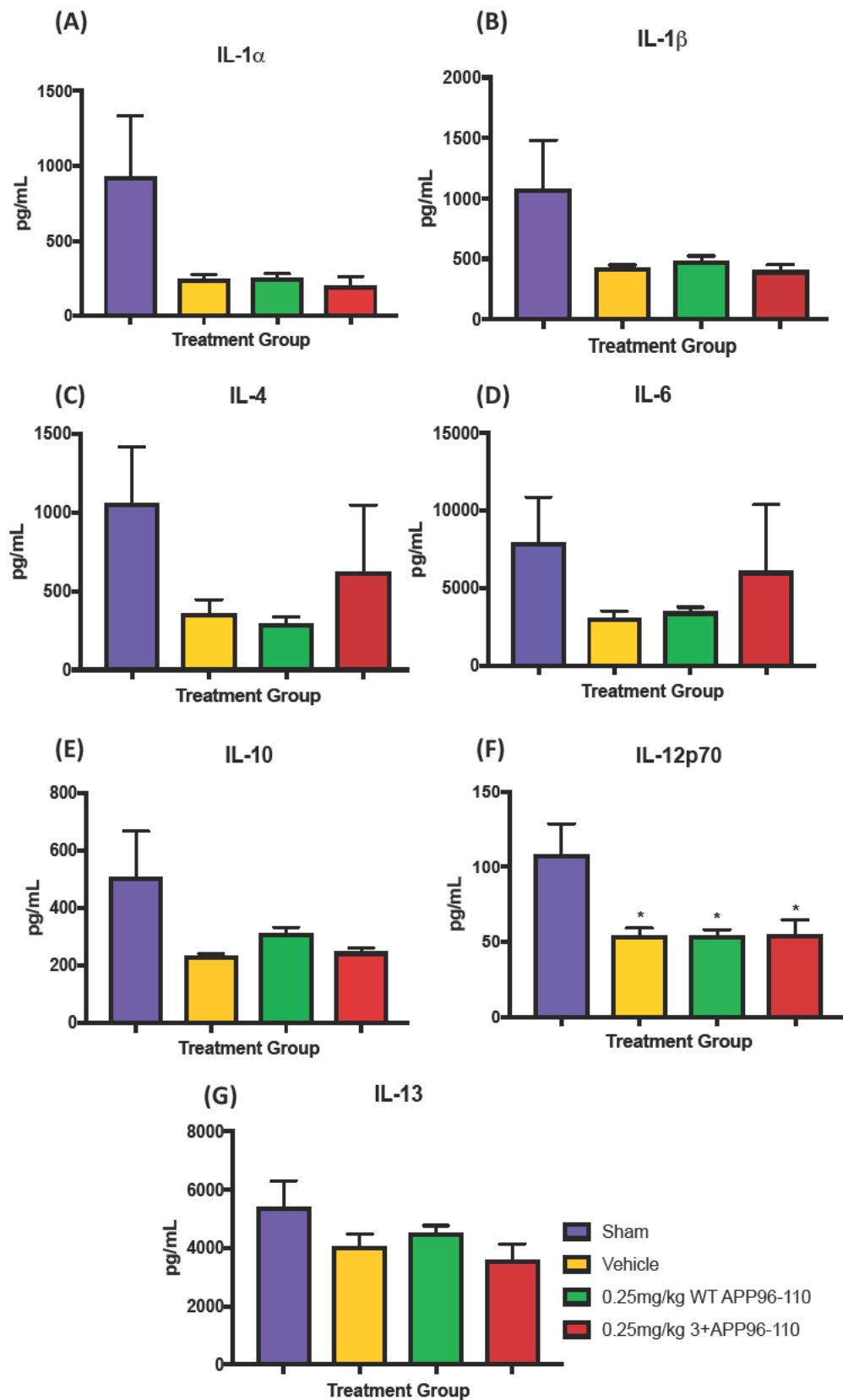
## **Appendix**

## Multiplex

Acute cytokine activity in the hippocampus at 24 hours post TBI was measured using a milliplex rat 8 plex cytokine kit (Millipore/Abacus ALS). Samples were loaded onto a 96 well plate in duplicates, and run in accordance to manufacturer's instructions. The plate was read using Magpix Luminex multiplex array (Abacus ALS, Queensland), and data expressed as pg/ml of concentration. Experimental data was calibrated against standard curves of all 8 cytokines, which were fitted using a 5 parameter log fit through Analyst software (Millipore, Australia). The values for TNF $\alpha$  fell below the detection range and were excluded from the final analysis. Multiplex data was analysed using a multivariate analysis of variance (MANOVA). Significant differences were only observed with IL 12(p70) between each of the treatment groups (vehicle control, 0.25mg/kg WT APP96 110 and 0.25mg/kg 3+APP96 110) with sham animals ( $p < 0.05$ ). No differences were seen with other cytokines.

### Neuroinflammatory cytokines analysed as part of the multiplex assay

Cytokine	M1 Vs M2 Characteristics	Function	Brain Region Analysed
IL 1 $\alpha$	M1	Pro inflammation	Left hippocampus
IL 1 $\beta$	M1	Pro inflammation	Left hippocampus
IL 4	M2	Anti inflammation	Left hippocampus
IL 6	M1	Pro inflammation	Left hippocampus
IL 10	M2	Anti inflammation	Left hippocampus
IL 12(p70)	M1	Anti inflammation	Left hippocampus
IL 13	M2	Anti inflammation	Left hippocampus
TNF $\alpha$	M1	Pro inflammation	Left hippocampus



Preliminary multiplex analysis of IL-1 $\alpha$  (A), IL-1 $\beta$  (B), IL-4 (C), IL-6 (D), IL-10 (E), IL-12(p70) (F) and IL-13 (G) in the left hippocampus at 24 hours post-TBI (n=3-5 per group). \*p<0.05, compared to sham animals.